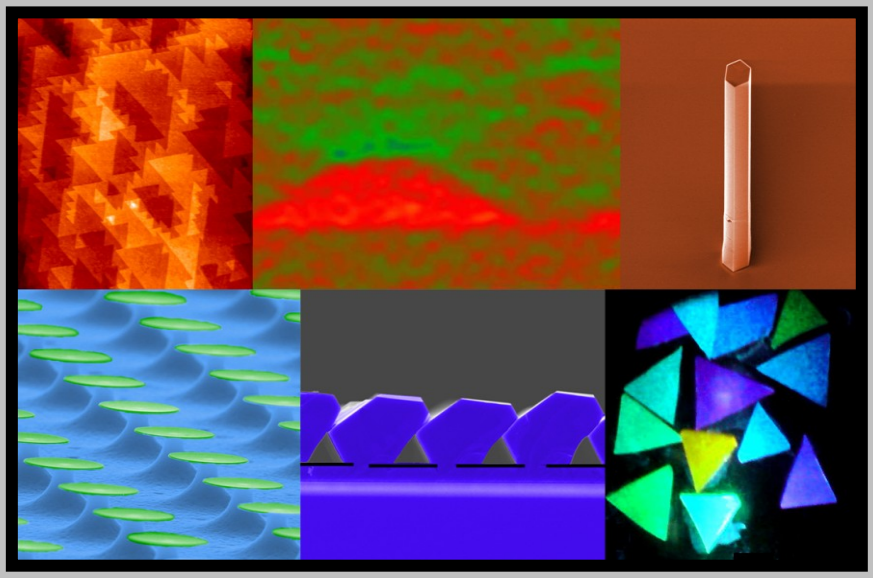

CRHEA

Centre de Recherches sur l'Hétéro-Epitaxie et ses Applications

Activity report

2006-2010

Université Nice SOPHIA ANTIPOLIS

cnrs advancing the frontiers

CONTENTS

GLOBAL REPORT

RESEARCH TEAMS

SCIENTIFIC HIGHLIGHTS

SCIENTIFIC PRODUCTION OF THE LABORATORY

GLOBAL REPORT

Head of laboratory : Jean-Yves DUBOZ
Contact: jyd@crhea.cnrs.fr

Mission and activity of the laboratory

CRHEA is a CNRS (Centre National de la Recherche Scientifique) research laboratory which also works in relation with the University of Nice-Sophia Antipolis. The staff amounts to about 55 including permanent, non permanent, PhD students.

CRHEA is highly specialized in the epitaxy of semiconductors. The core activity is to develop the heteroepitaxy and also the homoepitaxy of thin films, heterostructures, and nanostructures. Although there is still some activity related to arsenides with the InGaAsN materials, the lab really focuses on wide band gap materials. GaN and related alloys are the major research topic. ZnO and alloys is gaining importance, while SiC remains a specialty of the lab. All epitaxy techniques from MBE (6 reactors) to CVD (3 reactors), MOCVD (3 reactors) and HVPE (1 reactor) are developed at CRHEA. Material grown at CRHEA is mainly characterized on site, which allows a fast and efficient feedback. Hence, CRHEA has also developed a strong expertise in wide band gap semiconductor characterization such as X-ray diffraction (2 diffactometers), scanning electron microscopy (2 microscopes), atomic force microscopy (2 systems)), scanning tunneling microscopy under UHV (1 system coupled to a MBE reactor) and TEM (1 microcope). Optical characterization relies on UV-visivble-IR photoluminescence, reflectivity, micro-photoluminescence and excitation /selective photoluminescence. Cathodoluminescence and XPS surface analysis will be available soon.

Finally, CRHEA has its own clean room in order to process test devices which allow us to assess the optoelectronic properties of the heterostuctures grown in the lab. Optical and electronic lithography, metal and dielectric deposition systems, and reactive ion etching enable us to fabricate all the test devices that are needed to validate the material properties.

A particularity of the lab is to provide material for a large French and European community, either for further characterization, for fundamental physics

experiments or for sophisticated devices processing. For that reason, CRHEA is widely open to collaboration and has a large number of partners to works with, either on informal bases or in the frame of national or international contracts. CRHEA's model is to focus his efforts on the epitaxy and collaborate with external laboratories for further studies. CRHEA's portfolio of publications very clearly shows the importance of these collaborations.

Given the importance of semiconductors for industrial application, CRHEA has numerous relations with industrial partners. It has a common research lab with RIBER and with NOVASIC, and closely works with many others. The collaboration with RIBER aims at developing the MBE equipment for the epitaxy of GaN, both by the ammonia and the plasma approaches. NOVASIC in collaboration with CRHEA works on the CVD epitaxy of SiC and develops the equipment and the process for producing 4H-SiC epilayers on an industrial scale.

Education is also one of the goals of the laboratory. Every year, in average, three students are starting a PhD, and three are defending it. As the thesis duration is three years (in France), there are about 10 PhD students in the lab. A special agreement has been established with the University of Bochum which allows some students from CRHEA to spend a part of their time in Bochum, and vice versa. These PhD students at the end become Doctors of both the Bochum and Nice-Sophia Antipolis universities.

CRHEA is an active member of local and national research networks. For instance, for transmission electron microscopy, CRHEA contributes to a national program which allows to use various facilities in France (practically Grenoble and Marseille) and to a regional program which promotes the exchange of know how, the open access of various facilities (including CRHEA's one). Concerning the nanoscience, CRHEA is a member of the regional "C'nano" newtwork, which promotes the collaboration between local partners working in nanoscience (from physics to biology, and chemistry). CRHEA is also coordinating the development of the nanotechnology tools and processes at the regional scale and organizes the investment for new equipments in three clean rooms (2 in Marseille and the third one at CRHEA).

Research labs are evaluated in general every fourth years. For some pratical reasons, CRHEA is going to be evaluated in 2011 over a five year period that goes from 2006 to 2010. The present report thus cannot present all the results obtained during this period, but rather shows some representative highlights.

Organisation

CRHEA is organized around four teams :

-ELECTRO works on the epitaxy of GaN and SiC for electronics applications
-OPTO deals with the epitaxy of GaN and InGaAsN for optoelectronics applications
-OXTRO develops the epitaxy of ZnO for optics and spintronics
-NANO explores the nanosciences and nanotechnologies in epitaxy

These teams were created in 2007 in order to better cover the research topics in terms of physics and applications, while the laboratory was previously organized along the epitaxy techniques. With the growing maturity of wide band gap semiconductors, the growth technique was not a differentiating parameter anymore. The new organization allows for a better comparison of different technical approaches for a given application. This is particularly true for the OPTO team where many epitaxial techniques can be compared or even combined in order to fabricated complex devices such as lasers, white LEDs, etc…

Obviously, there is a large overlap between these teams, and this overlap is highly positive and encouraged. There is no clear frontier between teams and many subjects are explored by more than one team. These teams get a strong support in characterization from a common group of structural and optical analyses.

Finally, administrative and technical services provide the necessary support for the laboratory daily tasks.

The main research axes of each team are presented in a dedicated section starting on page 12, without entering into details. Key results are presented in the next section as scientific highlights. In agreement with the overlap between team activities mentioned above, many highlights have been obtained by more than one team.

CRHEA's staff and groups

Head of CRHEA
Jean-Yves DUBOZ

Technical services:
Isabelle CERUTTI, Marjorie TOLMONT, Michèle PEFFERKORN, Anne Marie GALIANA, Eric DREZET, Patrick CHALBET, Gérard MOLINO, Noureddine SLAMA

Analysis group:
Mathieu LEROUX, Monique TEISSEIRE, Maud NEMOZ, Sébastien CHENOT, Philippe VENNÉGUÈS, Olivier TOTTEREAU, Luan NGUYEN

Team ELECTRO:
Yvon CORDIER (HEAD), Adrien MICHON, Marc PORTAIL, Marcin ZIELINSKI (NovaSic), Thierry CHASSAGNE (NovaSic), Thierry BOURGOIN (NovaSic), Marc BUSSEL (NovaSic), Magdalena CHMIELOWSKA (post doc), M. Reda RAMDANI (Post Doc), Eric FRAYSSINET (Post Doc), Martin JOUK (Doc), Zhi CAO (Doc), Sai JIAO (Doc), Tasnia Hossain (Doc).

Team OPTO
Jean MASSIES (Head), Philippe DE MIERRY, Benjamin DAMILANO, Julien BRAULT, Mohamed AL KHALFIOUI, Gilles NATAF, Denis LEFEBVRE, Aimeric COURVILLE, Hyonju CHAUVEAU (Post doc), Thomas HUAULT (Doc), Abdelkarim Kahouli (Doc), Nasser Kriouche (Doc)

Team NANO
Jesús Zúñiga-PÉREZ (Head), Jean-Yves DUBOZ, Marc DE MICHELI, Fabrice SEMOND, Blandine ALLOING, Stéphane VÉZIAN, Emmanuel BERAUDO, Boris POULET, Sylvain SERGENT (Doc), M. J. RASHID (Doc)

Team OXTRO
Christian MORHAIN (Head), Christiane DEPARIS, Borge VINTER, Jean-Michel CHAUVEAU, Dimitri TAINOFF (Post Doc)

Scientific production

The list of publications is given at the end of this document. Note that not all publications of the year 2010 are included. As already said, CRHEA relies on collaborations to fully exploit the samples grown in the lab. As a consequence, a large number (about 70% of the total) of papers are co-published with external groups.

The following figures show the number of publications per year for CRHEA and per year and per researcher, as a function of time. The annual publication per researcher is increasing and reaches a very satisfactory value of about 5.

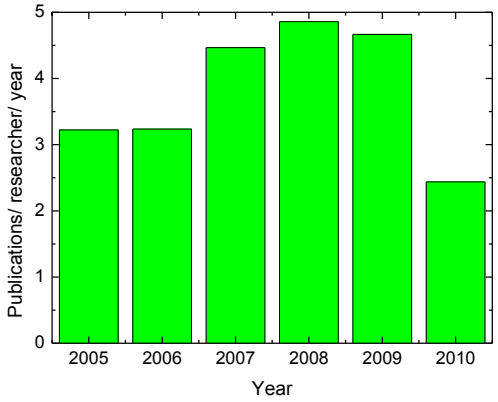

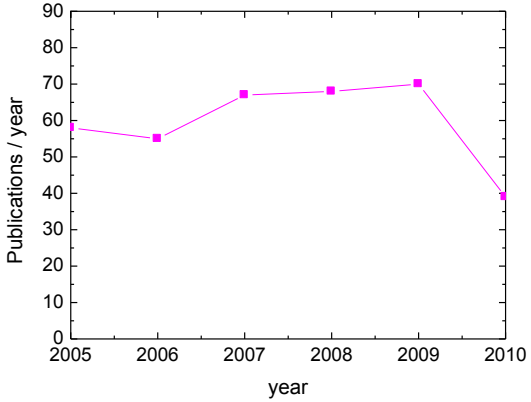

Research teams

ELECTRO

Head: *Yvon CORDIER* ***Contact:*** *yc@crhea.cnrs.fr*

Research topics

The ELECTRO team develops the epitaxy of semiconductors for electronics applications, including high power electronics, high frequency electronics and also sensors and micro-nanosystems. As GaN substrate remain small and expensive, the substrate of choice for the epitaxy of GaN is the Si in one considers the perspective of large volume/ low price applications. This, however, is at the expense of technical difficulties due to the large lattice and thermal expansion coefficent mismatches between nitrides and silicon. This is a central issue in our research activity. Another point that we focus our attention to is the control of residual doping levels as electronics devices often require both conductive channels and insulating layers.

The ELECTRO team activities are distributed along 6 main lines:

1-Heteroepitaxy of 3C-SiC on silicon :

For a few years, the epitaxy of 4H-SiC is mainly the goal of NOVASIC for industrial pruposes and our research activity in SiC focuses on cubic 3C-SiC grown on Si. SiC is mainly grown on Si (100) et (111) for fabricating devices such as diodes, but also microsystems in collaboration avec NOVASIC and the LMP laboratory in Tours (high power electronics lab). The emphasize is put on undestanding the physical mechanisms which occur during the nucleation and the subsequent growth along the (100) direction, but also along the (111), (211) et (110) orientations. These thin 3C-SiC layers on Si can then be used for the epitaxy of GaN/AlGan structures (***H1, H3)***.

2-Doping of 3C-SiC :

It is of paramount importance to control the level of doping in 3C-SiC films in order to fabricate structures with a precise electrical conductivity which can go from resistive to very conductive depending on applications. We study the incorporation of donors such as N as a function of the cristalline orientation. We closely collaborate with the LMP lab (Tours) in order to develop ohmic and Schottky contacts on 3C-SiC/Si. We also started to work on the p doping (Al acceptor) in 2010.

3- Graphene :

Since 2008, we have been working on the synthesis of graphene by annealing SiC surfaces in ultra high vacuum (collaboration with LPN lab in Marcoussis) and in an argon atmosphere in a SiC CVD reactor. Interestingly, we obtained similar behaviors on 3C-SiC / Si(111) to those reported on hexagonal SiC surfaces. More recently, we demonstrated the epitaxy of graphene by directly sending propane on a SiC surface (***H2***).

4-Heteroepitaxy of thick GaN on silicon:

High power electronic devices such as GaN rectifying Schottky diodes or transistors require the growth of thick (>5µm) GaN layers. This is very challenging on Si substrates due to the mechanical tensile strain which induces cracking in thick layers. New strategies have to be developed in order to avoid the formation of cracks and go beyond the usual 3µm thick GaN layers on Si reported by many groups. As an additional constrain, this thick GaN layer should not contain any AlN interlayer (***H3***).

5-Developement of AlGaN/GaN HEMTs:

AlGaN/GaN heterostructures with high electron mobility (HEMTs) are developed both for low frequency power applications and for high frequency applications. Due to the large volume market envisioned, the substrate of choice is Si. Si (111) is the most commonly used due to its hexagonal symmetry, but Si(100) and Si(110) have a larger potential in terms of processing and integration with the C-MOS technology (***H5***). Piezoelectric resonators on Si have also been fabricated based on these structures. Finally, the growth of similar AlGaN/GaNheterostructures on different substrates (3C-SiC / Si(111), 4H-SiC, GaN/saphir, AlN/saphir, GaN) allows to compare the optimisation and benchmark the performance (***H4***).

6-Vertical transport in AlGaN/GaN heterostructures

Understanding the vertical transport in AlGaN/GaN heterostructures is mandatory for the development of GaN based infrared or THz emitters and quantum cascade laser. Vertical transport is investigated in structures with AlGaN barriers as thin as a few nm. While non linearities have been measured in simple and double tunnel barriers, obtaining reproducible results requires to reduce the device dimensions by processing or to measure the current by AFM in conductive mode.

OPTO

Responsable: *Jean MASSIES* ***Contact:*** *jm@crhea.cnrs.fr*

Research topics

The OPTO team develops the epitaxy of semiconductors for optoelectronic applications. This applies in the near infrared with InGaAsN compounds but also and mostly in the visible and near UV with the nitride family. In this later material system, the OPTO team can take advantage of having access to all epitaxial techniques (MBE, MOCVD, HVPE) for growing the GaN based heterostructures. This unique and very favorable peculiarity allows us to compare and combine different growth techniques for fabricating original structures and related optoelectronic devices.

The OPTO team activities are distributed along 5 main lines:

1- Semi and non polar nitrides for LEDs : Nitrides have so far been mostly grown along their (0001) orientation (z axis of the wurzite structure). In this case, heterostructures are submitted to an intense piezoelectric field which reduces the radiative efficiency, in particular for LEDs based on QWs. One solution consists in growing the heterostructures along other directions, either perpendicular to the z axis (non polar material) or oblique to it (semipolar). The growth is however more difficult and lead to a poorer quality than along the (001) direction. Hence, new strategies must be implemented in order to improve the cristalline quality to a level that allows for the fabrication of devices such as LEDs or lasers. We have developed different epitaxy processes on full wafers as these solutions can be transfered to production ***(H6)***.

2- Monolithic white LEDs : The initial concept proposed by CRHEA was to directly emit different wavelengths from different QWs of the same LED, thus creating a white LED by color mixing. However these devices suffer from an inhomogenous carrier injection in all QWs and a color mixing that was difficult to control and optimize. The new concept patented by CRHEA in 2006 combines a QW based blue LED and a light converter based on QWs or QDs grown below the blue LED. The converter absorbs part of the blue light coming from the LED

and emits at longer wavelengths (typically yellow), thus replacing the fluorescent material usually deposited during the LED processing. This monolithic approach could thus simplify the white LED fabrication process and reduce its cost, which is the main limitation to the massive spreading out of LEDs for general lighting ***(H7 and H8)***.

3- Green laser based on nitrides : In the frame of an european project we are developing the epitaxy of nitride laser structures with the aim of pushing the wavelength up to the green region. Compared to other groups, the originality of our project consists in replacing the usual AlGaN bottom cladding layer by an AlInN one. The advantage is a better light confinement at large wavelength, and a better lattice matching on GaN substrates. The difficulty is to grow thick high quality AlInN layers which can be conductive enough to serve as electrical bottom contact. Some success has been obtained at wavelengths up to 436 nm with lasers fabricated by Tyndall Institute, one of our partner in the project, based on structures grown at CRHEA ***(H9)***.

4- Ultraviolet detectors based on AlGaN : AlGaN alloys have a direct band gap which can be adjusted from 200 to 365 nm by varying the Al content. They are thus ideal material for UV detectors, in particular for solar blind detectors (null response for wavelengths above 300 nm). These materials can be also used for extreme UV detectors. With our partner, Thales Research & Technology, we have demonstrated state of the art detectors, 2D detector arrays and integrated cameras based on structures grown at CRHEA ***(H10).***

5- Diluted nitrides (Ga,In)(N,As) : GaInNAs alloys are used for growing laser structures on GaAs substrates aiming at an emission between 1.31 and 1.55 µm. Unfortunately, for reaching a laser wavelength above 1.3 µm, one must increase the In and N contents to a level where many defects are created during the epitaxy, which severely degrades the laser performance. The material quality can in large part recover after a annealing step. We have studied in detail the effect of such annealing on GaInNAs QWs and on InAs QDs encapsulated in GaInNAs layers. Physical mechanisms related to the annealing have been elucidated ***(H11)***. Structures based on InAs QDs with GaInNAs barriers are currently under study in order to reach a lasing wavelength at 1,5 µm.

NANO

Responsable: *Jesús ZUNIGA-PEREZ* ***Contact:*** *jzp@crhea.cnrs.fr*

Research topics

The NANO team explores the epitaxy of nano-objects. It also works on larger objects such as microcavities. The materials involved in these studies are GaN and ZnO. As these nano-objects can be applied to any domain, the activity of the NANO team is feeding the activity of other teams. Inversely, there is also nanoscience in all other teams as epitaxy is by nature a nanoscience. This is the case for instance for quantum dots which are mainly investigated in the OPTO team. Hence, there is large overlap between the activities of this team and the one of the others.

The activities of the NANO spread in three main directions:

1-Nanophotonics

We have been working on microcavities for a few years, starting with GaN based cavities. This has been extended more recently to ZnO cavities. We were even able to combine ZnO and GaN in the same structure. After the demonstration of strong coupling at room temperature in both materials (**H12**), the aim is now to demonstrate polariton lasing and/or Bose Einstein condensation. We also work on photonic crystal with an original approach based on conformal epitaxy (**H13**). Microdisks are also studied and encouraging results have been obtained already (**H13**).

2-Nanowires

We explore the epitaxy of GaN nanowires. The appoach is essentially bottom up. There are many issues to explore such as the growth mechanisms, the strain relaxation by the free surfaces of the wire, the dislocation recombination. As we are able to use both MBE and MOCVD, we can play with the differences in growth modes between both techniques to grow axial or core shell heterostructures, finally leading to real 3D nano-objects. In order to grow the nanowires at a precise location, some top down preparation of the substrate is introduced **(H15)**. Nanowires will be used for optical applications (axial optical cavity, whispering gallery modes, strong coupling, sigle photon source…) and/or for electronics (resonant tunnel diode, 1D transistor, …).

3- Micro-nano-resonators

Acoustic resonators are needed for filtering high frequency signals such as in a cell phone at a few GHz or can be used as sensors that are very sensitive to pressure, temperature, acceleration…We have taken advantage of our expertise in the growth of AlN/Si to demonstrate bulk acoustic wave resonators (**H14**). Electromechanical resonators were also fabricated in collaboration with external groups (IEMN in Lille , CNM in Barcelona) (**H14**).

OXTRO

Responsable: *Christian MORHAIN* ***Contact:*** *cm@crhea.cnrs.fr*

Research topics

The research of the OXTRO team is focused on ZnO and its alloys such as non-magnetic (Zn,Mg)O or magnetic (Zn,Co)O. The scientific interests and the potential applications lie in the fields of optoelectronics and spintronics. Epitaxy is done by MBE.

Very high quality material and heterostructures have been obtained and have led to some state-of-the-art results:

- 2005 : First observation and measurements of very high piezoelectric fields (~MV/cm) in polar QWs based on (Zn,Mg)O/ZnO
- 2006 : First demonstration of the magnetic anisotropy of the Co ion in (Zn,Co)O, establishing a criterion for intrinsic ferromagnetism in these alloys (***H16***)
- 2007 : First demonstration of the antiferromagnetic coupling between Co ions and demonstration that a high density of free electrons ($n>10^{20}cm^{-3}$) does not induce any ferromagnetic transition in ZnCoO (***H16***)
- 2007 : First observation that the piezoelectric fields do not exist in non-polar (Zn,Mg)O/ZnO QWs (***H17***)

The OXTRO team activities follow 4 main lines:

1- Magnetic alloys :

Diluted magnetic semiconductors (DMS) based on ZnO were theoretically predicted to be good candidates for ferromagnetism at room temperature, opening the way to spintronic devices based on semiconductors. We first investigated (Zn,Co)O alloys and we optimized its growth so that a high crystallographic quality was achieved. This has led to scientific results of prime importance (**H16**). It turned out, *in fine*, that undoped and n-type doped ZnCoO and ZnMnO show no intrinsic ferromagnetism. As the latter alloy has the advantage that its optical properties for emission are much better than those of ZnCoO, we finally chose to further investigate the ZnMnO family. We are convinced that ZnMnO cannot be ferromagnetic without a strong coupling between ions mediated by holes. Efforts are now dedicated to magnify and control the magnetic properties of ZnMnO in sophisticated heterostructures. In

parallel we had also started investigating the ZnGdO alloys. First results were not convincing and the study has been stopped.

2- (Zn,Mg)O/ZnO quantum wells :

We have grown polar and non-polar ZnMgO/ZnO QWs with a state-of-the-art crystalline quality. This has been obtained thanks to an important effort dedicated to investigating the growth mechanisms and understanding the relationship between structural and electronic properties of quantum wells. Our ability to master the material quality has enabled us to demonstrate the presence of piezoelectric fields in polar heterostructures and their absence in non-polar ones (**H17**).

3- Homoepitaxy:

As ZnO substrates were initially very rare and expensive, the epitaxy of ZnO thin films and heterostructures was first carried out on foreign substrates, the physical properties of which (crystallographic symmetry, lattice parameter, thermal expansion coefficient) are different from those of ZnO. This heteroepitaxy leads to the generation of a high density of structural defects (dislocations, stacking faults, twins, grain boundaries…). We have mainly used sapphire substrates with various orientations ***(H17)***) but also polar AlN and GaN templates, and have obtained good results. Nevertheless, the optimum situation remains the homoepitaxy. Since ZnO substrates have become available and affordable, we could start homoepitaxy of ZnO in 2009. This effort was subsequently intensified through a national collaboration with several partners. In particular, we have first worked on the surface preparation of these substrates (not epiready) before starting the epitaxy. Homoepitaxy has already yielded excellent results, for instance for ZnO/ZnMgO QW structures ***(H18)***.

4- Residual doping and intentional p doping:

Efforts have been done to reduce the residual n type doping of ZnO films grown on sapphire first and more recently on ZnO substrates. A world record value of $1x10^{14}cm^{-3}$ has recently been measured for the residual doping N_d-N_a in homoepitaxially grown ZnO films, while the minimum value in ZnO grown on sapphire was $10^{16}cm^{-3}$. Then we have incorporated p type impurities, focusing our efforts on nitrogen activated in an *rf* plasma source, as nitrogen forms a relatively shallow acceptor level (165 meV). We discovered that the N incorporation is limited when ZnO is grown along the c-axis in O-polarity. Therefore we now investigate N incorporation in ZnO grown along various orientations in collaboration with Léti-CEA-Grenoble.

SCIENTIFIC HIGHLIGHTS

H01: 3C-SiC Heteroepitaxy on Silicon substrates

Thierry Bourgoin, Thierry Chassagne, Jean Michel Chauveau, Yvon Cordier, Sai Jiao, Maxim Korytov, Adrien Michon, Maud Nemoz, Marc Portail, Philippe Vennéguès, Marcin Zielinski

The cubic polytype of silicon carbide (3C-SiC) is the only one which can be grown on a host substrate, offering the possibility to dispose of the interesting electrical and mechanical properties of SiC at a low cost. The group activity is mainly focused on the elaboration of a high quality material reliable for the realization of pseudo substrates for group III-nitrides growth, the development of SiC based components (Schottky rectifiers) and micromechanical systems (MEMS). The achievement of such a material requires to address important issues: nucleation, doping and strain engineering.

During the period 2002-2006, many major technological advances have been achieved in close collaboration with the NOVASiC company. Originally designed resistively heated hot wall CVD reactors devoted to SiC epitaxy have been developed and optimized. That allowed demonstrating the growth of 3C-SiC layers both on 2'' and 4'' silicon substrates. Based on these advances, the 2006-2010 activity has been centered on the development of comprehensive analysis dedicated to highlight the major issues hindering the delivery of high quality epilayers suitable for electronic applications and for group III-nitrides regrowth.

The first issue concerns the understanding of SiC nucleation on silicon. The various applications to which the 3C-SiC epilayers are dedicated require to control the growth on differently oriented silicon substrates: (111) for polar and (100) or (211) for non or semi polar group III-nitrides regrowth. The influence of the carbonization step of the CVD process, used to nucleate SiC on Si, has been explored. It has been demonstrated that the carbon content during this step plays a major role conditioning the final crystalline quality of the epilayer with a significant reduction of the structural defects density, evidenced by X-ray Diffraction (XRD), as well as a better quality of the interface. In particular, both XRD and Transmission Electron Microscopy analysis revealed how the formation of stacking faults and twinned domains depends on the nucleation conditions The carbon enrichment of the gas phase during nucleation limits the formation of interfacial voids and Double Positioning Domains (Fig. 1). This work allowed to grow untwined 3C-SiC(111) films with thickness up to 3µm without any cracks [125;108]. These developments have been exploited for the growth of GaN/3C-SiC(111) based HEMTs [91] and 5µm thick crack-free GaN films *(see H3).* Furthermore, for certain applications, a reduced number of stress mitigating layers required to elaborate group III-nitride structures is one of the advantage of using the 3C-SiC(111) pseudo substrate.

The control of intentional doping being of prime importance regarding electronic applications, efforts were carried out to investigate the properties of doped epilayers. Our CVD reactors being initially designed for realizing n-type doping, we investigated the doping efficiency of nitrogen both on 3C-SiC(111) and 3C-SiC(100) epilayers. The influence of various growth parameters on dopant incorporation has been examined in details. The site competition effect of nitrogen with carbon atoms has been demonstrated and a more efficient doping incorporation has been evidenced for (100)

orientation [82]. The elaboration of highly doped/undoped 3C-SiC(100) epilayers for rectifier devices benefits from these investigations. In close collaboration with the LMP Lab (Université François Rabelais - Tours), within the scope of A. E. Bazin PhD thesis (2006-2009), both horizontal and vertical simple (non isolated) Schottky diodes have shown an ideality factor close to 1.2. The recent upgrade (2010) of the 2inches CVD reactor for realizing p type doping (TMAl) opens the way for the future development of p/n junctions but requires to overcome the problems related to this kind of doping, especially the memory effect that degrades the abruptness of p/n junctions.

Finally, in the past few years, the 3C-SiC epilayers grown on Si have become very attractive for the realization of surface machined Micro Electro Mechanical Systems (MEMS) owing to its high Young Modulus, as well as its chemical inertness which make it very suitable for resonators operating at high frequency (>20MHz) in harsh environment. The important problem of residual strain is well illustrated by upwards or downwards bendings of micrometer sized cantilevers designed either in 3C-SiC(111) or 3C-SiC(100) epilayers, related to the presence of a stress gradient within the film (Fig. 2). We have shown that the modification of the classical CVD process can be helpful for tuning the final deformation of the cantilevers [5].

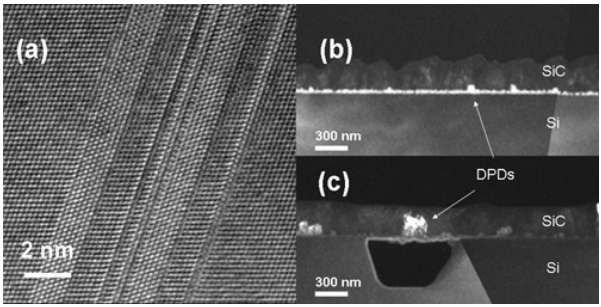

Fig. 1: (a) Stacking faults and twins in 3C-SiC(111) imaged by HRTEM; Reduction of Double Positioning Domains (DPDs) at the SiC/Si interface with optimized (b) and degraded (c) nucleation conditions.

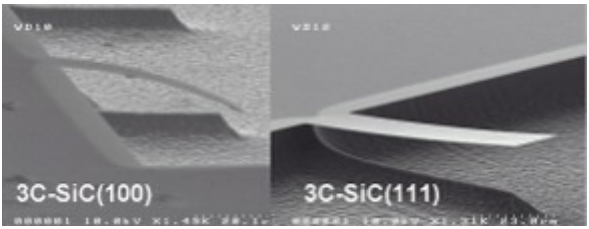

Fig. 2: 3C-SiC/Si cantilevers fabricated at LMP

H02: Graphene growth on 3C-SiC/Si and 6H-SiC

Thierry Chassagne, Yvon Cordier, Adrien Michon, Marc Portail, Stéphane Vézian, Marcin Zielinski

We have started in 2008 a new activity on the growth of graphene on SiC. Using ultra-high vacuum annealing, we have demonstrated that graphene can be obtained on 3C-SiC heteroepitaxially grown on Si(111) or Si(100). We have also developed a new approach based on the direct epitaxy of graphene via propane chemical vapor deposition. This method succeeds in growing graphene films on 6H and 3C-SiC/Si(111) with thicknesses lying between 1 and 7 monolayers.

Graphene is a promising material for both fundamental and applied physics. Following first works on graphene sheets obtained using the laborious exfoliation of few monolayers from graphite, some groups have worked on more determinist methods to obtain graphene. One of the more interesting methods is SiC annealing, which allows to obtain graphene films on entire substrates. The challenge is now to understand in details graphene formation to get a better control of its morphology and of its electron transport properties.

On the basis of its experience in SiC heteroepitaxy and homoepitaxy, CRHEA has naturally started a new research activity on graphene growth on SiC in 2008. But costs and relatively small available diameters of hexagonal SiC substrates compromise the realization of graphene-based devices at industrial scale. A possible way to circumvent this limitation is to use 3C-SiC films heteroepitaxially grown on silicon as low-cost and large-area substrate. The original feature of our activity is to use 3C-SiC pseudo substrates elaborated on silicon by chemical vapor deposition (CVD) and CRHEA is one of the pioneers in this field. We have shown, in collaboration with the Laboratoire de Photonique et de Nanostructures (LPN), that we can obtain graphene by ultra-high vacuum annealing on 3C-SiC(111) [151]. Surprisingly, we have also shown that we can obtain graphene (6-fold symmetry) on 3C-SiC(100) in spite of the 4-fold symmetry of the substrate surface. Furthermore, graphene obtained on (100) surfaces presents structural properties similar to what is observed on (000-1) hexagonal SiC substrates (C-face).

Pioneering works consisting in vapor phase annealing of hexagonal SiC substrates have shown that this method leads to the formation of graphene with good structural properties and an improved thickness homogeneity *[K.V. Emstev et al, Nat. Mat. 8 (2009) 203]*. In addition, vapor phase processes are more adapted to scale-up the fabrication of graphene. Nevertheless, graphene formation under vapor phase generally requires temperatures of about 1600°C, which is not compatible with 3C-SiC/Si substrates (silicon fusion temperature is 1420°C).

In order to address this issue, we have explored an alternative original solution consisting in feeding directly the surface with carbon via a propane flow for graphene formation. This method has allowed us to obtain graphene on 6H-SiC at a reduced temperature of 1350°C in our CVD reactor [167a]. Graphene grown using propane CVD on 6H-SiC(0001) presents structural and morphological properties similar to that

observed on (000-1) face (Fig. 1). This is attributed to the presence of hydrogen (vector gas) during growth that saturates the SiC dangling bonds. When increasing temperature, the expected $6\sqrt{3}\times6\sqrt{3}$ R30° interface reconstruction appears.

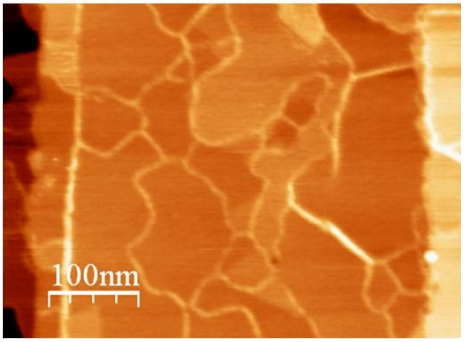

Fig. 1: AFM view (z-scale = 2.5 nm) of graphene grown on SiC by propane CVD. This morphology, commonly observed on (000-1) face is surprisingly observed on our sample grown on (0001) face. We can observe domains of 2 or 3 graphene monolayer, few Å tall walls, and atomic steps on both sides of the image.

Our first growth study shows that graphene thickness depends directly on propane flow and growth time. This confirms that graphene growth is fed by the propane flow, and not by the substrate as in classical annealing recipe. Direct control of the thickness by the growth parameters have allowed us to obtain samples containing graphene domains of 1 or 2 monolayers (Fig. 2). Finally, thanks to a reduced growth temperature, we have also succeeded in growing graphene/3C-SiC on 2 inches Si(111) substrates in a single growth sequence.

Direct epitaxy of graphene on SiC is still an unexplored domain (only 2 papers using MBE and 1 using CVD) but expected to grow. Our first growth study already revealed amazing features such as the possibility to control interface reconstruction and thickness. In addition, the reduced growth temperature allows to grow graphene on low-cost and large area 3C-SiC/Si pseudo-substrates. These promising results open the way to the potential integration of graphene material within Si technology.

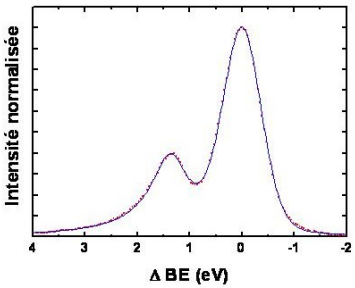

Fig. 2: XPS spectrum of graphene on 6H-SiC grown by propane CVD. The fit allows estimating thickness to 1.5 graphene monolayer.

H03: Strain engineering in GaN structures

N. Baron, T. Chassagne, J-M. Chauveau, M. Chmielowska, Y. Cordier, E. Frayssinet, T.Hossain, S. Joblot, M. Korytov, J-C. Moreno, F. Natali, M. Nemoz, M. Portail, J. Rashid, S. Roy, F. Semond, P. Venneguès, M.Zielinski

Applications such as GaN power electronics on silicon require the growth of several micron thick layers and strain engineering is necessary for avoiding layer cracking. Furthermore, optimizations in this field benefit to other applications using thinner structures

The lack of large size cost competitive GaN substrates makes necessary the growth on foreign substrates. Among these substrates, silicon appears as the most competitive in terms of size and cost. Efforts have then been done for growing good quality GaN based structures in spite of the large lattice and thermal expansion coefficient (TEC) mismatch, responsible for huge residual stress and risk of cracking of the epilayers. The most efficient way to achieve good quality structures is to grow GaN layers on top of a strain relaxed AlN nucleation layer. Indeed, thanks to the 2.5% lattice mismatch between both materials, GaN can be grown compressively strained. This strain, even progressively relaxed, is useful to compensate for the 0.2-0.23% tensile strain generated during the cooling down after the growth, and responsible for cracking. The main two growth techniques (metal organic vapor phase epitaxy (MOVPE) and molecular beam epitaxy (MBE)) are studied. MOVPE presents the advantage of higher growth rates, easy monitoring of three-dimensional to two-dimensional growth modes, which is very useful for eliminating crystal defects. On the other hand, MBE proceeds at lower temperature which is an advantage for slowing the strain relaxation of GaN growth on AlN and smaller thermal strain. Without strain engineering, the MBE growth of a GaN layer on silicon is limited to about 1 µm to avoid cracking. The use of a 3C-SiC buffer (H1) has been shown to reduce the resulting tensile stress in the GaN layers, allowing the growth of 2 µm thick crack free GaN. The same tendency but with thinner crack-free layers is observed with MOVPE. During the last years, intense efforts have been devoted to understand the mechanisms involved in the strain relaxation of GaN. Indeed, limiting the strain relaxation rate in GaN grown on AlN is one key point for obtaining thick crack free structures.

We discovered several years ago that the insertion of an AlN interlayer into the GaN buffer was very efficient to enable the growth of thicker crack free GaN (up to 3 µm with MBE, up to 2 µm with MOVPE). Since 2004, the patented MBE growth process to produce crack-free GaN HEMTs on silicon is licensed to Picogiga International (SOITEC group). During the last years, we studied more deeply how the strain was relaxed into these structures. Using X-ray diffraction, transmission electron microscopy, photoluminescence and in-situ curvature measurements, we have been able to understand the primary role of growth temperature and of the dislocation density on the GaN strain relaxation rate [122,262]. We studied the role played by AlN interlayers and by 3D growth enhanced with the insertion of silicon nitride layers in the lowering of the dislocation density [D.Schenk et al, J. Crystal Growth 2010]. Various optimizations have allowed us to establish the state of the art for GaN on silicon in terms of thickness of crack free layers. For example, 4.5 µm crack-free GaN can be grown by MBE and about 4 µm by MOVPE [E.Frayssinet et al, submitted to Physica Status Solidi c]. For applications

such as high power Schottky diodes (project G2REC leaded by STMicroelectronics) the growth of a silicon doped GaN bottom contact electrode layer is necessary. The strain relaxation being even more efficient in silicon doped layer, this makes the growth even more difficult. Again, the use of new strategies is necessary. For instance, the use of 3C-SiC/Si(111) substrates has presently resulted in the growth of a 4 µm undoped on 1µm Si doped crack-free GaN continuous layers [Y.Cordier et al, ISGN3 July 2010]. The results of these works do not apply only for high power devices on thick buffer layers such as Schottky rectifiers, MOSFETs and HEMTs. With less constrains on the residual strain, high quality layers for light emitting diodes, high frequency transistors and micro-systems can also be grown, not only on the {111} orientation of silicon, but also on C-MOS compatible orientations such as {100} and {110} (see H4).

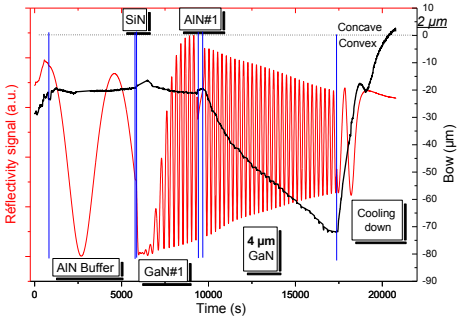

Fig.1: In situ curvature measurement performed during the growth of a thick GaN layer on silicon; the growth of the final GaN layer generates a convex curvature that compensates for the effect observed during cooling.

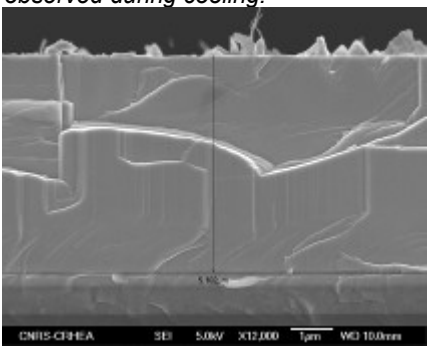

Fig.2: SEM cross-sectional view of 4 µm thick GaN grown crack-free on 1 µm thick GaN layer doped with 2x10^{18} atoms/cm^3 of silicon on a 3C-SiC/Si(111).

Optimizations on the epitaxial structures are underway, but other ways are explored such as local area growth that can lead to 8 µm thick crack-free GaN on areas up to 200 µm x 200 µm [M. J. Rashid et al, IWN 2010, Tampa, September 2010].

H04: AlGaN/GaN High Electron Mobility Transistors

M. Azize, N. Baron, S. Chenot, M. Chmielowska, Y. Cordier, E. Frayssinet, S. Joblot, M. Portail, F. Semond, M. Ramdani

We develop the epitaxy of nitride based High Electron Mobility Transistors for applications in the field of microwaves, power eletronics, micro-systems and sensors. AlGaN/GaN heterostructures are grown on various substrates such as silicon, silicon carbide, GaN or AlN templates and free standing GaN.

An intense effort is devoted to the growth of the AlGaN/GaN material system, considered as the most mature for future mass production in the field of telecommunications, radars, power switching and sensors. Nevertheless, the lack of large size cost competitive GaN substrates implies the growth on foreign substrates. Among these substrates, silicon appears as the most competitive in terms of size and cost. Efforts have then been done for growing good quality GaN based structures in spite of the large lattice and thermal expansion coefficient mismatch, responsible for huge residual stress and risk of cracking of the epilayers (*see H3*). HEMT device active layers require good crystal quality and sharp interfaces for reliability and for high electron mobility. Furthermore, the electrical behavior of the polar surface, as well as the need for high electrical resistivity buffer layers, are critical for these applications.

Substrate	Si(111)	3C-SiC	MOCVD-GaN	MOCVD-AlN
GaN thickness	1.7 µm	1.7 µm	4-7 µm	2 µm
Dislocation density (/cm²)	3-6x10^{9}	<5x10^{9}	<1x10^{9}	2-3x10^{9}
2DEG density (/cm²)	8x10^{12} 1x10^{13}	1.1x10^{13}	1x10^{13}	9x10^{12}
RT electron mobility (cm²/V.s)	1800 2000	2050	2030-2150	2085
LT electron mobility (cm²/V.s)	8500 13700		26500 31000	
Residual doping level n (cm^{-3})	2-4x10^{14}	1-2x10^{14}	<3x10^{14}	<3x10^{14}

Tab.1 : Material and device properties of AlGaN/GaN HEMTs grown on Silicon, 3C-SiC and MOCVD grown GaN and AlN templates on sapphire.

HEMT epilayers have been grown by molecular beam epitaxy on silicon substrates with various orientations: the <111> orientation well known to be compatible with hexagonal lattice of nitrides, but also the <100> and <110> orientations which are C-MOS compatible but present different surface symmetries (see *H5*). Optimizations led to structures with state of the art quality on Si(111) [122]. The use of a 3C-SiC buffer was shown to reduce the residual stress in the layers (*H1, H3*), and HEMT structures with a quality at least as good as on bare silicon have been obtained [91]. Concerning micro-system applications, 1 MHz MEMS resonators with fully integrated HEMT transducers have been developed at the IEMN in Lille on Si(111) [92].

HEMT structures are developed on other substrates such as 4H silicon carbide, GaN or AlN templates on sapphire with various resulting dislocation densities, strain states and thermal dissipation coefficients of the substrate. The regrowth on GaN based substrates

has necessitated the development of new strategies based on the use of acceptors (Fe, Mg, C) to avoid any electrical conduction at the regrowth interface. An enhancement of the resistive properties of the buffer layers at high temperature has been achieved, which is a benefit for HEMT power devices, but also for less temperature dependant Hall sensors [148] as shown in Fig.1. Furthermore, in the frame of a project with IES (ANR AITHER), enhanced transmission of radiations at 300 GHz has been obtained with such structures grown on sapphire; this is the first step in the demonstration of THz amplification.

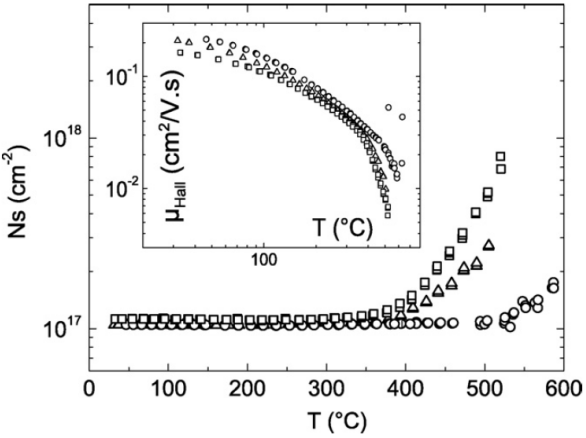

Fig.1: Evolution of the Hall carrier density and mobility with the temperature in AlGaN/HEMTs with different buffer layers.

Another result is that in DC conditions, the drain current collapse of HEMTs on Si(111) is noticeably smaller than on GaN on sapphire templates (Fig.2). However, pulsed I-V measurements with (Vds=0V, Vgs=0V) quiescent bias show the same reduced current collapse for both kinds of devices, whereas relatively small gate lag and drain lag effects appear on silicon in spite of the absence of any passivation of the devices. This attests the quality of these devices.

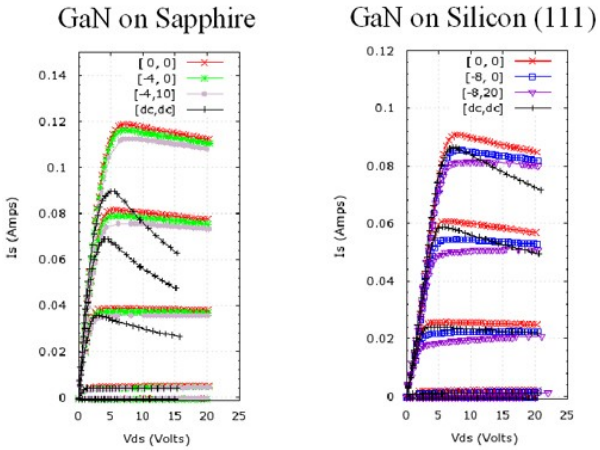

Fig.2: DC and pulsed output characteristics of HEMT devices on GaN/Sapphire and Si(111).

H05: Integration of GaN with silicon technology

N. Baron, S. Chenot, Y. Cordier, E. Frayssinet, S. Joblot, F. Semond

We develop the epitaxy of nitride based High Electron Mobility Transistors for integration with silicon technology. After demonstrating the feasibility of growth on silicon substrates with various orientations, we show the first AlGaN/GaN HEMT integrated with a silicon MOS process.

Combination of GaN-based transistors and CMOS technology would allow for an expanded set of applications that can take advantage of the high voltage and high power handling capability of nitrides as well as the high density, simplicity and low power consumption of MOS digital circuitry. Additionally there is great interest in GaN-based chemical, gas, biological, pressure and mass sensors. Monolithic integration of AlGaN/GaN HFETs with the silicon MOSFETs opens the door for the integration of MOS devices along with GaN-based sensor, allowing for compact, low power read-out circuitry.

Substrate	Si(111)	Si(001)	Si(110)
GaN thickness	1.7 µm	0.8 µm	1.7 µm
Dislocation density (/cm²)	3-6x10^{9}	1x10^{10}	3.7x10^{9}
2DEG density (/cm²)	8x10^{12} 1x10^{13}	8x10^{12}	9.6x10^{12}
Electron mobility (cm²/V.s)	1800 2000	1800	1982
Residual doping level n (cm^{-3})	2-4x10^{14}	5x10^{14}	4x10^{14}

Tab. 1: Material and device properties of AlGaN/GaN HEMTs grown on Silicon

A first step in the demonstration of the feasibility of integration was the growth of HEMT epilayers by molecular beam epitaxy on silicon substrates with the <100> and <110> orientations which are C-MOS compatible but present a different surface symmetry compared to the one of GaN.

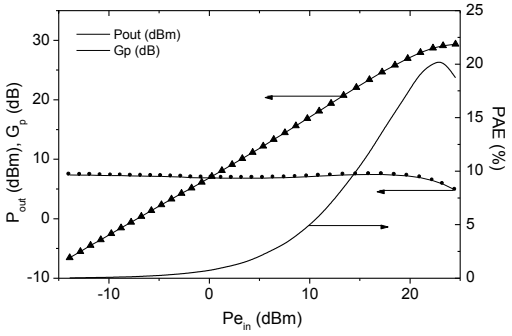

Fig.1: Power characteristics at 10 GHz for a 2x150x0.3 µm² AlGaN/GaN HEMT on (001) Si substrate (Vds=30V,Vgs=-2V). (from [3])

The structures have been compared with those optimized on Si(111)[122] (Tab.1). Surprisingly, the HEMT structures and devices grown on Si(110) are very similar in quality to those grown on Si(111) [91]. On the contrary, a big effort has been necessary to achieve good quality structures on Si(100). Nevertheless HEMT devices on Si(001) processed at IEMN showed an output power density of 2.9 W/mm with a power added efficiency of 20% at 10 GHz (Fig.1), establishing the state of the art for this system [148].

A second step consists in integrating both GaN and silicon device technologies. In collaboration with the IMS-NRC and Carleton University (Ottawa, Canada) we have developed a windowed growth technique, also called differential epitaxy technique, to grow AlGaN/GaN HEMT layers on Si substrates while leaving protected areas of atomically smooth silicon in which MOSFETs are subsequently built (Fig.2) [123].

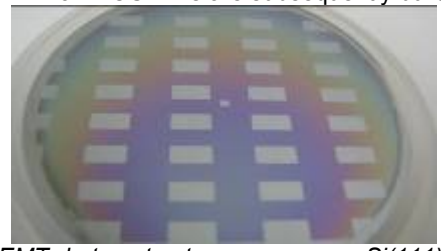

Fig.2: 2" AlGaN/GaN HEMT heterostructure grown on Si(111) with silicon window openings for MOS integration

Thanks to this method we successfully demonstrated the first monolithic integration of AlGaN/GaN HEMTs and silicon MOSFETs (Fig.3) [163].

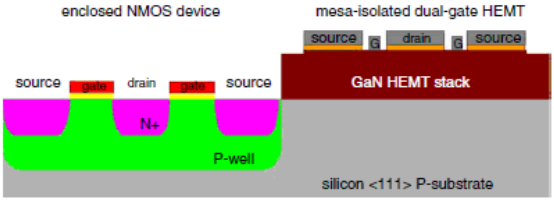

Fig.3: Schematic of integrated process. NMOS device shown on left, mesa-isolated GaN HEMT on right

The way how the protection is realized and the minimization of the thermal budget during MOS processing turn out to be key issues for accomplishing this integration. We found out that the HEMT performance was not compromised by the integration process. Also high channel electron mobilities were obtained in the MOSFETs, meaning that the quality of the silicon surface is preserved all along this process. Work in underway to transfer this integration process to more industrially relevant silicon (110) substrates.

H06: Defect reduction in semipolar nitrides by selective epitaxy

S. Chenot, A. Courville, P. De Mierry, N. Kriouche, M. Leroux G. Nataf, M. Némoz, P. Vennéguès.

III-N compounds of wurtzite symmetry exhibit spontaneous and piezoelectric polarizations along the (0001) c-axis of the unit cell. Growth of heterostructures along this direction leads to strong polarization fields which reduce the internal quantum efficiency in quantum wells-based light emitting diodes. This effect is known as the quantum confined Stark effect (QCSE). Growth of nitrides along a direction different from [0001] allows decreasing or suppressing the QCSE. In particular, semipolar (11-22) GaN could be obtained by heteroepitaxy on (1-100) m-plane sapphire. These layers exhibit almost no polarization fields along the growth axis but present a high density of structural defects in comparison with polar (0001) GaN. We present 2 methods which efficiently reduce the defects densities.

In semipolar GaN, basal stacking faults (BSFs) and partial dislocations (PDs) lye in the (0001) plane and can extend to the surface during growth. Two different approaches were used to decrease the defects density. The first one is based on the overgrowth of GaN from a semipolar GaN template patterned with SiO_2 stripes, called AS-ELO (asymmetric epitaxial lateral overgrowth) [109,138]. The second one consists in growing (11-22) GaN from ridge-patterned (10-12) r-plane sapphire substrates obtained by wet chemical etching [147].

1)AS-ELO.

Fig.1a) shows the shape of GaN crystals at an intermediate stage of ELO. The growth conditions are chosen to enhance the growth rate along the +c axis. The crystal expands both laterally and vertically until a situation where it overgrows the adjacent crystal. This situation is propitious for stopping the propagation of inclined stacking faults and threading dislocations, as shown by the schematic image in Fig.1b).

2) Semipolar (11-22) GaN on etched r-plane sapphire.

The sapphire substrate was etched in an acidic solution in order to reveal the c and m facets (Fig.2a)). A 30 nm-thick GaN nucleation layer was first deposited at 580°C. This layer was then heated at 1100°C. During this step, the initial nucleation layer covering the surface experienced a major morphologic change by forming 3D GaN crystals by mass transport recrystallization toward the *c*-facet of the patterned sapphire. The morphology of the annealed nucleation layer is shown in Fig.2b).The crystal is oriented in the [11-22] growth direction, with the *c*-axis tilted by about 58° from the surface normal. Growth was then pursued at 1100 °C. Figure 2c) shows the shape of the GaN stripes after 30 min growth. A two-dimensional film is obtained after coalescence of the *c*-plane growth fronts, according to the schematic view in Fig. 2d).

Both methods are shown to dramatically enhance the crystalline quality and decrease the BSFs and PDs densities. They are low cost attractive alternatives to the homoepitaxial growth approach developed in particular by the Santa Barbara University group *(Appl. Phys. Express 2 (2009) 021002)*. Furthermore, this open the way to the realization of semipolar optoelectronic devices on large scale 2 inches sapphire.

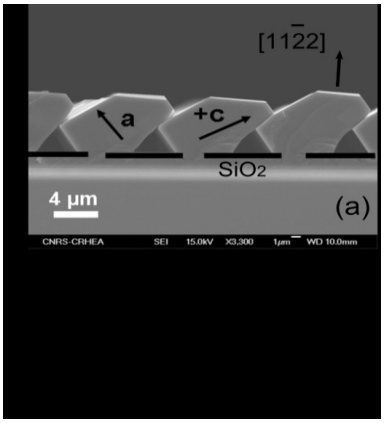

Fig.1 a) cross-sectional SEM image of the crystals after 1 hour of ELO, b) schematic image showing the progress of the crystal during ELO. The inclined lines represent the BSFs. The dotted lines indicate the location of the coalescence front between adjacent crystals

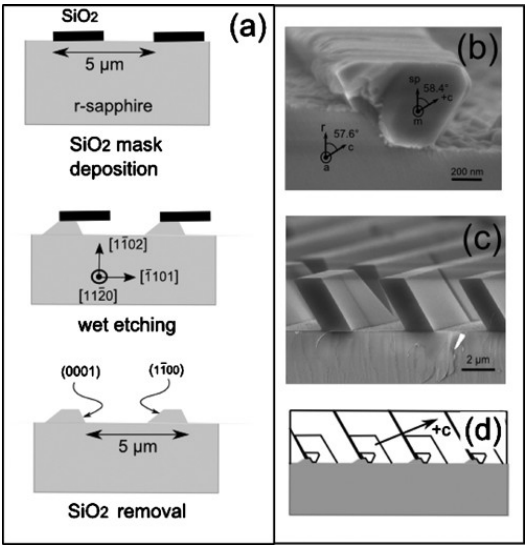

FIG. 2. (a) Schematic of the process development of the sapphire etching. Cross-sectional SEM image of GaN crystals on etched r-sapphire, (b) after deposition of the low temperature nucleation layer and recrystallization at 1100 °C, (c) at an intermediate step of growth (30 min). (d) Schematic view showing the progress of the crystal growth. The arrows depict the r [1-102], a [11-20], m [1-100], sp [11-22], and c [0001] orientations.

H07: Monolithic white light emitting diodes

J. Brault, B. Damilano, P. De Mierry, P. Demolon, T. Huault, J. Massies, F. Natali

Today the realization of white light emitting diodes (WLED) is based on hybrid structures combining a (Ga,In)N blue LED and different phosphorescent materials (phosphors) deposited on top of the LED. This implies the association of very different materials and complicates the fabrication process compared to a blue LED. The general purpose of this work is to find a way to directly obtain white light emission from a monolithic approach using epitaxial growth. Such approach avoids the post-epitaxial growth phosphor deposition. Thus the fabrication process is simplified, decreasing then the cost production which is a key issue for solid state lighting. Furthermore, avoiding the use of phosphors should increase the WLED reliability. One of the main difficulties for monolithic white LEDs is to get chromaticity coordinates independent of the injection current. Towards this end, we introduce here a new concept of monolithic white LED using an epitaxial light converter.

We have demonstrated in 2001 (B. Damilano et al., Jpn. J. Appl. Phys. 40, L918, 2001) the first monolithic white light emitting diodes (WLEDs). It was based on the mixing of blue and yellow quantum wells (QW) in the LED active zone (Figure 1, "standard"). Since that time, such a concept of monolithic WLED has been explored by many other groups and in particular by the company Nichia. However, this concept suffers from intrinsic limitations such as nonhomogeneous and current dependent carrier injection in each QW inside the active region. One of the consequences is that the chromaticity coordinates strongly depend on the injection current.

To avoid this drawback, we have proposed in 2006 a different approach which consists in combining a blue (Ga,In)N/GaN QW LED and a light converter (typically blue to yellow) based on a stacking of nitride quantum dots or quantum wells (Al,Ga,In)N inserted during the epitaxial growth of the structure (Figure 1, right, French patent N°06/50842). This is still a monolithic approach which simplifies the fabrication and should then reduce the fabrication cost, which is nowadays a limiting factor of the use of WLEDs for the general lighting. This work has been supported by the ANR-PNANO (DEMONI, 2007-2010, in partnership with Riber and Lumilog).

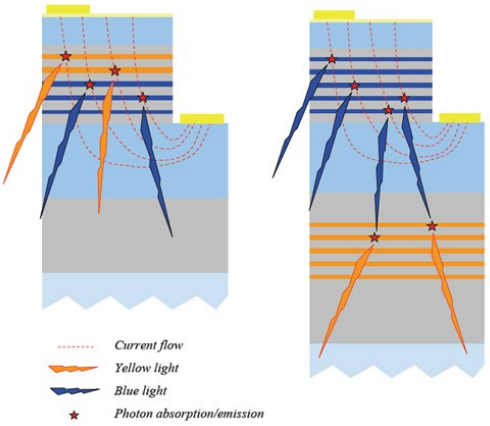

Figure 1. Left : Standard monolithic white LED. Right: Monolithic white LED with light converter.

A good performance has been obtained for the blue LED pump: LEDs realized on GaN substrates (Lumilog) deliver an optical power of 1.3 mW at 20 mA and more than 5 mW at 100 mA (these values correspond to on wafer measurements, i.e. the extraction efficiency is limited to 4%). A first demonstrator of monolithic WLED according to the patented concept has been fabricated (Figure 2). We have shown that, as expected for this new kind of monolithic WLED, the chromatic coordinates are almost insensitive to the injection current (between 10 and 100 mA) [96,164]. This is a significant improvement compared to our initial approach of monolithic WLED where quantum wells emitting at different wavelengths are inserted directly inside the LED p-n junction [210]. Beyond this proof of concept, the objective is now to improve the luminous efficiency (~1 lm/W) by a factor 4 to 5 to really be in the race for practical applications. The limiting factor is the light converter internal quantum efficiency. Several approaches are currently investigated to improve the efficiency of the light converter: mainly GaN/InGaN/AlGaN asymmetric multiple quantum wells [284] and the use of semi-polar orientations to increase the quality of GaInN layers with large In composition.

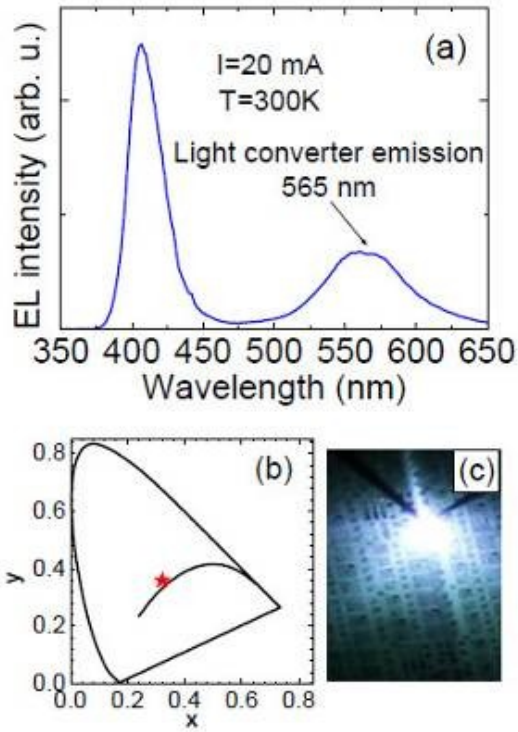

Figure 2. (a) 300K electroluminescence spectrum at 20 mA for a monolithic white light emitting diode with a light converter at 565 nm, corresponding chromaticity coordinates (b) and picture (c).

H08: GaN/AlGaN nanostructures: from quantum dots to dashes

J. Brault, B. Damilano, T. Huault, M. Korytov, M. Leroux, J. Massies, F. Natali, P. Vennéguès

Tri-dimensional confinement of carriers in quantum dots strongly improves the luminescence efficiency of nitride heterostructures which are usually highly defective. By taking advantage of the internal electric field in samples grown along [0001], we have in particular shown ten years ago that it is possible to obtain a photoluminescence emission covering the entire visible spectrum range for GaN/AlN quantum dots. In the present work, the GaN/$Al_xGa_{1-x}N$ nanostructures formation has been studied as a function of the Al concentration. Nanostructures formation via a 2D/3D transition has been observed for $x \geq 0.4$. A morphological transition of the nanostructures (quantum dots → dashes) is evidenced depending on the growth procedure. A striking feature of quantum dashes is the possibility to obtain a photoluminescence emission in a wider wavelength range compared to quantum dots, which could be useful for the realisation of white light LEDs.

In the framework of the monolithic white light emitting diode (LED) project (see Highlight « Monolithic white LED »), we have investigated the possibility to realize quantum dots (QDs) in the GaN/$Al_xGa_{1-x}N$(0001) system with the aim of obtaining an emission over the entire visible range, as demonstrated ten years ago for the case of GaN/AlN quantum dots (B. Damilano et al. Appl. Phys. Lett. 75 (1999) 962). Since n-type and p-type $Al_xGa_{1-x}N$ (with $x \leq 0.5$) layers can be obtained with carrier concentrations above 10^{17} cm^{-3} at room temperature - contrary to AlN -, it should be possible, on one hand, to realize LEDs and, on the other hand, to reduce the epitaxial stress in heterostructures to avoid the formation of cracks (the lattice-mismatch is $\Delta a/a \sim 2.4\%$ between GaN and AlN). However, the formation of GaN quantum dots being obtained through a stress driven 2D-3D - Stranski-Krastanov like - morphological transition, the reduction of the epitaxial stress could become a problem. Indeed, in previous studies, GaN/$Al_xGa_{1-x}N$ quantum dots have been obtained by using different approaches to compensate the low lattice-mismatch (stressed $Al_xGa_{1-x}N$: Y. Hori et al., J. Appl. Phys. 102 (2007) 024311 ; Si exposed $Al_xGa_{1-x}N$: S. Tanaka et al., Appl. Phys. Lett. 69 (1996) 4096).

Nevertheless, we have shown that GaN quantum dots can be obtained on $Al_xGa_{1-x}N$ for $x \geq 0.4$, by simply triggering the 2D-3D transition by a growth interruption, as for GaN/AlN QDs. Moreover, a luminescence in the violet-blue range (400 – 420 nm) is observed [74,139] whereas previous studies reported a UV luminescence (< 360 nm).

Unfortunately, it was not possible to cover the entire visible spectrum range by increasing the GaN deposited thickness: a wavelength emission limited to the blue region ($\lambda_{max} \sim 470$ nm) has been obtained in the thickness range compatible with the formation of dots (fig. 1a). By modifying the GaN surface energy, through a change in the growth interruption process used for the formation of dots, we have evidenced a transition in the nanostructure shape from a dot to a dash-like shape [135]. By adjusting the NH_3 pressure during the 2D-3D transition, the shape can be efficiently controlled in order to favour one type of nanostructure and to obtain mainly dots or dashes (fig. 1). Furthermore, the GaN deposited thickness range to grow quantum dashes is larger than for QDs.

Besides the fundamental interest of such a transition, the possibility to grow quantum dashes with a larger GaN amount has also some important consequences on the density and the size of the nanostructures. By simply adjusting the GaN deposited thickness of the quantum dashes, the combined effects of quantum confinement and built-in electric field result in a luminescence which can be extended from the violet-blue to the green-orange range (fig. 1b) [128]. These results show that GaN nanostructures have a potential interest for the realization of visible light sources using low-dimensionality GaN active regions. An important prospect also concerns the fabrication of nanostructures with a reduced/suppressed electric field, using the so-called nonpolar or semipolar surfaces (see Highlight « Defects reduction in semipolar group III nitrides by selectively localized epitaxy »), to further extend the field of applications to UV light emitters.

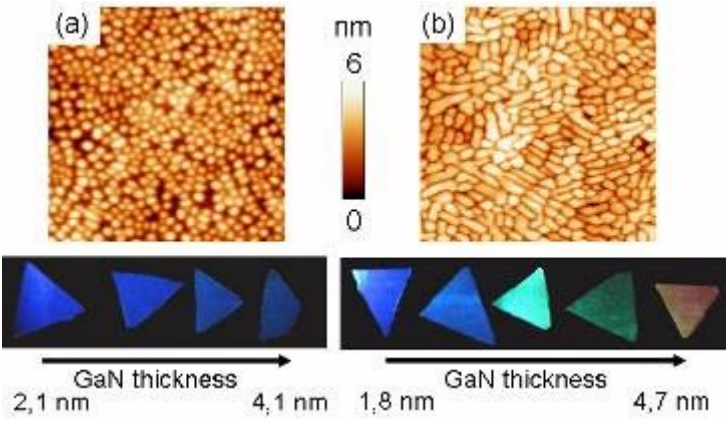

Figure 1. AFM pictures and photographs of the light emitted from different samples (triangular cleaved pieces) (a) quantum dots and (b) quantum dashes (excitation: unfocused laser at 244 nm).

H09: Towards a green laser based on nitrides

H. Chauveau, P. Demolon, J.-Y. Duboz, E. Frayssinet, P. de Mierry

We develop the epitaxy of nitrides to extend semiconductor lasers towards the green. Our original approach consists in replacing the bottom AlGaN cladding by AlInN to increase the optical confinement. Lasers were obtained up to 436 nm

A large effort is devoted in the world to the fabrication of nitride based green laser for many applications including full color displays. The difficulty in extending current blue GaN laser into the green lies in the phase separation in the In rich GaInN QWs, the strong piezoelectric in the QWs, and in the optical confinement (the optical index contrast between the waveguide claddings and core is reduced). Concerning the optical confinement, we have chosen to replace the traditional AlGaN bottom cladding by AlInN [275,276]. Hence, our strategy is to start from the usual laser structure at 400 nm, then replace the bottom cladding, and finally increase the wavelength. We use standard (0001) polar orientation which is easier to grow, but our approach is compatible with the use of semipolar nitrides orientations (see H1) which appear the best solution in the long term.

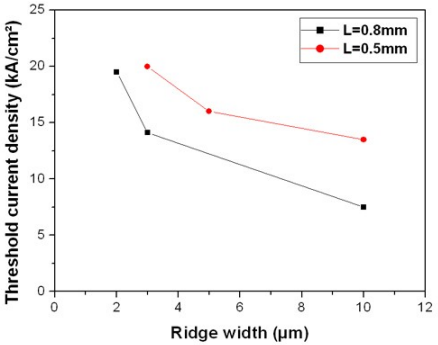

Fig.1 Jth versus laser geometry for AlGaN cladding laser at 410 nm.

When growing by MOCVD thick (500 nm) AlInN layers lattice matched (17% In) with GaN, V-shape pits appear and the material quality, in particular the surface, dramatically degrades. As a GaN layer allows to smooth the surface when v-pits start to appear in AlInN, we introduced periodic GaN layers (fig.2). 5 nm GaN /50 nm AlInN allows to keep a smooth surface (fig.3)

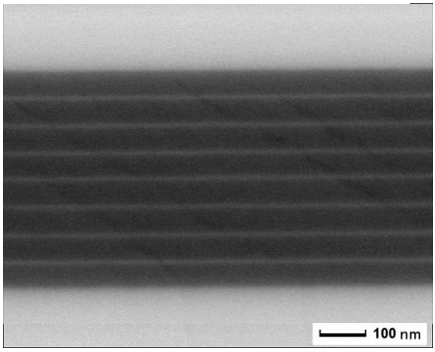

Fig.2: SEM image of the periodic AlInN (50 nm)/ GaN(5nm) used for the laser cladding layer

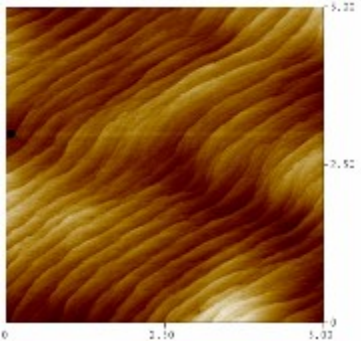

Fig.3 : AFM picture (5×5 µm) of the AlInN cladding (9 × (50nm AlInN/5nm GaN)), rms=0.56nm

We first obtained a laser with an AlGaN cladding with a performance still far below the state of the art, in particular for the threshold current density. Fig.1 shows its variation with the laser geometry, showing that both the material and the process (made by Tyndall Inst.) still need improvement. Laser structures were grown with this AlInN bottom cladding. The cristallographic quality of the whole structure is shown by the XRD, which allows to measure the composition of both the top AlGaN and bottom AlInN cladding layers (fig.4).

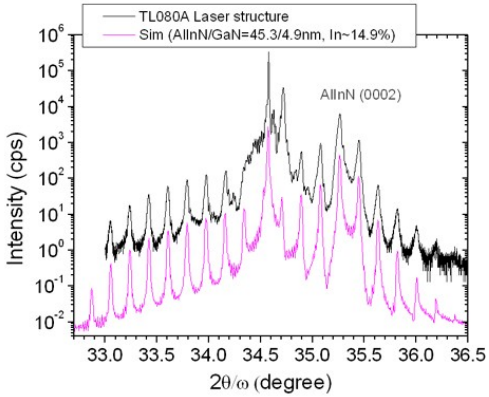

Fig.4: XRD of the whole laser structure

Lasers have been processed and measured by Tyndall. Laser emission was obtained at 400 nm first and then 436 nm. These lasers are the first one in the world obtained with AlInN cladding, where the current is injected through the doped and conductive AlInN layer. Further improvements in epitaxy and processing remain necessary to reduce the threshold current density.

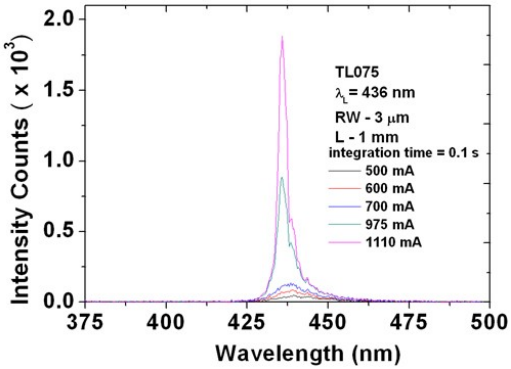

Fig.5: Electrical lasing of a structure with AlInN bottom cladding (50ns pulse, 0.1 % duty cycle).Jth=30 kA/cm2.

H10: Detectors based on AlGaN

J. Brault, J-Y. Duboz, E. Frayssinet, F. Semond

Optical detection based on AlGaN heterostructures has been developed to yield state of the art imaging arrays both in the UV and extreme EU. In the X-ray range, the fundamentals of the photoresponse in GaN have been elucidated.

Solar blind detectors based on AlGaN layers have been developed for many years in collaboration with Thales R&T. Individual Schottky diodes grown on sapphire by MBE have reached an excellent spectral selectivity and a good detectivity [17]. After the fabrication of linear arrays [14], the focus in the last years was put on the fabrication of 2D arrays. A UV camera prototype has been fabricated based on an AlGaN Schottky diode array hybridized to a commercial Si circuit (Indigo, 320x256 pixels with a pitch of 30µm). The cut off wavelength can be adjusted to any value from 260 to 360 nm by changing the chip. The performance is at the state of the art with an excellent rejection ratio (4-5 decades in response between wavelengths of 280 and 400 nm), a low noise (120-300 electrons rms per pixel) and a good uniformity (4% deviation) [280]. This camera is driven by a PC and is easy to move and operate. It is integrated in a commercial package (Raptor) so that this prototype can be readily put on the market (fig.1).

Fig.1 : solar blind camera based on AlGaN heterostructures (commercial package Raptor).

The detection activity has been extended to extreme UV (1-200 nm). In collaboration with Thales R&T, we developed Schottky diodes based on thin AlGaN layers grown by MBE on Si. During the device fabrication, the Si substrate is removed in order to allow illumination from the back side. Using the same read out circuit and integration package as in the UV we fabricated the world first EUV array based on nitrides. The camera was tested at Soleil to image the beam (fig.2) [254].

Fig.2: Image of the split beam of Soleil DISCO line taken at 130 nm by the EUV camera based on AlGaN heterostructures

The electrical performance is similar to the one for the UV camera with a dark current below 1fA at –1V, and a noise of 150 electrons, per pixel. The spectral response (fig.3) shows a high rejection above 300 nm, a high response at 250-300 nm and below 20 nm. The response is weaker in the central 50-150 nm region. At the Lyman α (121nm), the efficiency can reach a few % but is very sensitive to the technology. Arrays with smaller pitch (10µm) are also developed with IMEC for solar observation, based on AlGaN Schottky diodes grown on Si [102]. Measurements at Bessy show the importance of external photoemission from 50 to 150 nm which is problematic for imaging.

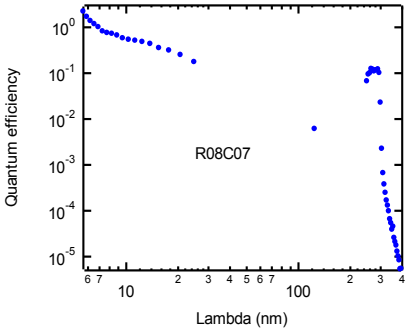

Fig.3: Spectral response of AlGaN Schottky diodes measured at Soleil (CNES study).

In the X-ray range, GaN MSM and Schottky diodes were tested from 6 to 22 keV. The Schottky diodes perform better as their geometry is better suited to the thick layers required by the low absorption coefficient [90]. Some parasitic effects related to the electrical activation of defects by high energy photons and to the tunnel effect in lightly doped Schottky diodes have been evidenced and modeled [134]. The spectral response was measured at Soleil (fig.4). A decent sensitivity (slightly below the Si one) is already obtained around 15 keV [166].

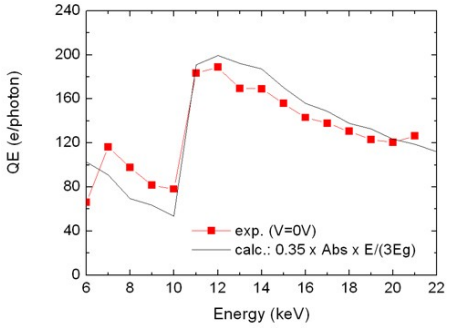

Fig.4: Spectral response of GaN (10 µm thick layers grown by MOCVD) Schottky diodes measured at Soleil. It agrees with the absorption spectrum we measured.

H11: Dilute nitride (Ga,In)(N,As) : from material to laser diodes

M. Al Khalfioui, B. Damilano, J.Y. Duboz, M. Hugues, J. Massies

The dilute nitride (Ga,In)(N,As) is an attractive material system based on GaAs substrates for optical telecommunications in the 1.3-1.5 µm wavelength range, as a lower cost alternative to the standard InP based platform. As a consequence, this material has been thoroughly investigated in the last decade. However, obtaining efficient laser diodes above 1.3 µm remains a key issue. This is in particular due to defect generation increasing with the N incorporation used to lower the band-gap energy. The present work is intended first to study annealing performed to cure these defects and get 1.3 µm QW laser diodes and second to assess the use of InAs/(Ga,In)(N,As) QDs for longer wavelength emission applications.

(Ga,In)(N,As) quantum wells:

Adding small amounts of nitrogen in InGaAs induces a strong reduction of band-gap energy in such a way that 1.3-1.55 µm telecoms wavelengths can be reach. Moreover, the (Ga,In)(N,As) (GINA) can be lattice matched to GaAs and then is a low cost potential alternative to the InP based material system. However, the In and N concentrations (around 40% and 4% respectively) necessary to obtain 1.55 µm laser diodes are at the origin of a strong degradation of the laser performances. Actually, nitrogen incorporation provokes the generation of a high point defect density which strongly decreases the radiative efficiency even for very low N concentration. These defects are partly cured by thermal annealing but this in turn induced an undesired blue-shift. Seeing their crucial role, we have studied in detail the thermal annealing effects in GINA QWs (*M. Hugues, Thèse Université de Nice, December 2007).* The QW blue-shift observed after low temperature annealing (below 750°C) has been attributed to atomic reorganization while, at higher temperature, In-Ga and N-As interdiffusion processes have been shown to be responsible for the blue shift increase [35]. On the other hand, the origin of photoluminescence intensity quenching with temperature of GINA QWs emitting near 1.5 µm has been clarified. Two different processes are responsible for the intensity decrease: exciton dissociation in the low temperature range and thermal hole escape out of QW to the barrier for temperatures above 200 K [41]. Characteristic temperatures (T0) of (Ga, In)(N, As)/GaAs have been investigated for GINA laser diodes emitting in the 1.3-1.5 µm [59]. Edge emitting laser around 1.3µm (fig. 1) are currently made in our lab in partnership with Telekom Malaysia Research and Development (TMRD) with the final objective of demonstrating 1.31µm VCSELs operating at 300K with a low threshold current density.

InAs/(Ga,In)(N,As) quantum dots:

InAs/InGaAs QD high performance lasers at 1.3 µm have been demonstrated by T. J. Badcock et al *(Appl. Phys. Lett.* ***90*** *(2007) 111102)*. We have shown that the emission wavelength can be increased up to 1.5 µm by using InAs QDs capped with GINA [18]. However, the addition of N in the capping layer reduces the emission intensity. It is improved by thermal annealing, but still an undesired blue-shift emission is obtained. The effect of annealing on long wavelength emitting InAs/ $Ga_{0.85}In_{0.15}N_xAs_{1-x}$ ($0 \leq x \leq 0.023$)

QDs has been investigated. After optimum annealing, the QD PL emission exponentially blue-shifts with the nitrogen composition. To achieve emission at 1.55um, it has been concluded that the nitrogen composition should be limited to 1.7-2% and the In composition increased up to 20-25% [75]. In partnership with ISOM Universitad Politécnica de Madrid, we have realized InAs QD LEDs with GINA capping layers. Room temperature electroluminescence close to 1.5 µm was recently demonstrated *(fig. 2)* [257] and work is in progress to obtain 1.5 µm InAs/(Ga,In)(N,As) QD lasers.

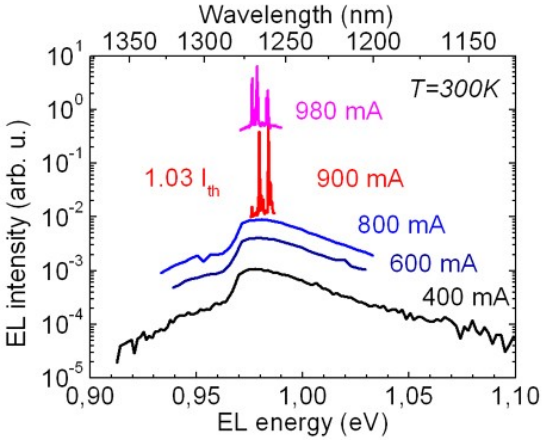

Fig 1: Electroluminescence of GINA quantum wells laser

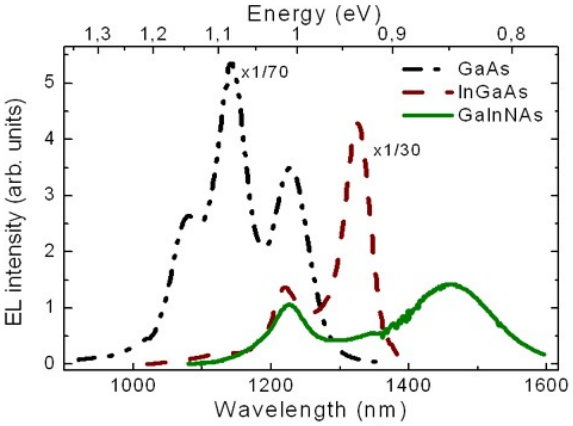

Fig 2: RT Electroluminescence of the as-grown QD-LEDS

H12: Strong-coupling at room temperature: GaN and ZnO microcavities

J. Y. Duboz, E. Frayssinet, M. Leroux, J. Massies, J. C. Moreno, I. R. Sellers, F. Semond, S. Sergent, J. Zúñiga-Pérez

Optical microcavities based on GaN and ZnO are fabricated by MBE in order to study the light-matter interaction in such wide-bandgap materials. The development of the required building blocks (Distributed Bragg Reflectors and active materials) and the understanding of their optical properties aim at fabricating low threshold polariton lasers working at room temperature. Rabi splittings in the order of 50 meV and 100 meV have been measured in GaN- and ZnO-based cavities, respectively, and peculiarities of polariton relaxation in these materials have been studied.

Due to their large oscillator strengths and large exciton binding energies, greater than the thermal energy at room temperature, GaN and ZnO are ideal candidates for maintaining the strong-coupling regime up to room temperature. However, contrary to the growth of other materials traditionally employed in semiconductor optical microcavities (GaAs and CdTe), the growth of GaN and ZnO heterostructures is still an open issue and the fabrication of high quality cavities is still challenging.

In 2005 we showed for the first time the strong coupling regime at room temperature in a low quality factor (Q=40) GaN-based cavity using angle-dependent reflectivity measurements. Subsequently, and by improving the quality factor (Q>160), the strong-coupling regime could be evidenced using both reflectivity and photoluminescence (Fig. 1) [15,23,62,63].

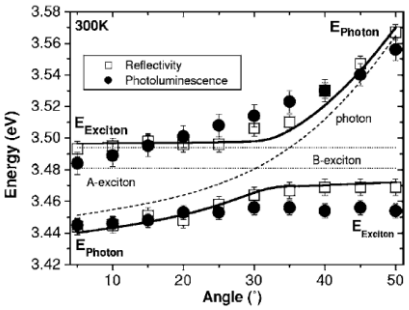

Fig. 1: Dispersion of the polariton branches in a GaN λ/2 cavity measured at room temperature by reflectivity and photoluminescence.

In order to increase the Rabi splitting/polariton linewidth ratio, microcavities based on ZnO active layers were considered. In 2009, and almost simultaneously with two other teams, we published the observation of microcavity polaritons on a planar ZnO-based cavity for the first time (Fig. 2) [105,113,141]. However, due to the much larger exciton oscillator strength in ZnO and the larger absorption by the continuum, the upper polariton branch (UPB) cannot be observed unless very thin cavities ($d_{ZnO} \sim \lambda/2$ or thinner) are used. This is illustrated in Fig. 2, where the UPB can only be detected in the cavity with an optical ZnO thickness of $\lambda/4$. Furthermore, as can be seen in Fig. 2(b), at the onset of the continuum (~3.42 eV) the UPB seems to split into two components. Again, this effect could be simulated and explained in terms of the sudden increase of the absorption coefficient.

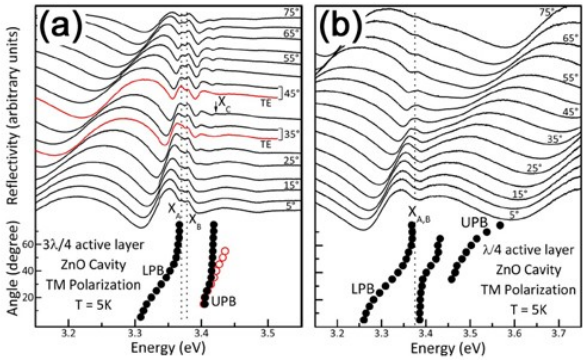

Fig. 2: Angle-dependent reflectivity of ZnO-based cavities of thickness λ (a) and λ/2 (b).

For achieving polariton lasing, or Bose-Einstein condensation, polaritons need to relax to the bottom of the LPB. However, to achieve this we must on the one hand overcome the "relaxation bottleneck" observable in both kind of cavities [76] (Fig. 3), and on the other hand we must increase the polaritons lifetime to allow them to condensate. The first problem was solved by increasing the temperature and the excitation intensity, thereby enhancing polariton relaxation towards k=0 via phonon-assisted and polariton-polariton interactions, respectively. The second problem arises from the photonic component of polaritons, which results in typical polariton lifetimes of some ps. This effect is particularly important in our cavities, which typically show Qs smaller than 200. To overcome this limitation and observe nonlinearities in the cavity emission the absolute reflectivity of both mirrors must be increased, which we currently try to achieve by using a fully-hybrid approach, with two dielectric DBRs, or by using different microcavity geometries (disks and wires).

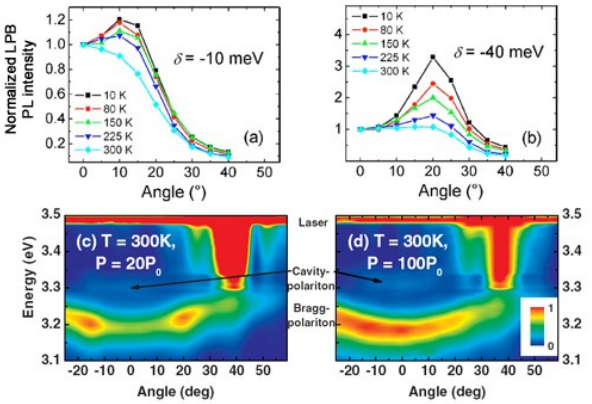

Fig. 3: Normalized PL intensity of the LPB in a GaN cavity at two detunings: (a) -10meV and (b) -40meV. Angle-resolved PL spectra of a ZnO cavity for two excitation intensities: (c) and (d).

H13: GaN Nanophotonics on silicon

S. Chenot, M. Leroux, M.J. Rashid, F. Semond, S. Sergent

By using (Al,Ga)N layers grown on silicon substrates, we fabricated free-standing photonic cavities operating in the UV. 2D photonic crystal cavities are realized by an original fabrication process and Q factors up to 350 are measured. AlN-based microdisk resonators containing GaN QDs exhibiting Q factors up to 6600 in the UV range are demonstrated.

Nitrides have become the dominant materials for short wavelength semiconductor light sources. However in order to expand their field of applications, device performances have still to be improved and their emission wavelength range needs to be extended and likely, new class of devices would be very welcome. One important step toward the demonstration of novel GaN-based optoelectronic devices is the ability to control the light emission by an increased coupling of the active material with optical modes. Much effort has already been done with other material systems using cavities such as photonic crystal (PC), micropillars or microdisks (μdisks). Thanks to their large quality factors (Q) and small modal volumes, it is possible to observe attractive phenomena such as the Purcell effect, strong coupling and low-threshold lasing. Thus, embedding III-N active layers into such cavities could lead to novel devices emitting in the UV operating up to RT. However, because of the chemical inertness of III-N materials, the realization of free-standing membrane photonic structures remains difficult.

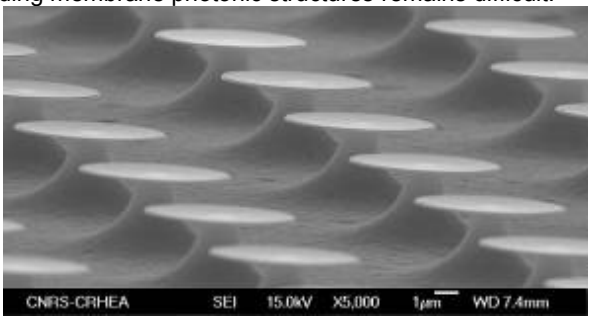

Fig.1: AlN microdisks standing up on silicon posts.

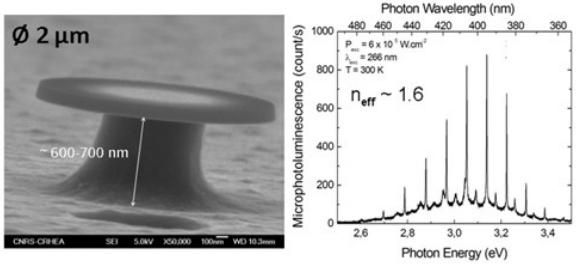

Fig.2: μPL spectrum at RT of a 2 μm diameter AlN μdisk containing GaN QDs.

The originality of this work is the use of Si substrates to circumvent the inertness of III-N materials and ease the realization of free-standing cavities (Fig.1). The main drawback of this approach is that the optically active layers have to be grown close to the Si substrate (typically 50 nm above the hetero-interface where a large density of structural defects exist) in order to fabricate single mode operation devices. We demonstrated the possibility to obtain optically active GaN/(Al,Ga)N QD stacks in such thin epilayers (100-120 nm) grown on Si [112]. Indeed, despite the vicinity of the Si substrate interface, GaN QDs embedded in thin (Al,Ga)N layers exhibit PL up to RT. We then optimized the fabrication process of µdisk resonators [285]. Q factors up to 6600 are obtained at 390 nm which are the highest values ever reported in nitrides (Fig.2).

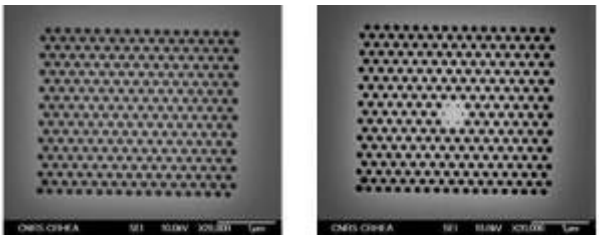

Fig.3: AlN photonic crystal membranes. Left, PC with no cavity mode (only slow velocity mode). Right, PC with a H1 modified cavity defect.

Photonic crystal membrane cavities are far more difficult to fabricate especially at the very short wavelengths we intend to reach. For this purpose, an original patented fabrication process is developed: a PC is first defined into a Si substrate, then the PC structure is transferred from the Si substrate to a nitride epilayer by conformal epitaxy, and the release of the PC membrane is finally realized by selective etching of Si (Fig.3). This innovative approach overcomes the difficulty associated with the etching of nitrides. So far slow group velocity and cavity modes with Q factors up to 350 have been measured (Fig.4).

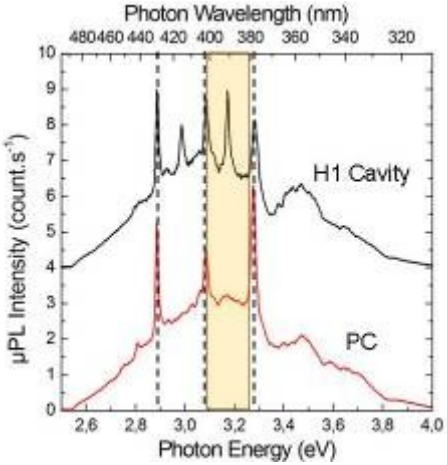

Fig.4: µPL spectra at RT of structures shown in Fig.3. The bandgap region of the PC is highlighted. Both, slow group velocity and cavity modes are observed.

This work allows to studying the coupling between GaN QDs and confined optical modes at short wavelengths. Building-blocks developed in this study pave the way to the demonstration of optically pumped UV low threshold micro-nanolasers integrated on silicon.

H14: Nitrides for micro-nano-resonators

Y. Cordier, J.C. Moreno, F. Semond

Using nitride-based layers grown on Si, suspended microstructures and resonators are fabricated. A bulk acoustic wave (BAW) resonator operating at 16 GHz is demonstrated using a thin (180 nm) AlN epitaxial layer. Mechanical resonators are fabricated and characterized. Combining the piezoelectric and semiconducting properties of nitrides, a fully integrated electromechanical resonator for actuation and detection of nanoscale motion is also demonstrated.

Nitrides exhibit interesting mechanical, chemical, physical and optical properties. Their use for filtering, sensing and actuating is attracting more attention but free-standing structures are usually needed for such applications. Epitaxy of nitrides on silicon substrates is obviously of great interest regarding the fabrication of suspended micro-nanostructures (Fig. 1).

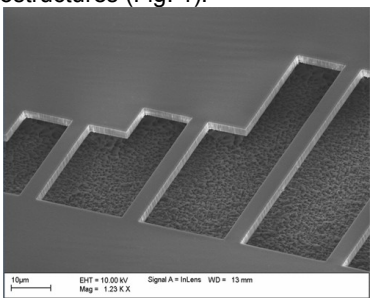

Fig.1: Suspended GaN/AlN bridges.

Highly textured sputtered AlN thick films (1-2 µm) are currently widely used as the piezoelectric material in the fabrication of all commercial bulk acoustic wave (BAW) filters for RF applications (2-4 GHz). In order to fabricate filters operating at much higher frequency (10-30 GHz) much thinner (100-200 nm) high quality AlN films are required. It turns out that sputtering could not laed to such thin high quality AlN films. In collaboration with STMicroelectronics and Leti, we have investigated the properties of very thin (100-200 nm) AlN epitaxial layers grown by MBE on Si to fabricate high operating frequency BAW devices. The sound velocity of acoustic waves (11500-12000 m/s) and the piezoelectric coefficient e31 (1 C/m2) are at least as good as or even better than those obtained for state of the art sputtered thick (1-2 µm) AlN films. A very first BAW structure using a thin (180 nm) AlN films has been fabricated. Despite a rather low electromechanical coupling and a poor Q factor, indicating that the fabrication process still needs to be improved, a resonance frequency of 16 GHz has been achieved (Fig.2).

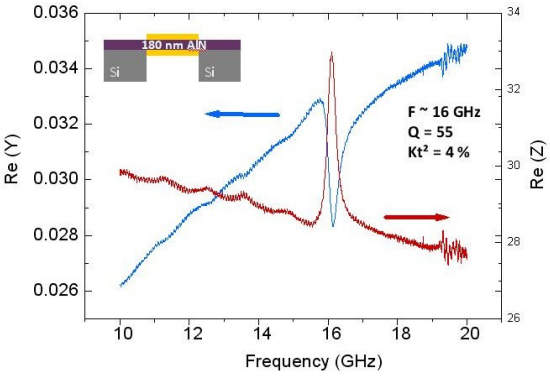

Fig.2: Resistance and conductance of a BAW fabricated from a 180 nm AlN films.

AlN is also interesting regarding the fabrication of highly sensitive mechanical devices. In collaboration with the CNM (Barcelona), AlN-based cantilevers have been fabricated and resonance frequencies have been measured (Fig.3) [58,267]. The Young's modulus value has been evaluated to 279 GPa. Interestingly, the high tensile stress measured in bridge structures would be advantageous to increase the resonance frequency and the quality factor of resonators.

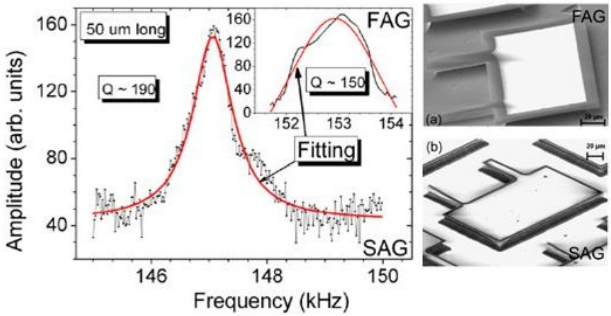

Fig.3: 50 µm long AlN cantilevers fabricated by 2 approaches and measured resonant frequencies.

Combining their outstanding properties (mechanical, piezoelectric, semiconducting) and the possibilities of epitaxial growth of complex heterostructures, nitrides offer many routes for the implementation of new functionalities. As an example, a fully integrated electromechanical resonator for actuation and detection of nanoscale motion has been fabricated at IEMN [116].

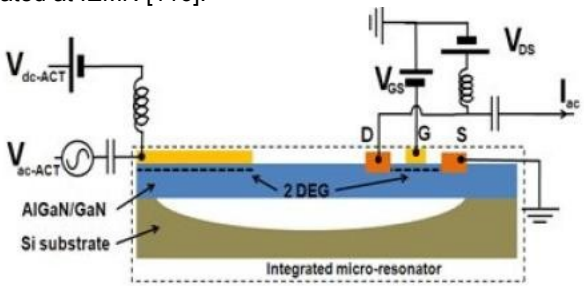

Fig.4: Schematic of the GaN microresonator showing the measurement setup.

Starting from an AlGaN/GaN heterostructure grown on Si, a suspended bridge microstructure is fabricated (Fig. 4). Actuation is provided by a Schottky diode and the 2DEG as a bottom electrode that allows using the d31 coefficient of the AlGaN barrier for the excitation of vibration modes. Detection of strain variation is provided by a resonant high-electron-mobility transistor. In this device, we take advantage of the polarization field divergence originated by mechanical flexural modes for generating piezoelectric doping. This enables a modulation of the carrier density which results in a large current flow and thus constitutes a motion detector with intrinsic amplification.

H15: Growth and characterization of GaN nanowires

B. Alloing, E. Beraudo, S. Chenot, M. Leroux, J. Massies, M. Nemoz, O. Tottereau, P. Vennéguès, S. Vézian, J. Zuniga-Perez

The growth of epitaxial GaN nanowires has been achieved by ammonia-assisted MBE and MOVPE on sapphire and silicon substrates. Their structural and optical properties have been characterized and, in particular, their polarity has been determined and their strain-free condition confirmed.

Compared to continuous layers, nanowires (NWs) offer the advantage of being dislocation-free even for heteroepitaxial growth on large lattice-mismatch substrates due to an efficient strain-relaxation via lateral free surfaces. This is especially important for materials such as GaN, which is most often grown on highly mismatched substrates (silicon carbide, sapphire or silicon).

We achieved for the first time the growth of GaN NWs by molecular beam epitaxy using ammonia as a nitrogen precursor (ammonia-MBE), instead of classically using plasma-assisted MBE method. Preliminary STM-RHEED studies of the AlN nucleation on Si(111) allowed us to obtain a selective GaN growth on AlN clusters and formation of NWs with vertical facets on silicon [43]. Similarly, as shown in Fig. 1, GaN NWs could also be grown on Al_2O_3(0001) substrates by ammonia-MBE. The main difference between the NWs grown on these substrates is their polarity: whereas on Al_2O_3(0001) GaN NWs are mostly N-polar and systematically present inversion domains, on Si(111) substrates the GaN NWs are Ga-polar and show no inversion domains. Both results are consistent with the growth conditions employed during the nucleation stage, which allow for the coexistence of both polarities on Al_2O_3(0001) and guarantee the nucleation of a single (metal) polarity on Si(111). Low-temperature photoluminescence measurements on NWs ensembles reveal the high optical quality of the nanostructures, with a PL linewidth of 4meV, and confirm the completely relaxed strain state that is commonly assumed [167b].

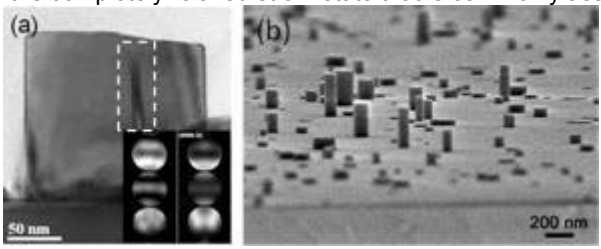

Fig. 1: GaN NWs grown on Al_2O_3 (0001) with ammonia-MBE: (a) TEM image in bright field. Inset: CBED patterns (experimental, left, and simulated, right) establishing the absolute N-polarity of the nanowires. The dashed rectangle surrounds an inversion domain of Ga-polarity. (b) SEM pictures of GaN NWs.

GaN NWs and microwires, with diameters ranging from some hundreds of nanometers to several micrometers, were also grown on sapphire substrates by metal organic vapor phase epitaxy (MOVPE). The Vapor-Liquid-Solid approach, with Ni as metal catalyst, was first investigated and NWs growing along the nonpolar <10-10> axis could be obtained. However, the nanowires grew randomly on the substrates surface.

Thus, we abandoned the VLS approach and concentrated on catalyst-free growth. Upon optimization of the growth conditions, we could achieve epitaxial

GaN NWs on Al_2O_3(0001) without any catalyst or dielectric mask, as well as AlN/GaN heterostructures. In this case, SiH_4 was required during the initial growth stage to promote a preferential growth along the <0001> axis. Fig. 2(a) shows a typical SEM picture of a single GaN microwire grown by catalyst-free MOVPE. Moreover, a very good spatial selectivity could be achieved using a dielectric mask with both MOVPE (Fig. 2b) and MBE (not shown). Interestingly, the MOVPE-grown wires showed always a mixture of N- and Ga-polarity [B. Alloing, submitted 2010].

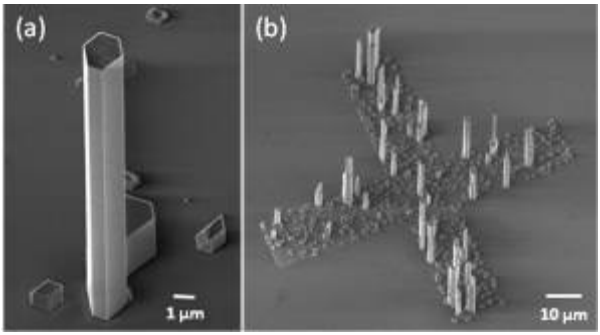

Fig.2: SEM pictures of GaN NWs grown with catalyst-free MOVPE (a) on Al_2O_3(0001), (b) on patterned Al_2O_3(0001) substrate with a SiO_2 mask.

Due to their single-crystalline and strain-free nature, GaN NWs are used as seeds for the growth of high-quality GaN templates within the European project SMASH, whose goal is to obtain high performance LEDs. We have achieved (Fig. 3(a)) the coalescence of GaN NWs grown by plasma assisted MBE in UPM (Spain) and the subsequent growth of a continuous GaN template. In parallel, on patterned *c*-plane Al_2O_3(0001) substrates, we carried out the whole process (growth of NWs+coalescence) (Fig 3(b)).

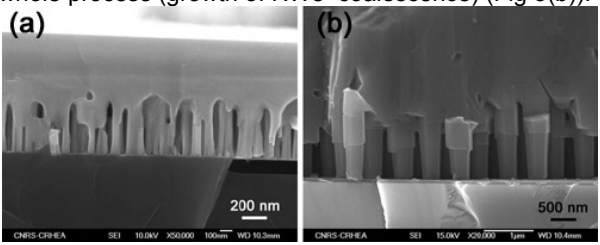

Fig. 3: (a) GaN layer grown by MOVPE at CRHEA on GaN NWs grown by plasma MBE at UPM on Silicon; (b) GaN NWs and coalesced layer grown with MOVPE on (0001) Al_2O_3.

Finally, and thanks to a home-made microPL setup, whispering gallery modes (WGMs) could be observed on single GaN MOVPE-grown wires. Furthermore, in collaboration with the Institut Néel we could observe for the first time the strong coupling regime at 300K between WGMs and excitons in GaN wires. These results are very promising for using GaN wires as high-quality optical microcavities.

H16: Intrinsic properties of (Zn,Co)O magnetic alloys

C. Deparis, C. Morhain, B. Vinter

Progress in spintronics requires the development of active-type spin devices that can strongly polarize, transport, detect and manipulate spins. The ideal would be a ferromagnetic semiconductor. ZnO-based diluted semiconductors (DMS) have attracted a great deal of research attention over the past decade, sparked by predictions of above room-temperature ferromagnetism in transition metal (TM)-doped ZnO. In this context, we have optimized the growth of (Zn,Co)O films by MBE, explored their properties and clarified the nature of the magnetic coupling in this DMS.

The predictions by Dietl et al. and Sato et al. in 2001, based on two different types of calculations, the mean-field model and LSDA respectively, that $Zn_{1-x}TM_xO$ alloys could produce above room-temperature ferromagnetic semiconductors have been at the origin of a surge of reports of ferromagnetism in $Zn_{1-x}TM_xO$ thin films. However, reported values of magnetic moments and Curie temperature are inconsistent, which leads to controversy over the origin of the observed magnetism. A considerable debate has been ongoing whether the observed ferromagnetism was an intrinsic property of the material, the result of the formation of secondary magnetic phases, or was controlled by an interaction between the magnetic ions and the free carriers (electrons or holes) or native defects (vacancies, and other defect centres).

In this context, our efforts have been focused on mastering the growth of $Zn_{1-x}TM_xO$ epilayers by MBE, controlling in-situ their conductivity and doping levels that should be tunable over several orders of magnitude, clarifying and understanding the magnetic coupling of magnetic ions in ZnO using appropriate spectroscopies.

The work has mostly been focused on ZnCoO alloys, as the incorporation of Co had been predicted to be the most promising in early ab-initio calculations: (i) undoped material should be ferromagnetic with a high Curie temperature (ii) the Curie temperature could be further increased by doping the material n-type.

Optimization of the MBE growth

An important work has been devoted to the optimization of the growth conditions of the ZnCoO alloys, that was observed to differ considerably from the growth conditions used for ZnO epilayers, as shown in Fig. 1.

The marked improvement in the morphology of the thin films correlates with a strong improvement in their crystalline quality (no twinning or texturation and reduced in-plane twist), while the growth becomes 2D (RHEED) and the rms roughness is drastically reduced to values in the range of 1nm (AFM). Series of samples with Co contents ranging from very diluted (0.01%) to highly alloyed (35%) have been grown. The doping level was tuned from $n\sim10^{17}cm^{-3}$ to $4x10^{20}cm^{-3}$ using Ga as a dopant during the growth for many x_{Co} in order to investigate the influence of free electrons on the magnetic ordering.

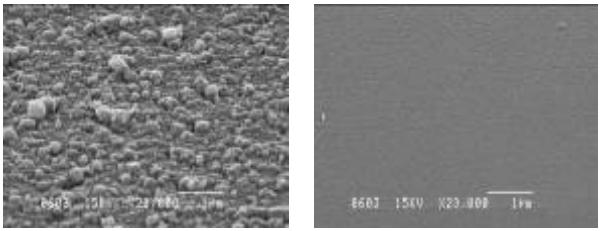

Fig.1: SEM pictures of the surface of a $Zn_{0.9}Co_{0.1}O$ grown on sapphire substrates in standard ZnO growth conditions (left) and optimized growth conditions (right).

Spectroscopy of isolated Co

For low x_{Co}(<5%), detailed EPR and magneto-optical spectroscopies of the transitions related to the Co ions, indicate that all isolated ions are substituting the Zn atoms (2006) in films with optimized growth. The g factor is not dependent on the Co content, a behavior characteristic of paramagnetic materials.

Furthermore, the measurements also reveal that isolated Co^{2+} ions in ZnO possess a strong single ion anisotropy which leads to an "easy plane" ferromagnetic state when the ferromagnetic Co-Co interaction is considered. We suggest that this anisotropy can be viewed as a signature of intrinsic ferromagnetism in (Zn,Co)O materials [13]. As this anisotropy has not been observed by any group, we conclude that an intrinsic ferromagnetic DMS at room temperature has not yet been obtained, despite many claims. Interestingly, anisotropy was also found in our ZnMnO films [106].

The near band edge spectroscopy reveals a giant Zeeman splitting that confirms the spin-carrier coupling of paramagnetic type, in ZnCoO. However, the exchange integrals that are derived are very different from those expected by Dietl et al. This demonstrates that the mean-field theory used to describe ferromagnetism in GaAs and ZnTe-based DMS, is no longer valid in ZnO [12].

Co-Co interactions

For x_{Co} >3%, Co-Co interactions take place, that are shown to be anti-ferromagnetic from magnetization measurements (SQUID)[45]. Moreover, we found (Fig.2) that n-type doping has no influence on the magnetization ordering contrary to early LSDA predictions.

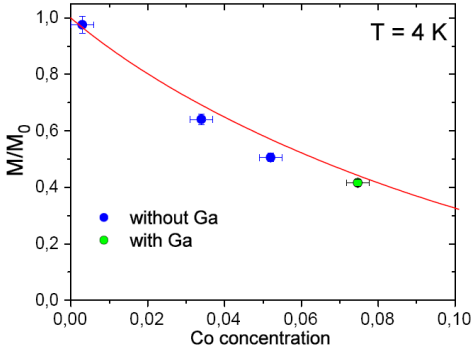

Fig.2: Magnetization of undoped (●) and degenerate (●) ZnCoO epilayers. The curve corresponds to calculations (LSDA+U) for anti-ferromagnetic.

H17: Nonpolar (Zn,Mg)O/ZnO heterostructures

J.-M. Chauveau, C. Deparis, C. Morhain, M. Teisseire, B. Vinter

We develop the epitaxy of ZnO/(Zn,Mg)O heterostructures along different crystallographic orientations. We study the influence of anisotropic residual strain on the optical properties of nonpolar quantum wells.

In 2005, the OXTRO group gave clear evidence of the presence of large internal electric fields in (Zn,Mg)O/ZnO heterostructures grown along the *c* axis (Coll. GES) [C. Morhain et *al*., Phys. Rev . B **72**, 241305 (2005); 57]. Nonpolar surfaces are of a particular interest since the *c*-axis of the layer lies in the growth plane in this case. As a result it is expected that (Zn,Mg)O/ZnO quantum well structures (QW) can be grown without any field effect on the exciton energies. Our strategy was therefore to develop and optimize the growth of nonpolar ZnO and its related alloys on sapphire (see H16). Based on this know-how, we were able to fabricate for the first time nonpolar QWs with different widths and different Mg content, and demonstrated the absence of Quantum Confined Stark Effect [199].

However, a strong anisotropy of the initial strain is observed due to the differences of the crystallographic structures between ZnO and Sapphire. In addition we have demonstrated that the relaxation process was also anisotropic [69]. As a result, we have shown that the in-plane lattice parameters of the (Zn,Mg)O barriers exhibited a very unusual and anisotropic behavior (Fig. 1).

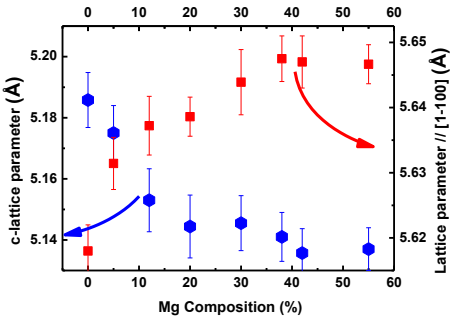

Fig.1: Evolution of the in-plane lattice parameters of (Zn,Mg)O layers as a function of the Mg content.

Then we have studied the effects of this anisotropic strain state on the luminescence emission from QW. Therefore we have calculated the bulk exciton energies and polarizations of strained ZnO [66]. In Fig. 2 we show the calculated A-exciton energy as a function of the strain components. Experimentally, we have checked the validity of our calculations by comparing the positions of A-exciton in bulk *a*-ZnO substrate and in *a*-ZnO grown on Sapphire (Fig.3). The UV-shift observed in *a*-ZnO grown on sapphire was fully explained by the strain measured in X-ray. The huge anisotropy in the (Zn,Mg)O barrier (Fig.1) induces an unusual strain state in the ZnO QW (both in-plane tensile and compressive strains). We found that A-exciton energy was 3.41 eV for ZnO strained under this experimental condition (red star in Fig. 2).

In order to avoid the influence of localization effects, photoluminescence excitation (PLE) have been performed on the series of QWs. Figure 4 displays the observed PLE energies of the lowest energy exciton as a function of the QW width. It shows the

absence of Quantum Confined Stark Effect in nonpolar QWs because the QW emission is still above the ZnO bulk position even for wide QWs.

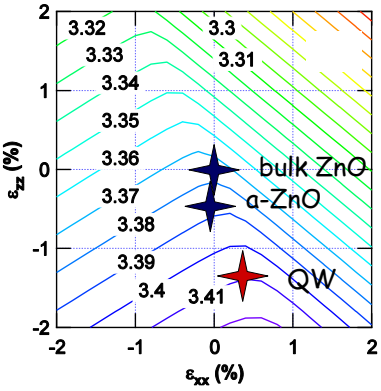

Fig.3: Reflectivity spectra recorded at 2K with linear polarization set perpendicular to the c-axis of the epilayer and the ZnO substrate.

Fig.2: Calculated lowest bulk exciton energy (eV) of ZnO as a function of in-plane strain components.

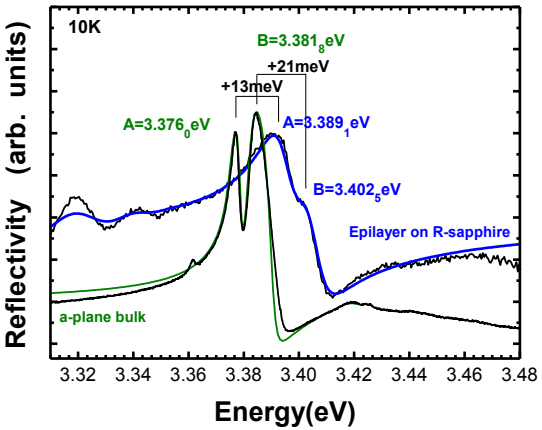

The PLE energies of the QWs were satisfactorily simulated when taking into account the variation of the exciton binding energy with the QW width and the anisotropic strain state (Fig. 4). The main limitation of QWs is the large density of structural defects (H20). We show a drastic improvement of structural and optical properties by using ZnO substrates (see H18).

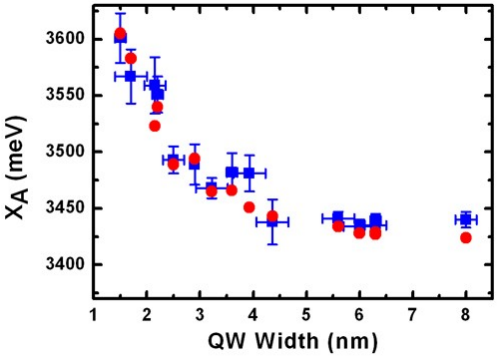

Fig.4: Ground state energies (PLE) from a series of QWs. Calculated transitions corrected by the exciton binding energy and the anisotropic strain (circles).

H18: Heteroepitaxy and Homoepitaxy of ZnO and related alloys

J.-M. Chauveau, C. Deparis, H. Kim-Chauveau, C. Morhain, M. Teisseire, D. Taïnoff, B. Vinter

We develop the epitaxy of ZnO and its related alloys on different substrates. We demonstrate some benefits of homoepitaxy on the properties of nonpolar (Zn,Mg)O/ZnO quantum wells on a-plane ZnO substrates

Controlling the structural quality of ZnO-based alloys is a prerequisite for all the applications that require heterostructures such as light emitting devices, high electron mobility transistors, microcavities, spin injection, … Unfortunately ZnO based alloys -(ZnCo)O, (Zn,Mn)O, (Zn,Mg,Cd)O,…- are not stable thermodynamically and exhibit strong composition fluctuations up to phase separation. Our strategy is to use molecular beam epitaxy to push the limit of the phase transition in order to provide a large range of band gap engineering.

A significant progress has been demonstrated in the control of (Zn,Co)O or (Zn,Mn)O alloys along polar orientations (see H16). We also have studied the effect of Co incorporation on surface morphology in nonpolar orientations [200] and used (Zn,Co)O and (Zn,Mn)O alloys as buffer layers on sapphire to successfully grow quantum wells (QWs) [71].

In order to grow QWs it is very important to precisely control the Mg content as well as the quality of the (Zn,Mg)O alloy as a confinement barrier. In 2005, the phase transition of (Zn,Mg)O (wurtzite to cubic) was expected to be below 30% of Mg. After a precise optimization of our growth conditions along different crystallographic orientations, we have demonstrated the possibility to grow single phase (Zn,Mg)O up to ~ 60% Mg [71,66] which allows to tune the emission energy on a much wider range (Fig.1).

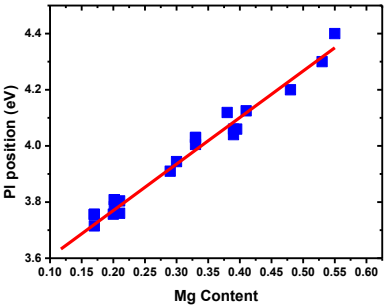

Fig.1: PL emission (eV) of single phase wurtzite (Zn,Mg)O as a function of the Mg content.

Polar and nonpolar ZnO and GaN layers exhibit large densities of dislocations and stacking faults when they are grown on sapphire (see H19). From this viewpoint, ZnO offers a unique opportunity in the field of wurtzite wide band gap semiconductors. Indeed ZnO substrates are commercially available. Therefore, the OXTRO group has started to develop the homoepitaxial growth in 2009 from the preparation of the ZnO substrate surface to the growth of heterostructure and doping (*coll*. CEA-LETI, RIBER, Novasic). Recently, we have demonstrated huge improvements of the structural and optical

properties when the QWs are grown on ZnO substrates. For instance X-Ray full width at half maximum (FWHM) and surface roughness were strongly reduced (Fig. 2) [142].

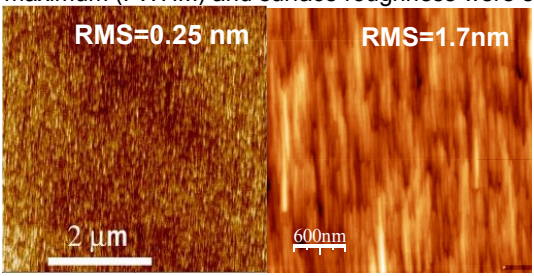

Fig.2: Surface morphologies from homoepitaxial (left) and heteroepitaxial (right) nonpolar (Zn,Mg)O/ZnO QW

The high resolution transmission electron microscopy images exhibit smooth interfaces between the (Zn,Mg)O barriers and the QW, without extended defects (Fig. 3).

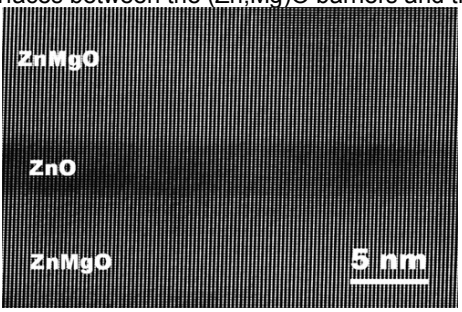

Fig.3: High resolution TEM image of a nonpolar QW

The drastic improvement of the structural properties leads to a strong enhancement of the photo-luminescence (PL) properties, especially along nonpolar orientations. The QW emission can be as narrow as 3.5 meV at 8K for QWs larger than 4nm. Their intensity is about 50 times stronger than that of QWs grown on sapphire (Fig.4). It is also remarkable that the room temperature PL emission of nonpolar homoepitaxial QWs is still one order of magnitude more intense than that of the nonpolar heteroepitaxial QW taken at low temperature [142]. Our work clearly demonstrates the benifits of homoepitaxial ZnO quantum well structures for bright UV emitters.

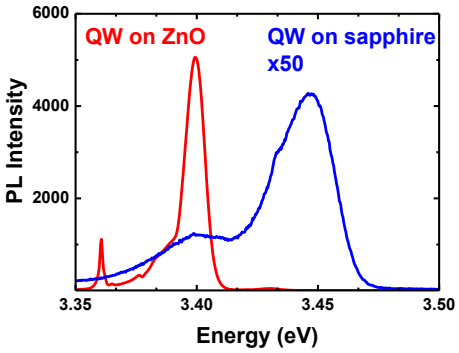

Fig.4: Comparison between PL spectra from homoepitaxial and heteroepitaxial QWs (3.5 nm).

H19: Quantitative TEM of GaN/($Al_{0.5}$,$Ga_{0.5}$)N quantum dots

J. Brault, T. Huault, M. Korytov, O. Tottereau, P. Vennégues

Local lattice strain measurement by high resolution transmission electron microscopy (HRTEM) has been implemented to study GaN/(Al0.5Ga0.5)N quantum dots grown by molecular beam epitaxy (MBE). The observed phase separation mechanism in the AlGaN barrier has been quantitatively analyzed.

The active parts of III-Nitrides optoelectronics devices contain, most of the time, nanometric size objects (quantum wells or quantum dots). HRTEM is therefore the tool of choice to study their structure. We adapted the technique of local strain measurement in HRTEM images to the wurztite structure of III-Nitrides and used it to analyze GaN/($Al_{0.5}Ga_{0.5}$)N quantum dots (QDs) grown by MBE (see H7). The imaging conditions for reliable measurement of strain distributions around these 3D-nanostructures in both the in- and out-of plane directions have been determined thanks to HRTEM image simulations. The out-of-plane strain can be determined with the JEOL2010F installed at CRHEA using two-beam imaging off-axis conditions whereas the in-plane strain measurement requires the use of up-to-date microscopes equipped with a corrector of spherical aberrations. Thanks to the METPACA and METSA networks, we had access to such a microscope (Titan 80-300, CP2M, Marseille).

Both surface and buried QDs have been studied. Different characteristic phenomena original for nitride semiconductors have been observed:

- A shape transition of surface QDs from perfect to truncated pyramids with an increase of the deposited GaN thickness.
- A shape transition between surface and buried QDs, with buried QDs being always truncated pyramids.
- An increase of the QD volume due to the QD capping.
- A phase separation mechanism in the AlGaN barriers covering QDs.

The phase separation phenomenon has been studied in details by HRTEM [101,124]. In Fig. 1, the QDs are not visible in the in-plane strain map (b) indicating that all the structure adopts the in-plane lattice parameter of the ($Al_{0.5}Ga_{0.5}$)N template. On the other hand, zones of different contrast are observed in the out-of-plane strain map (c): the QDs (appearing in red), Al-rich zones in ($Al_{0.5}Ga_{0.5}$)N above the QDs (in green) and Ga-rich zones between the QDs. Assuming a biaxial strain the chemical composition in the Al-rich regions is estimated to be about 70-75%. This value has been confirmed by electron energy loss spectrometry (EELS) (M. Benaissa, CNRST-Rabat, experiments performed in Stuttgart, Germany).

To understand the mechanism of phase separation, we studied a set of samples at different stages of QD covering with ($Al_{0.5}Ga_{0.5}$)N. To discriminate between strain and chemical contrast, this study has been conducted using scanning transmission electron microscopy in high angle annular dark field mode (STEM-HAADF) (INAC Grenoble and CP2M Marseille). ($Al_{0.5}Ga_{0.5}$)N is first deposited on the wetting layer between the QDs

and then it gradually fills the space between them. The phase separation occurs as soon as $(Al_{0.5}Ga_{0.5})N$ grows on top of the QDs. We proposed a qualitative model based on the elastic strains experienced by the covering $(Al_{0.5}Ga_{0.5})N$, which takes into account both the in- and out-of-plane mismatches with the GaN 3D-QDs.

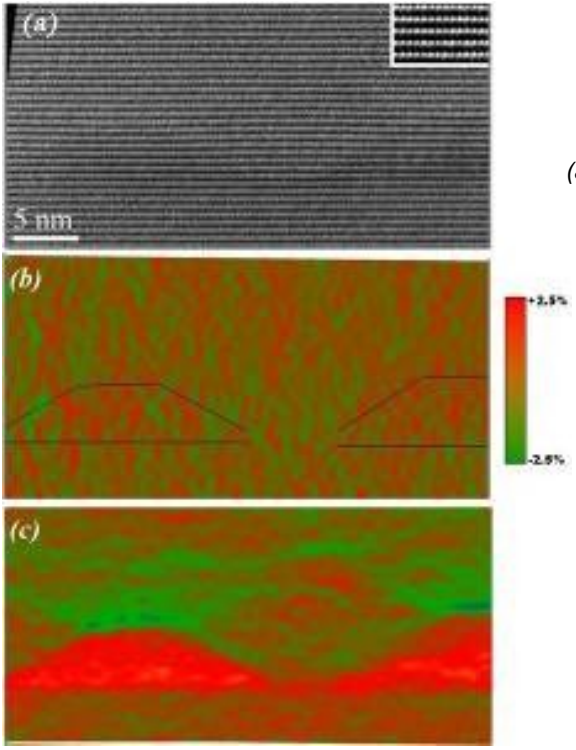

Fig.1:
(a) *HRTEM image of buried QDs along the [1-100] zone axis acquired on the FEI Titan 80-300 Cs-corrected microscope. The inset shows a zoom.*
(a)(b) Out-of-plane strain.
(c) In-plane strain. The position of the left QD is shown.
The reference lattice parameters are chosen in the $(Al_{0.5}Ga_{0.5})N$ template.

This model has been compared to elastic calculations (J. Budagoski, Université de Valence). The calculated strains are in good agreement with our simple model but, on the other hand, the configuration with a homogeneous $(Al_{0.5}Ga_{0.5})N$ barrier has a lower elastic energy than an $(Al_{0.5}Ga_{0.5})N$ barrier with a phase separation which indicates that the surface energies have also to be taken into account in the calculations.

The detailed study of these nanometric scale characteristics phenomena in GaN/$(Al_{0.5}Ga_{0.5})N$ structures have been made possible thanks to quantitative HRTEM measurement. This demonstrates that, when properly adapted to the studied materials (structure, geometry…), such a technique, in conjunction with other TEM-based methods (EELS, STEM-HAADF, …) provides invaluable structural information on the active layers of optoelectronic devices.

H20: Microstructure of non and semipolar wurtzite heteroepitaxial films

J. Brault, J.M. Chauveau, R. Chmielowski, T. Gühne, N. Kriouche, P. De Mierry, O. Tottereau, P. Vennégues

Heteroepitaxial non and semipolar wurzite films contain numerous extended defects. TEM allows us to study in details the epitaxial relationships, the nature and origin of the structural defects and to evaluate the processes used to improve the crystalline quality.

In order to avoid or to decrease the influence of internal electric fields on the properties of heterostructures, the growth of wurtzite semiconductors (III-Nitrides and ZnO-based alloys) along non and semipolar orientations is nowadays explored (H5 and H17). The heteroepitaxy on foreign substrates leads to the formation of numerous extended defects. The study of their microstructure especially by transmission electron microscopy (TEM) is therefore of primary importance. Heteroepitaxial films grown on different types of substrates (AlN and GaN on 6H-SiC [156], ZnO and GaN on R-sapphire [67] and ZnO and GaN on M-sapphire [103]) have been investigated. The epitaxial relationships have been determined and explained in terms of interfacial structure. The focus has been put on the orientation of the polar c-axis obtained using convergent beam electron diffraction (CBED): on R-plane sapphire, the films are unipolar whereas regions of opposite polarities (inversion domains) are present in the films epitaxied on M-sapphire (figure 1). This behavior is explained by the difference of surface symmetries between the sapphire R- and M-surfaces, the presence of an inversion center on the M-surface explaining the equivalent probability for both in-plane polarities [103].

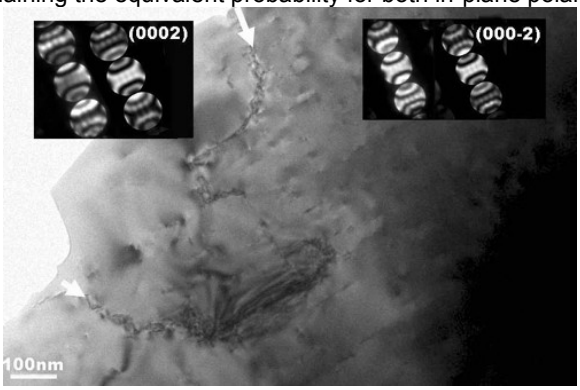

Fig. 1: Plan-view image of a nonpolar GaN film deposited on M-Sapphire. The comparison of simulated and experimental CBED patterns allows to evidence the presence of inversion domains [2].

The nature and origin of the extended defects present in the films have been determined. The dominant defects are basal stacking faults (BSF) with their associated defects (partial dislocations and prismatic stacking faults). On sapphire substrates, for both nonpolar and semipolar orientations and for GaN and ZnO-based materials, the BSF

are of I_1 type, corresponding to the introduction of one cubic stacking in the hexagonal wurtzite structure. The ensemble BSF+partial dislocations may correspond to dissociated *a* or *a+c* perfect dislocations as shown on the Burger circuit drawn around a BSF (fig. 2).

The density of extended defects in heteroepitaxial films is too high to allow the fabrication of efficient devices. Thanks to the availability of good quality nonpolar ZnO substrates, efforts for this material are now put on the development of homoepitaxy (H17). On the other hand, GaN nonpolar substrates being still of very small size, different strategies have been developed in CRHEA in order to increase the crystalline quality of III-Nitrides heteroepitaxial films, as the use of a better adapted substrate (ZnO) or the epitaxial lateral overgrowth method (ELO), method which proves its efficiency for polar c-oriented heterostructures. The AS-ELO, described in H5, consists in overgrowing a highly defective seed layer by a good quality crystal expanding laterally. The cross-section dark field images shown in figure 3 demonstrate that both the partial dislocations (visible in both dark field images) and the BSF (only visible in the g = {10-10} dark field image) are blocked in the coalescence boundary resulting in films with a drastically improved crystalline quality [138].

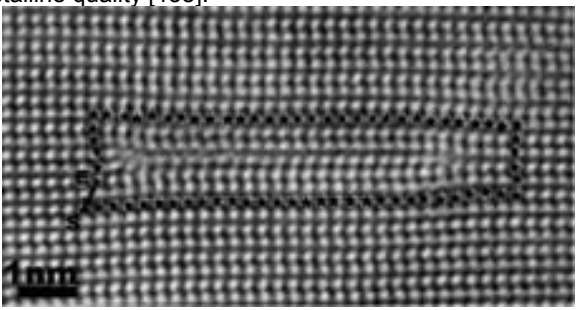

Fig. 2: High resolution TEM image of a I_1 BSF in a nonpolar ZnO film deposited on R-sapphire [3].

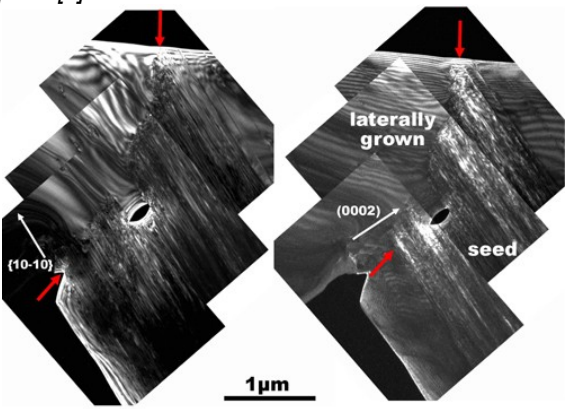

Fig. 3: Cross-section dark field images of a coalescence boundary in a semipolar GaN AS-ELO film. The position of the curved coalescence boundary is shown by the red arrows.

Scientific production of the laboratory

Regular papers

2006

1. Comparison of carrier dynamics in GaN quantum dots and GaN quantum wells embedded in low-Al-content AlGaN waveguides
Y.H. Cho, H. S. Kwack, B. J. Kwon, J. Barjon, J. Brault, B. Daudin, Le Si Dang
Appl. Phys. Lett. 89 (2006) 251914

2. Photoluminescence of single GaN/AlN quantum dots on Si(111): spectral diffusion effects
R. Bardoux, T. Guillet, P. Lefebvre, T. Taliercio, T. Bretagnon, S. Rousset, B. Gil, F. Semond
Phys. Rev. B 74 (2006) 195319

3. High temperature pulsed measurements of AlGaN/GaN HEMTs on high resistive Si(111) substrate
M. Werquin, D. Ducatteau, N. Vellas, E. Delos, Y. Cordier, R. Aubry, and C. Gaquiere
Microwave and Optical Technology Letters 48, No. 11 (2006) 2303-2305

4. Role of elastic scattering mechanisms in GaInAs/AlInAs quantum cascade lasers
A. Vasanelli, A. Leuliet, C. Sirtori, A. Wade, G. Fedorov, D. Smirnov, G. Bastard, B. Vinter, M. Giovannini, and J. Faist
Appl. Phys. Lett. 89 (17) (2006) 172120-3

5. Generation-recombination reduction in InAsSb photodiodes
M. Carras, C. Renard, X. Marcadet, J. L. Reverchon, B. Vinter, and V. Berger
Semicond. Sci. Tech. 21 (12) (2006) 1720-3

6. Crack-free highly reflective AlInN/AlGaN Bragg mirrors for UV applications
E. Feltin, J.-F. Carlin, J. Dorsaz, G. Christmann, R. Butté, M. Laügt, M. Ilegems, and N. Grandjean
Appl. Phys. Lett. 88 (2006) 051108

7. Strain Tailoring in 3C-SiC Heteroepitaxial Layers Grown on Si(100)
G. Ferro, T. Chassagne, A. Leycuras, F. Cauwet, Y. Monteil
Chem. Vap. Deposition 12 (2006) 483–488

8. Application of LTPL Investigation Methods to CVD-Grown SiC
J. Camassel, S. Juillaguet, M. Zielinski, C. Balloud
Chem. Vap. Deposition 12 (2006) 549–556

9. Stress relaxation during the growth of 3C-SiC/Si thin films
M. Zielinski, A. Leycuras, S. Ndiaye, T. Chassagne
Appl. Phys. Lett. 89 (2006) 131906

10. Epitaxial orientation of III-Nitrides grown on R-plane sapphire by metalorganic-vapor-phase-epitaxy
P. Vennéguès and Z. Bougrioua
Appl. Phys. Lett. 89 (2006) 111915

11. Optical monitoring of nonequilibrium carrier lifetime in freestanding GaN by time-resolved four-wave mixing and photoluminescence techniques
T. Malinauskas, K. Jarasiunas, S. Miasojedovas, S. Jursenas, B. Beaumont, P. Gibart
Appl. Phys. Lett. 88 (2006) 202109

12. Effect of the s,p-d exchange interaction on the excitons in $Zn_{1-x}Co_xO$ epilayers
W. Pacuski, D. Ferrand, J. Cibert, C. Deparis, J. A. Gaj, P. Kossacki, and C. Morhain
Phys. Rev. B 73 (3) (2006) 035214-13

13. Magnetic Anisotropy of Co^{2+} as Signature of Intrinsic Ferromagnetism in ZnO:Co
P. Sati , R. Hayn, R. Kuzian, S. Regnier, S. Schafer, A. Stepanov, C. Morhain, C. Deparis, M. Laügt, M. Goiran, , Z. Golacki
Phys. Rev. Lett. 96 (2006) 017203-4

14. An AlGaN Based Linear Array for UV Solar Blind Imaging from 240 nm to 280 nm
G. Mazzeo, J.L. Reverchon, J.-Y. Duboz, A. Dussaigne
IEEE Sensors Journal 6(4) (2006) 957-63

15. Strong coupling of light with A and B excitons in GaN microcavities on silicon
I.R.Sellers, F. Semond, M. Leroux, J. Massies, P. Disseix, A-L. Henneghien, J. Leymarie and A. Vasson
Phys. Rev. B 73 (2006) 033304

16. Characterization of high-k Ta_2/Si oxidized films on 4H-SiC and Si substrates as gate insulator
A. Pérez-Tomas, P. Godignon, J. Montserrat, J. Millan, N. Mestres, P. Vennéguès and J. Stoemenos
J. Electrochem. Soc. 152(4) (2006) G259-65

17. Solar blind AlGaN photodetectors with a very high spectral selectivity
J.-Y. Duboz , N. Grandjean, A. Dussaigne,M. Mosca, J.L. Reverchon,P.G. Verly, R. H. Simpson
Eur. Phys. J. Appl. Phys. 33 (2006) 5

18. Long wavelength emitting InAs/$Ga_{0.85}In_{0.15}$Nas Quantum Dots on GaAs substrate
M. Richter, B. Damilano, J.-Y. Duboz, J. Massies, A. Wieck
Appl. Phys. Lett. 88 (2006) 231902

19. Optimum indium composition for (Ga,In)'(N,As) /GaAs quantum wells emitting beyond 1.5µm
M. Hugues, B. Damilano, J.-Y. Duboz, and J. Massies
Appl. Phys. Lett. 88 (2006) 91111

20. AlGaN/GaN HEMTs on (001) silicon substrates
S. Joblot, Y. Cordier, F. Semond, P. Lorenzini, S. Chenot and J. Massies
Electron. Lett. 42 (2006) 117-118

21. Sensitivity of synchrotron radiation x-ray diffraction to the chemical ordering in epitaxial perovskite multilayers
M. Nemoz, E. Dooryhee, J.-L. Hodeau, C. Dubourdieu, H. Roussel, P. Bayle-Guillemaud
J. Appl. Phys 100 (2006) 124110

22. On the determination of the structural parameters of $Ga_xIn_{1-x}As/AlAs_ySb_{1-y}$ superlattices by X-ray diffraction
C. Renard, X. Marcadet, J. Massies
J. Cryst. Growth 297 (2006) 272

23. Polariton emission and reflectivity in GaN microcavities as a function of angle and temperature
I.R. Sellers, F. Semond, M. Leroux, J. Massies, M. Zamfirescu, F. Stokker-Cheregi, M. Gurioli, A. Vinattieri, M. Colocci, A. Tahraoui, and A.A. Khalifa
Phys. Rev. B 74 (2006) 193308

24. Fast, high-efficiency, and homogeneous room-temperature cathodoluminescence of ZnO scintillator thin films on sapphire
M. Lorenz, R. Johne, T. Nobis, H. Hochmuth, J. Lenzner, M. Grundmann, H.P.D. Schenk, S.I. Borenstain, A. Schön, C. Bekeny, T. Voss, and J. Gutowski
Appl. Phys. Lett. 89 (2006) 243510

25. Optoelectronic properties of GaN epilayers in the region of yellow luminescence
C. Grazzi, H.P. Strunk, A. Castaldini, A. Cavallini, H.P.D. Schenk, and P. Gibart
J. Appl. Phys 100 (2006) 073711

26. Growth and optical and structural characterizations of GaN on freestanding GaN substrates with an (Al,In)N insertion layer
K. Bejtka, R.W. Martin, I.M. Watson, S. Ndiaye, M. Leroux
Appl. Phys. Lett. 89 (2006) 191912

27. Properties of (InGa)As/GaAs QW (1200 nm) facet-coated edge-emitting diode laser
T. Gühne, V. Gottschalch, G. Leibiger, H. Herrnberger, J. Kovác, J. Kovác, Jr., R. Schmidt-Grund, B. Rheinländer, and D. Pudis
Laser Physics (2006) 441

28. Investigation of AlN films grown by molecular beam epitaxy on vicinal Si(111) as templates for GaN quantum dots
M. Benaissa,P. Vennéguès, O. Tottereau, L. Nguyen and F. Semond
Appl. Phys. Lett. 89 (2006) 231903

29. Spin-exchange interaction in ZnO-based quantum wells
B. Gil, P. Lefebvre, T. Bretagnon, T. Guillet, J. A. Sans, T. Taliercio, and C. Morhain
Phys. Rev. B, 74, 153302, (2006)

30. Growth of Ag thin films on ZnO(000-1) investigated by AES and STM
E. Duriau, S. Agouram, C. Morhain, T. Seldrum, R. Sporken, J. Dumont
App. Surf. Science, 253, 549, (2006)

2007

31. Low electron mobility of field-effect transistor determined by modulated magnetoresistance
R. Tauk, J. Lusakowski, W. Knap, A. Tiberj, Z. Bougrioua, M. Azize, P. Lorenzini, M. Sakowicz, K. Karpierz, C. Fenouillet-Beranger, M. Casse, C. Gallon, F. Boeuf, T. Skotnicki
J. Appl. Phys. 102 (2007) 103701

32. Photoinduced current transient spectroscopy of deep levels and transport mechanisms in iron-doped GaN thin films grown by low pressure-metalorganic vapor phase epitaxy
P. Muret, J. Pernot, M. Azize, Z. Bougrioua
J. Appl. Phys. 102 (2007) 053701

33. Optical determination of the effective wetting layer thickness and composition in InAs/Ga(In)As quantum dots
M. Hugues, M. Teisseire, J. M. Chauveau, B. Vinter, B. Damilano, J. Y. Duboz, and J. Massies
Phys. Rev. B 76 (7) (2007) 075335-6

34. Positron annihilation spectroscopy for the determination of thickness and defect profile in thin semiconductor layers
A. Zubiaga, J. A. García, F. Plazaola, F. Tuomisto, J. Zúñiga-Pérez, V. Muñoz-Sanjosé
Phys. Rev. B 75 (2007) 205305

35. Blue-shift mechanisms in annealed GaInNAs/GaAs quantum wells

M. Hugues, B. Damilano, J.-M. Chauveau, J.-Y. Duboz and J. Massies
Phys. Rev. B 75 (2007) 045313

36. Nanogoniometry with Scanning Force Microscopy: A Model Study of CdTe Thin Films
E. Palacios-Lidón, L. Guanter, J. Zúñiga-Pérez, V. Muñoz-Sanjosé, and J. Colchero
Small 3 (2007) 474

37. Radiative lifetime of a single electron-hole pair in GaN/AlN quantum dots
T. Bretagnon; P. Lefebvre; P. Valvin; R. Bardoux; T. Guillet; T. Taliercio; B. Gil-; N. Grandjean-; F. Semond; B. Damilano; A. Dussaigne; J. Massies
Phys. Rev. B 73(11) (2007) 113304-1-4

38. Microcrack-induced strain relief in GaN/AlN quantum dots grown on Si(111)
G. Sarusi, O. Moshe, S. Khatsevich, D. H. Rich, and B. Damilano
Phys. Rev. B 75 (2007) 075306

39. Investigation of Non-Radiative Processes in InAs/(Ga,In)(N,As) Quantum Dots
M. Hugues, M. Richter, J.-M. Chauveau, B. Damilano, J.-Y. Duboz, J. Massies, T. Taliercio, P. Lefebvre, T. Guillet, P. Valvin, T. Bretagnon, B. Gil, A. D. Wieck
Jpn. J. Appl. Phys 46, N14 (2007) L317-L319

40. Annealing effects on GaInNAs/GaAs quantum wells analyzed using thermally detected optical absorption and ten band k.p calculations
T. Bouragba, M. Mihailovic, F. Reveret, P. Disseix, J. Leymarie, and A. Vasson, B. Damilano, M. Hugues, J. Massies and J. Y. Duboz
J. Appl. Phys 101 (2007) 073510

41. Exciton dissociation and hole escape in the thermal photoluminescence quenching of (Ga,In)(N,As) quantum wells
M. Hugues, B. Damilano, J.-Y. Duboz, J. Massies
Phys. Rev. B 75 (2007) 115337

42. Ordered growth of tilted ZnO nanowires: morphological, structural and optical charcaterization
J. Zúñiga-Pérez, A. Rahm, C. Czekalla, J. Lenzner, M. Lorenz, M. Grundmann
Nanotechnology 18 (2007) 195303

43. Selective epitaxial growth of AlN and GaN nanostructures on Si(111) by using NH3 as nitrogen source
S. Vézian, A. Le Louarn and J. Massies
J. Cryst. Growth 303 (2007) 419

44. Energy levels and intersubband transitions in InGaAsN/AlGaAs quantum wells
J.-Y. Duboz
Phys. Rev. B 75 (2007) 045327

45. Antiferromagnetic Interactions in Single Crystalline $Zn_{1-x}Co_xO$ Thin Films
P. Sati, C. Deparis, C. Morhain, S. Schafer, and A. Stepanov
Phys. Rev. Lett. 98 (13) (2007) 137204-4

46. Formation and rupture of Schottky nanocontacts on ZnO nanocolumns
B. Pérez-García, J. Zúñiga-Pérez, V. Muñoz-Sanjosé, J. Colchero, and E. Palacios-Lidón
Nano Letters 7 (2007) 1505

47. Anisotropic morphology of nonpolar a-plane quantum dots and quantum wells
S. Founta, C. Bougerol, H. Mariette, B. Daudin and P. Vennéguès
J. Appl. Phys 102 (2007) 074304

48. AlGaN/GaN HEMTs regrown by MBE on epi-ready semi-insulating GaN-on-sapphire with inhibited interface contamination
Y. Cordier, M. Azize, N. Baron, S. Chenot, O. Tottereau, J. Massies
J. Cryst. Growth 309 (2007) 1–7

49. AlGaN/GaN HEMTs on a (001)-Oriented Silicon Substrate Based on 100-nm SiN Recessed Gate Technology for Microwave Power Amplification
S. Boulay, S. Touati, A. A. Sar, V. Hoel, C. Gaquière, J.-C. De Jaeger, S. Joblot, Y. Cordier, F. Semond, and J. Massies
IEEE Transactions on Electron Devices 54, No. 11 (2007) 2843-2848

50. Growth of freestanding GaN using pillar-epitaxial lateral overgrowth from GaN nanocolumns
Z. Bougrioua, P. Gibart, E. Calleja, A. Trampert, J. Ristic, M. Utrera, G. Nataf
J. Cryst. Growth 309 (2007) 113-120

51. InAs/AlAsSb based quantum cascade lasers
X. Marcadet, C. Renard, M. Carras, M. Garcia, J. Massies
Appl. Phys. Lett. 91 (2007) 161104

52. (In,Ga)N/GaN microcavities with double dielectric mirrors fabricated by selective removal of an (Al,In)N sacrificial layer
F. Rizzi, P.R. Edwards, K. Bejtka, F. Semond, X.N. Kang, G.Y. Zhang, E. Gu, M.D. Dawson, I.M. Watson, and R.W. Martin
Appl. Phys. Lett. 90 (2007) 111112

53. Cathodoluminescence spectroscopy of epitaxial-lateral-overgrown nonpolar (11-20) and semipolar (11-22) GaN in relation to microstructural characterization
T. Gühne, M. Albrecht, Z. Bougrioua, P. Vennéguès, and M. Leroux
J. Appl. Phys. 101 (2007) 113101

54. Microstructural characterization of semipolar GaN templates and epitaxial-lateral-overgrown films deposited on M-plane sapphire by metalorganic-vapor-phase-epitaxy
P. Vennéguès, Z. Bougrioua and T. Guehne
Jpn. J. Appl. Phys 46, n° 7A (2007) 4089

55. Screening the built-in electric field in 4H silicon carbide stacking faults
S. Juillaguet, J. Camassel, M. Albrecht and T. Chassagne
Applied Physics Letters 90, (2007), 111902

56. Cathodoluminescence investigation of stacking faults extension in 4H-SiC
Juillaguet S., Camassel J., Albrecht M. and Chassagne T.
Physica Status Solidi (a) 204, N°. 7, (2007), 2222-2228

57. Barrier composition dependence of the internal electric field in ZnO/Zn1-xMgxO quantum wells
T. Bretagnon, P. Lefebvre, T. Guillet, T. Taliercio, B. Gil, C. Morhain
Appl. Phys. Lett., 90, 201912, (2007)

2008

58. Highly sensitive strained AlN on Si(111) resonators
M. Placidi, J.C. Moreno, P. Godignon, N. Mestres, E. Frayssinet, F. Semond, C. Serre
Sensors and Actuators A: Physical 150 (2008) 64-68

59. Analysis of the characteristic temperatures of (Ga,In)(N,As)/GaAs laser diodes
M. Montes, A. Hierro, J. M. Ulloa, A. Guzmán, B. Damilano, M. Hugues, M. Al Khalfioui, J.-Y. Duboz and J. Massies
JPhys D:Appl Phys 41 (2008) 155102

60. Magnesium diffusion profile in GaN grown by MOVPE
Z. Benzarti, I. Halidou, Z. Bougrioua, T. Boufaden, B. El Jani
J. Cryst. Growth 310 (2008) 3274

61. Polarized emission from GaN/AlN quantum dots: single-dot spectroscopy and symmetry-based theory
R. Bardoux, T. Guillet, B. Gil, P. Levebvre, T. Bretagnon, T. Taliercio, S. Rousset, F. Semond
Phys. Rev. B 77 (2008) 235315

62. Strong light-matter coupling in ultrathin double dielectric mirror GaN microcavities
K. Bejtka, F. Réveret, R.W. Martin, P.R. Edwards, A. Vasson, J. Leymarie, I. Sellers, J.-Y. Duboz, M. Leroux, and F. Semond
Appl. Phys. Lett. 92 (2008) 241105

63. Influence of the mirrors in the strong coupling regime in planar GaN microcavities
F. Réveret, P. Disseix, J. Leymarie, A. Vasson, F. Semond, M. Leroux, J. Massies
Phys. Rev. B 77 (2008) 195303

64. Structural and electrical properties of Au and Ti/Au contacts to n-type GaN
L. Dobos, B. Pecz, L. Toth, Z.J. Horvath, Z.E. Horvath, B. Beaumont, Z. Bougrioua
Vacuum 82 (2008) 794

65. Mechanism of mobility increase of the two-dimensional electron gas in AlGaN/GaN heterostructures under small dose gamma irradiation
A.M. Kurakin, S.A. Vitusevich, S.V. Danylyuk, H. Hardtdegen, N; Klein, Z. Bougrioua, B.A. Danilchenko, R.V. Konakova, A.E. Belyaev
J. Appl. Phys. 103 (2008) 083707

66. Residual strain in nonpolar a-plane $Zn_{(1-x)}Mg_xO$ (0< x <0.55) and its effect on the band structure of *(Zn,Mg)O/ZnO quantum wells*
J.-M. Chauveau, J. Vives, J. Zúñiga-Pérez, M. Laügt, M. Teisseire, C. Deparis, C. Morhain, and B. Vinter
Appl. Phys. Lett. 93 (2008) 231911

67. Interfacial structure and defect analysis of nonpolar ZnO films grown on R-plane sapphire by molecular beam epitaxy
P. Vennéguès, J.M. Chauveau, M. Korytov, C. deparis, J. Zúñiga-Pérez, and C. Morhain
J. Appl. Phys 103 (2008) 083525

68. Thickness and substrate effects on AlN thin film growth at room temperature
B. Abdallah, C. Duquenne, M.P. Besland, E. Gautron, P.Y. Jouan, P.Y. Tessier, J. Brault, Y. Cordier, and M.A. Djouadi
Eur. Phys. J. Appl. Phys. 43(3) (2008) 309-313

69. Interface structure and anisotropic strain relaxation of non polar wurtzite (11-20) and (10-10) orientations: ZnO epilayers grown on sapphire
J.-M. Chauveau, P. Vennéguès, M. Laügt, C. Deparis, J. Zúñiga-Pérez and C. Morhain
J. Appl. Phys 104 (2008) 073535

70. In-plane anisotropy characteristics of GaN epilayers grown on A-face sapphire substrates
HJ. Kim-Chauveau, P. De Mierry, H. Cabane, and D. Gindhart
J. Appl. Phys 104 (2008) 113516

71. Non-polar a-plane ZnMgO/ZnO quantum wells grown by molecular beam epitaxy
J. M. Chauveau, M. Laügt, P. Vennéguès, M. Teisseire, B. Lo, C. Deparis, C. Morhain, and B. Vinter

Semicond. Sci. Tech. 23 (3) (2008) 035005

72. Layer-by-layer epitaxial growth of Mg on GaN(0001)
S. Pezzagna, S. Vézian, J. Brault, and J. Massies
Appl. Phys. Lett. 92 (2008) 23111

73. Indium incorporation dynamics into AlInN ternary alloys for laser structures lattice-matched to GaN
H.P.D. Schenk, M. Nemoz, M. Korytov, P. Vennéguès, A.D. Dräger, and A. Hangleiter
Appl. Phys. Lett. 93 (2008) 081116

74. Blue-light emission from GaN/$Al_{0.5}Ga_{0.5}N$ quantum dots
T. Huault, J. Brault, F. Natali, B. Damilano, D. Lefebvre, L. Nguyen, M. Leroux, and J. Massies
Appl. Phys. Lett. 92 (2008) 051911

75. Optimum annealing temperature versus nitrogen composition in InAs/(Ga, In) (N, As) quantum dots
M Hugues, B Damilano, M Al Khalfioui, J.-Y. Duboz, J Massies, M Richter and A D Wieck
Semicond. Sci. Tech. 23 (2008) 035020

76. Polariton relaxation bottleneck and its thermal suppression in bulk GaN microcavities
F. Stokker-Cheregi, A. Vinattieri, F. Semond, M. Leroux, I.R. Sellers, J. Massies, D. Solnyshkov, G. Malpuech, M. Colocci, M. Gurioli
Appl. Phys. Lett. 92 (2008) 042119

77. Symmetry of wurtzite nanostructures with the c-axis in the layer plane
P. Tronc and P. Vennéguès
Phys. Rev. B 77 (2008) 075336

78. Composition analysis of semiconductor quantum wells by energy filtered convergent beam electron diffraction
D. Jacob, J. Min Zuo, A. Lefebvre, Y. Cordier
Ultramicroscopy 108 (2008) 358–366

79. Magnetotransport in Gd-implanted wurtzite GaN/$Al_xGa_{1-x}N$ high electron mobility transistor structures
F.-Y. Lo, A. Melnikov, D. Reuter, Y. Cordier, and A.D. Wieck
Appl. Phys. Lett. 92 (2008) 112111

80. Fabrication and characterization of ultrathin double dielectric mirror GaN microcavities
K. Bejtka, P.R. Edwards, R.W. Martin, F. Reveret, A. Vasson, J. Leymarie, I.R. Sellers, M. Leroux, and F. Semond
Semicond. Sci. Tech. 8 (2008) 045008

81. Bandgap and effective mass of epitaxial cadmium oxide
P. H. Jefferson, S. A. Hatfield, T. D. Veal, P. D. C. King, C. F. McConville, J. Zúñiga-Pérez and V. Muñoz-Sanjosé
Appl. Phys. Lett. 92 (2008) 022101

82. Nitrogen doping of 3C-SiC thin films grown by CVD in a resistively heated horizontal hot wall reactor
M. Zielinski, M. Portail, T. Chassagne, S. Juillaguet, H. Peyre
J. Cryst. Growth 310 (2008) 3174

83. Band gap narrowing and radiative efficiency of silicon doped GaN
H.P.D Schenk, S.I. Borenstain, A. Berezin, A. Schön, E. Cheifetz, S. Khatsevich, and D.H. Rich
J. Appl. Phys 103 (2008)

84. High doping level in Mg-doped GaN layers grown at low temperature
A. Dussaigne, B. Damilano, J. Brault, J. Massies, E. Feltin, and N. Grandjean
J. Appl. Phys 103 (2008) 013110

85. Band-edge Photoluminescence and Reflectivity of nonpolar (11-20) and semipolar (11-22) GaN formed by Epitaxial Lateral Overgrowth on sapphire
T. Gühne, Z. Bougrioua, S. Laügt, M. Nemoz, P. Vennéguès, B. Vinter, and M. Leroux
Phys. Rev. B 77 (2008) 075308

86. Demonstration of semipolar (11-22) InGaN/GaN blue-green light emitting diode
T. Gühne, P. DeMierry, M. Nemoz, E. Beraudo, S. Chenot, and G. Nataf
Electron. Lett. (2008) 231

87. Electronic structure of single-crystal rocksalt CdO studied by soft x-ray spectroscopies and ab initio calculations
L. F. J. Piper, A. DeMasi, K. E. Smith, A. Schleife, F. Fuchs, F. Bechstedt, J. Zúñiga-Pérez and V. Muñoz-Sanjosé
Phys. Rev. B 77 (2008) 125204

88. Investigation of AlGaN/AlN/GaN Heterostructures for Magnetic Sensor Application from liquid helium temperature to 300°C
L. Bouguen, S. Contreras, B. Jouault, L. Konczewicz, J. Camassel, Y. Cordier, M. Azize, S. Chenot, N. Baron
Appl. Phys. Lett. 92 (2008) 043504

89. Probing the band structure of InAs/GaAs quantum dots by capacitance-voltage and photoluminescence spectroscopy
W. Lei, M. Offer, A. Lorke, C. Notthoff, C. Meier, O. Wibbelhoff, and A.D. Wieck
Appl. Phys. Lett. 92 (2008) 193111

90. GaN for x-ray detection
J.-Y. Duboz, M. Laügt, H.P.D. Schenk, B. Beaumont, J.L. Reverchon, A.D. Wieck, and T. Zimmerling
Appl. Phys. Lett. 92 (2008) 263501

91. AlGaN/GaN high electron mobility transistors grown on 3C-SiC/Si(111)
Y. Cordier, M. Portail, S. Chenot, O. Tottereau, M. Zielinski, T. Chassagne
J. Cryst. Growth 310 (2008) 4417–4423

92. Demonstration of AlGaN/GaN High-Electron-Mobility Transistors Grown by Molecular Beam Epitaxy on Si(110)
Y. Cordier, J.-C. Moreno, N. Baron, E. Frayssinet, S. Chenot, B. Damilano, and F. Semond
IEEE Electron Device Letters 29 (2008) 1187-1189

93. Observation of quantized subband states and evidence for surface electron accumulation in CdO from angle-resolved photoemission spectroscopy
L. F. J. Piper, L. Colakerol, P. D. C. King, A. Schleife, J. Zúñiga-Pérez, P. A. Glans, T. Learmonth, A. Federov, T. D. Veal, F. Fuchs, V. Muñoz-Sanjosé, F. Bechstedt, C. F. McConville and K. E. Smith
Phys. Rev. B 78 (2008) 165127

94. Valence band offset of the ZnO/AlN heterojunction determined by x-ray photoemission spectroscopy
T.D. Veal, P.D.C. King, S.A. Hatfield, L.R. Bailey, C.F. McConville, B. Martel, J.C. Moreno, E. Frayssinet, F. Semond, and J. Zúñiga-Pérez
Appl. Phys. Lett. 93 (2008) 202108

95. Blue (Ga,In)N/GaN Light Emitting Diodes on Si(110) Substrate
B. Damilano, Fr. Natali, J. Brault, T. Huault, D. Lefebvre, R. Tauk, E. Frayssinet, J.-C. Moreno, Y. Cordier, F. Semond, S. Chenot, and J. Massies
Applied Physics Express 1 (2008) 121101

96. Monolithic white light emitting diodes using a (Ga,In)N/GaN multiple quantum well light converter
B. Damilano, A. Dussaigne, J. Brault, T. Huault, F. Natali, P. Demolon, P. De Mierry, S. Chenot, and J. Massies
Appl. Phys. Lett. 90 (2008) 101117

97. Refractive indices and elasto-optic coefficients of GaN studied by optical waveguiding
S. Pezzagna, J. Brault, M. Leroux, J. Massies, M. de Micheli
J. Appl. Phys 103 (2008) 123112

98. Luminescence upconversion in GaAs quantum wells
S. Eshlaghi, W. Worthoff, A.D. Wieck, and D. Suter
Phys. Rev. B 77 (2008) 245317

98a. Continuous-wave and ultrafast coherent reflectivity studies of excitons in bulk GaN
O. Aoudé, P. Disseix , J. Leymarie , A. Vasson, M. Leroux, E. Aujol, B.Beaumont, A. Trassoudaine, and Y. André
Phys. Rev. B 77, 045206 (2008)

2009

99. Anisotropic electron spin relaxation in bulk GaN
J.H. Buss, J. Rudolph, F. Natali, F. Semond, D. Hagele
Appl. Phys. Lett. 95 (2009) 192107

100. Interfacial properties of AlN and oxidized AlN on Si
M. Placidi, A. Perez-Tomas, J. C. Moreno, E. Frayssinet, F. Semond, A.Constant, P. Godignon, N. Mestres, A. Crespi and J. Millán
Surface science 604 (2009) 63

101. Phase separation in GaN/AlGaN quantum dots
M. Benaissa, L. Gu, M. Korytov, T. Huault, P. A. van Aken, J. Brault, and P. Vennéguès
Appl. Phys. Lett. 95 (2009) 141901

102. Backside illuminated GaN on Si Schottky photodiode for UV radiation detection
P. E. Malinowski, J. John, J. Y. Duboz, A. Lorenz, J. G. Rodriguez Madrid, C. Sturdevant, G. Hellings, K. Chen, M. Leys, J. Derluyn, J. Das, M. Germain, K. Minoglou, P. De Moor, R. Mertens, E. Frayssinet, F. Semond, J. Francois Hochedez and B. Giordaneng
Electron Device Lett 30 (2009) 1308

103. In-Plane Polarities of Nonpolar Wurtzite Epitaxial Films Deposited on m- and r-plane Sapphire Substrates
P. Vennéguès, T. Zhu, Z. Bougrioua, D. Martin, J. Zúñiga-Pérez, and N. Grandjean
Jpn. J. Appl. Phys. 48 (2009) 090211

104. Modelling of strong coupling regime in bulk GaN microcavities using transfer matrix and quasiparticle formalisms
F. Reveret, P. Disseix, J. Leymarie, F. Semond et al.
Solid State Com. 150 (2009) 122

105. Relaxation and emission of Bragg-mode and cavity-mode polaritons in a ZnO microcavity at room temperature
S. Faure, C. Brimont, T. Guillet, T. Bretagon, B. Gil, F. Médard, D. Lagarde, P. Disseix, J. Leymarie, J. Zúñiga-Pérez, M. Leroux, E. Frayssinet, J. C. Moreno, F. Semond, and S. Bouchoule
Appl. Phys. Lett. 95 (2009) 121102

106. Single-ion anisotropy in Mn-doped diluted magnetic semiconductors
A. Savoyant, A. Stepanov, R. Kuzian, C. Deparis, C. Morhain, and K. Grasza
Phys. Rev. B 80 (2009) 115203

107. Zinc oxide nanorod based photonic devices: recent progress in growth, light emitting diodes and lasers
M. Willander, O. Nur, Q. X. Zhao, L. L. Yang, M. Lorenz, B. Q. Cao, J. Zúñiga-Pérez, C. Czekalla, G. Zimmermann, M. Grundmann, A. Bakin, A. Behrends, M. Al-Suleiman, A. El-Shaer, A. Che Mofor, B. Postels, A. Waag, N. Boukos, A. Travlos, H. S. Kwack, J. Gu
Nanotechnology 20 (2009) 332001

108. Transmission electron microscopy investigation of microtwins and double positioning domains in (111) 3C-SiC in relation with the carbonization conditions
S. Roy, M. Portail, T. Chassagne, J. M. Chauveau, P. Vennéguès, M. Zielinski
Appl. Phys. Lett. 95 (2009) 081903

109. Improved semipolar (11-22) GaN quality using asymmetric lateral epitaxy
P. de Mierry , N. Kriouche, M. Nemoz, and G. Nataf
Appl. Phys. Lett. 94 (2009) 191903

110. Quantum confinement effect on the effective mass in two-dimensional electron gas of AlGaN/GaN heterostructures
A.M. Kurakin, S.A. Vitusevich, S.V. Danylyuk, H. Hardtdegen, N. Klein, Z. Bougrioua, A.V. Naumov, A.E. Belyaev
J. Appl. Phys. 105 (2009) 073703

111. Comparison between polar (0001) and semipolar (11-22) nitride blue-green light-emitting diodes grown on c-plane and m-plane sapphire substrates.
P.de Mierry, T. Guehne, M. Nemoz, S. Chenot, E. Beraudo, and G. Nataf
Jpn. J. Appl. Phys. 48 (2009) 031002

112. GaN Quantum Dots Grown on Silicon for Free-Standing Membrane Photonic Structures
S. Sergent, J.-C. Moreno, E. Frayssinet, S. Chenot, M. Leroux, and F. Semond
Applied Physics Express 2 (2009) 051003

113. Experimental observation of strong light-matter coupling in ZnO microcavities: Influence of large excitonic absorption
F. Medard, J. Zúñiga-Pérez, P. Disseix, M. Mihailovic, J. Leymarie, A. Vasson, F. Semond, E. Frayssinet, J. C. Moreno, M. Leroux, S. Faure, T. Guillet
Phys. Rev. B 79 (2009) 125302

114. AlN buffer layer growth for GaN epitaxy on (1 1 1) Si: Al or N first?
A. Le Louarn, S. Vézian, F. Semond and J. Massies
J. Cryst. Growth 311 (2009) 3278

115. Towards two-dimensional metallic behavior at $LaAlO_3/SrTiO_3$ interfaces
O. Copie, V. Garcia, C. Bödefeld, C. Carrétéro, M. Bibes, G. Herranz, E. Jacquet, J.-L. Maurice, B. Vinter, S. Fusil, K. Bouzehouane, H. Jaffrès, and A. Barthélémy
Phys. Rev. Lett. 102 (2009) 216804-4

116. Amplified piezoelectric transduction of nanoscale motion in gallium nitride electromechanical resonators
M. Faucher, B. Grimbert, Y. Cordier, N. Baron, A. Wilk, H. Lahreche, P. Bove, M. François, P. Tilmant, T. Gehin, C. Legrand, M. Werquin, L. Buchaillot, C. Gaquière, and D. Théron
Appl. Phys. Lett. 94 (2009) 233506

117. Homogeneous core/shell ZnO/ZnMgO quantum well heterostructures on vertical ZnO nanowires
B. Q. Cao, J. Zúñiga-Pérez, N. Boukos, C. Czekalla, H. Hilmer, J. Lenzner, A. Travlos, M. Lorenz, and M. Grundmann
Nanotechnology 20 (2009) 305701

118. Noise spectroscopy of AlGaN/GaN HEMT structures with long channels
S.A. Vitusevich, M.V. Petrychuk, A.M. Kurakin, S.V. Danylyuk, D. Mayer, Z. Bougrioua, A.V. Naumov, A.E. Belyaev, N. Klein
J. Stat. Mech. 1 (2009) P01046

119. Catalytic unzipping of carbon nanotubes to few-layer graphene sheets under microwaves irradiation
I. Janowska , O. Ersen , T. Jacob, P. Vennéguès, D. Bégin, M.-J. Ledoux, C. Pham-Huu
Applied Catalysis A:General 371 (2009) 22-30

120. GaN transistor characteristics at elevated temperatures
A. Pérez-Tomás, M. Placidi, N. Baron, S. Chenot, Y. Cordier, J. C. Moreno, A. Constant, P. Godignon, and J. Millán
J. Appl. Phys. 106 (2009) 074519

121. Signature of monolayer and bilayer fluctuations in the width of (Al,Ga)N/GaN quantum wells
F.Natali, Y.Cordier, J.Massies, S.Vezian, B.Damilano, M.Leroux
Phys. Rev. B 79 (2009) 035328

122. The critical role of growth temperature on the structural and electrical properties of AlGaN/GaN high electron mobility transistor heterostructures grown on Si(111)
N.Baron, Y.Cordier, S.Chenot, P.Vennéguès, O.Tottereau, M.Leroux, F.Semond, and J.Massies
J. Appl. Phys. 105 (2009) 033701

123. Windowed growth of AlGaN/GaN heterostructures on Silicon (111) substrates for future MOS integration

P. Chyurlia, F. Semond, T. Lester, J. A. Bardwell, S. Rolfe, Y. Cordier, N. Baron, J.-C. Moreno, and N. G. Tarr
Phys. Stat. Sol. A 206 (2009) 371-374

124. Effects of capping on GaN quantum dots deposited on $Al_{0.5}Ga_{0.5}N$ by molecular beam epitaxy
M. Korytov, T. Huault, M. Benaissa, T. Neisius, J. Brault, P. Vennéguès
Appl. Phys. Lett. 94 (2009) 143105

125. Comparative Study of the Role of the Nucleation Stage on the Final Crystalline Quality of (111) and (100) silicon carbide films deposited on silicon substrates
M. Portail, M. Zielinski, T. Chassagne, S. Roy, M. Nemoz
J. Appl. Phys 105 (2009) 083505

126. Anisotropic chemical etching of semipolar {10-1-1}/{10-1+1} ZnO crystallographic planes: polarity versus dangling bonds
E. Palacios-Lidon, B. Pérez-Garcia, P. Vennéguès, J. Colchero, V. Muñoz-Sanjosé, and J. Zúñiga-Pérez
Nanotechnology 20 (2009) 065701

127. Infrared detectors based on InGaAsN/GaAs intersubband transitions
J.-Y. Duboz, M. Hugues, B. Damilano, A. Nedelcu, P. Bois, N. Kheirodin, F. H. Julien
Appl. Phys. Lett. 94 (2009) 022103

128. Tailoring the shape of $GaN/Al_xGa_{1-x}N$ nanostructures to extend their luminescence in the visible range
J. Brault, T. Huault, F. Natali, B. Damilano, D. Lefebvre, M. Leroux, M. Korytov, and J. Massies
J. Appl. Phys 105 (2009) 033519

129. Unification of the electrical behavior of defects, impurities, and surface states in semiconductors: Virtual gap states in CdO
P. D. C. King, T. D. Veal, P. H. Jefferson, J. Zúñiga-Pérez, V. Muñoz-Sanjosé, and C. F. McConville
Phys. Rev. B 79 (2009) 035203

130. Elaboration of (111) oriented 3C-SiC/Si layers for template application in nitride epitaxy
M. Zielinski, M. Portail, S. Roy, T. Chassagne, C. Moisson, S. Kret, Y. Cordier
Mat. Sci. Eng. B 165 (2009) 9

131. Valence-band electronic structure of CdO, ZnO, and MgO from x-ray photoemission spectroscopy and quasi-particle-corrected density-functional theory calculations
P. D. C. King, T. D. Veal, A. Schleife, J. Zúñiga-Pérez, B. Martel, P. H. Jefferson, F. Fuchs, V. Munoz-Sanjosé, F. Bechstedt, and C. F. McConville
Phys. Rev. B 79 (2009) 205205

132. Highly sensitive determination of n+ doping level in 3C-SiC and GaN epilayers by Fourier Transform Infrared spectroscopy
M. Portail, M. Zielinski, T. Chassagne, H. Chauveau, S. Roy, P. De Mierry
Mat. Sci. Eng. B 165 (2009) 42

133. Comparison of GaN and ZnO epitaxial films for scintillator applications
H.P.D. Schenk, S.I. Borenstain, A. Berezin, A. Schön, E. Cheifetz, A. Dadgar, and A. Krost
J. Cryst. Growth 311 (2009) 3984

134. Anomalous photoresponse of GaN X-ray Schottky detectors
J.-Y. Duboz, B. Beaumont, J.-L. Reverchon and A. D. Wieck
J. Appl. Phys. 105 (2009) 114512

135. GaN/$Al_{0.5}Ga_{0.5}N$ quantum dots and quantum dashes
T. Huault, J. Brault, F. Natali, B. Damilano, D. Lefebvre, R. Tauk, M. Leroux, and J. Massies
Phys. Stat. Sol. (b) 246 (2009) 845-845

136. Combined structural and optical studies of stacking faults in 4H-SiC layers grown by chemical vapour deposition
M. Marinova, T. Robert, S. Juillaguet, I. Tsiaoussis, N. Frangis, E. Polychroniadis, J. Camassel, T. Chassagne
Phys. Status Solidi A 206, No. 8, (2009), 1924-1930

2010

137. Growth of GaN based structures on Si(1 1 0) by molecular beam epitaxy
Y. Cordier, J.-C. Moreno, N. Baron, E. Frayssinet, J.-M. Chauveau, M. Nemoz, S. Chenot, B. Damilano, F. Semond
J. Cryst. Growth 312 - n° 19 (2010) 2683-2688

138. Stacking faults blocking process in (1 1 −2 2) semipolar GaN growth on sapphire using asymmetric lateral epitaxy
N. Kriouche, P. Vennéguès, M. Nemoz, G. Nataf and P. De Mierry
J. Cryst. Growth 312 (2010) 2625

139. Carrier transfer and recombination dynamics of a long-lived and visible range emission from multi-stacked GaN/AlGaN quantum dots
J.-H. Kim, B.-J. Kwon, Y.-H. Cho, T. Huault, M. Leroux, J. Brault
Appl. Phys. Lett. 97 (2010) 061905

140. External efficiency and carrier loss mechanisms in InAs/GaInNAs quantum dot light-emitting diodes
M. Montes, A. Hierro, J. M. Ulloa, A. Guzmán, M. Al Khalfioui, M. Hugues, B. Damilano, and J. Massies

J. Appl. Phys. 108 (2010) 033104

141. Influence of the excitonic broadening on the strong light-matter coupling in bulk zinc oxide microcavities
F. Médard, D. Lagarde, J. Zúñiga-Pérez, P. Disseix, M. Mihailovic, J. Leymarie, E. Frayssinet, J. C. Moreno, F. Semond, M. Leroux, and S. Bouchoule
J. Appl. Phys. 108 (2010) 043508

142. Benefits of homoepitaxy on the properties of nonpolar (Zn,Mg)O/ZnO quantum wells on a-plane ZnO substrates
J.-M. Chauveau, M. Teisseire, H. Kim-Chauveau, C. Deparis, C. Morhain, and B. Vinter
Appl. Phys. Lett. 97 (2010) 081903

143. Polarized emission from GaN/AlN quantum dots subject to uniaxial thermal interfacial stresses
O. Moshe, D.H. Rich, B. Damilano and J. Massies
J. Vac. Sci.Technol.B 28 (2010) C5E25

144. Photoemission of Si 1s --> 2pz transition in GaAs/AlGaAs quantum well for zero-dimensional states infrared detection
T. Antoni, M. Carras, X. Marcadet, B. Vinter, and V. Berger
Appl. Phys. Lett. 97 (2010) 042102-3

145. Current Spreading Efficiency and Fermi Level Pinning in GaInNAs–GaAs Quantum-Well Laser Diodes
M. Montes Bajo, A. Hierro, J. M. Ulloa, J. Miguel-Sánchez, Á. Guzmán, B. Damilano, M. Hugues, M. Al Khalfioui, J.-Y. Duboz, and J. Massies
IEEE J Quantum Electron 46 (2010) 1058

146. Anomalous composition dependence of the band gap pressure coefficients in In-containing nitride semiconductors
I. Gorczyca, A. Kamińska, G. Staszczak, R. Czernecki, S. P. Łepkowski, T. Suski, H. P. D. Schenk, M. Glauser, R. Butté, J.-F. Carlin, E. Feltin, N. Grandjean, N. E. Christensen, and A. Svane
Phys. Rev. B 81 (2010) 235206

147. Semipolar GaN films on patterned r-plane sapphire obtained by wet chemical etching
P. de Mierry, N. Kriouche, M. Nemoz, S. Chenot, and G. Nataf
Appl. Phys. Lett. 96 (2010) 231918

148. AlGaN/GaN HEMTs on (001) Silicon Substrate With Power Density Performance of 2.9 W/mm at 10 GHz
J.-C. Gerbedoen, A. Soltani, S. Joblot, J.-C. De Jaeger, C. Gaquière, Y. Cordier, and F. Semond
IEEE Trans. Electron Devices 57 (2010) 1497-1503

149. Surface band-gap narrowing in quantized electron accumulation layers
P. D. C. King, T. D. Veal, C. F. McConville, J. Zúñiga-Pérez, V. Munoz-Sanjosé, M. Hopkinson, E. D. L. Rienks, M. Fuglsang Jensen, and Ph. Hofmann
Phys. Rev. Lett. 104 (2010) 256803

150. Luminescence properties of ZnO/$Zn_{1-x}Cd_xO$/ZnO double heterostructures
M. Lange, C. P. Dietrich, C. Czekalla, J. Zippel, G. Benndorf, M. Lorenz, J. Zúñiga-Pérez, and M. Grundmann
J. Appl. Phys. 107 (2010) 093530

151. Epitaxial graphene on Cubic SiC(111)/Si(111) substrate
A. Ouerghi, A. Kahouli , D. Lucot , M. Portail , L. Travers , J. Gierack , J. Penuelas , P. Jegou , A. Shukla , T. Chassagne, M. Zielinski
Appl. Phys. Lett. 96 (2010) 191910

152. Ti–Ni ohmic contacts on 3C–SiC doped by nitrogen or phosphorus implantation
A.E. Bazin, J.F. Michaud, C. Autret-Lambert, F. Cayrel, T. Chassagne, M. Portail, M. Zielinski, E. Collard, D. Alquier
Mat. Sci. Eng. B 171 (2010) 120

153. Two-dimensional confined photonic wire resonators: strong light-metter coupling
R. Schmidt-Grund, H. Hilmer, A. Hinkel, C. Sturm, B. Rheinlander, V. Gottschalch, M. Lange, J. Zúñiga-Pérez, and M. Grundmann
Phys. Stat. Sol. B 247 (2010) 1351

154. Whispering gallery modes in zinc oxide micro- and nanowires
C. Czekalla, T. Nobis, A. Rahm, B. Cao, J. Zúñiga-Pérez, C. Sturm, R. Schmidt-Grund, M. Lorenz, and M. Grundmann
Phys. Stat. Sol. B 247 (2010) 1282

155. Voltage tunable surface acoustic wave phase shifter on AlGaN/GaN
J. Pedros, F. Calle, R. Cuerdo, J Grajal, Z. Bougrioua
Appl. Phys. Lett. 96 (2010) 123505

156. Influence of Stacking Sequences and Lattice Parameter Differences on the Microstructure of Nonpolar AlN Films Grown on (1120) 6H-SiC by Plasma-Assisted Molecular Beam Epitaxy
P. Vennéguès, S. Founta, H. Mariette, and B. Daudin
Jpn. J. Appl. Phys. 49 (2010) 040201

157. Temperature dependence of electron spin relaxation in bulk GaN
J.H. Buss, J. Rudolph, F. Natali, F. Semond, D. Hagele
Phys. Rev. B 81 (2010) 155216

158. Room-temperature continuous-wave metal grating distributed feedback quantum cascade lasers

M. Carras,G. Maisons. B. Simozrag, M. Garcia, O. Parillaud, J. Massies, X. Marcadet
Appl. Phys. Lett. 96 (2010) 161105

159. Evidence of electrical activity of extended defects in 3C-SiC grown on Si
X. Song, J.F. Michaud, F. Cayrel, M. Zielinski, M. Portail, T. Chassagne, E. Collard, D. Alquier
Appl. Phys. Lett. 96 (2010) 142104

160. Raman scattering of cadmium oxide epilayers grown by metal-organic vapor phase epitaxy
R. Cusco, J. Ibanez, N. Domenech-Amador, L. Artus, J. Zúñiga-Pérez, and V. Munoz-Sanjose
J. Appl. Phys. 107 (2010) 063519

161. Tuning the lateral density of ZnO nanowires arrays and its applications as physical templates for radial nanowire heterostructures
B. Q. Cao, J. Zúñiga-Pérez, C. Czekalla, H. Hilmer, J. Lenzner, N. Boukos, A. Travlos, M. Lorenz, and M. Grundmann
J. Mater. Chem. 20 (2010) 3848

162. Self-organized growth of ZnO-based nano- and microstructures
M. Lorenz, A. Rahm, B. Cao, J. Zúñiga-Pérez, E. M. Kaidashev, N. Zhakarov, G. Wagner, T. Nobis, C. Czekalla, G. Zimmermann, and M. Grundmann
Phys. Stat. Sol. B 247 (2010) 1265

163. Monolithic integration of AlGaN/GaN HFET with MOS on silicon <111 > substrates
P.N. Chyurlia, F. Semond, T. Lester, J.A. Bardwell et al
Electron. Lett. 46 (2010) 240

164. Blue-green and white color tuning of monolithic light emitting diodes
B. Damilano, P. Demolon , J. Brault , T. Huault, F. Natali , J. Massies
J. Appl. Phys. 108 (2010) 073115

165. Electronic and optical properties of GaN/AlN quantum dots on Si(111) subject to in-plane uniaxial stresses and variable excitation
O. Moshe, D. H. Rich, S. Birner , M. Povolotskyi , B. Damilano , J. Massies
J. Appl. Phys. 108 (2010) 083510

166. X-ray detectors based on GaN Schottky diodes
J.-Y. Duboz, E. Frayssinet, S. Chenot, J.-L. Reverchon, M. Idir,
Appl. Phys. Lett. 97 (2010) 163504

167. Epitaxial graphene on 3C-SiC(111) pseudosubstrate: structural and electronic properties
A. Ouerghi, M. Marangolo, B. Belkhou, S. El Moussaoui, M. Silly, M. Eddrief, L. Largeau, M. Portail, B. Fain, F. Sirotti
Phys. Rev. B **82**, (2010) 125445

167a. Direct growth of few-layer graphene on 6H-SiC and 3C-SiC/Si via propane chemical vapor deposition
A. Michon, S. Vézian, A. Ouerghi, M. Zielinski, T. Chassagne, and M. Portail
Appl. Phys. Lett. **97**, 171909 (2010)

167b. GaN nanocolumns on sapphire by ammonia-MBE: From self-organized to site-controlled growth
S. Vézian, B. Alloing, J. Zúñiga-Pérez
Journal of Crystal Growth, In Press, Available online 4 November 2010

Conference papers (reviewed by a reading committee)

2006

168. Optimization of InAs/(Ga,In)As quantum dots in view of efficient emission at 1.5µm
M. Hugues, M. Richter, B. Damilano, J.-M. Chauveau, J.-Y. Duboz, J. Massies and A. D. Wieck
Phys. Stat. Sol. (c) **3** (2006) 3979

169. 1.5 µm luminescence from InAs/$Ga_xIn_{1-x}N_yAs_{1-y}$ quantum dots grown on GaAs substrate
M. Richter, M. Hugues, B. Damilano, J. Massies, J.-Y. Duboz, D. Reuter and A. D. Wieck
Phys. Stat. Sol. (c) **3** (2006) 3848

170. Magneto-optical spectroscopy of (Zn,Co)O epilayers
W. Pacuski, D. Ferrand, J. Cibert, C. Deparis, P. Kossacki, C. Morhain
Phys. Stat. Sol. B **243** (2006) 863

171. Time resolved photoluminescence study of ZnO/(Zn,Mg)O quantum wells
T. Bretagnon, P. Lefebvre, P. Valvin, B. Gil, C. Morhain, X.D. Tang
J. Cryst. Growth **287** (2006) 12

172. Structural and electrical characteristics of Ag/$Al_{0.2}Ga_{0.8}N$ and Ag/$Al_{0.3}Ga_{0.7}N$ Schottky contacts: an XPS study
B. Boudjelida, I. Gee, J. Evans-Freeman, S.A. Clark, M. Azize, J.M. Bethoux, and P. de Mierry
Phys. Stat. Sol. C **3** (2006) 1823

173. Room temperature Strong coupling in low finesse GaN microcavities
I.R. Sellers, F. Semond, M. Leroux, et al.
MRS symposium **892** (2006) 485-490

174. Structural evaluation of GaN/sapphire grown by epitaxial lateral overgrowth by X-ray microdiffraction
M. Drakopoulos, M. Laügt, T. Riemann, B. Beaumont, and P. Gibart

Phys. Stat. Sol. (b) **243, No. 7** (2006) 1545–1550

175. Quality and uniformity assessment of AlGaN/GaN Quantum Wells and HEMT heterostructures grown by molecular beam epitaxy with ammonia source
Y.Cordier, F.Pruvost, F.Semond, J.Massies, M.Leroux, P.Lorenzini, C.Chaix
Phys. Stat. Sol. (c) **3, N°6** (2006) 2325-2328

176. Growth by molecular beam epitaxy of AlGaN/GaN high electron mobility transistors on Si-on-polySiC
Y.Cordier, S.Chenot, M.Laügt, O.Tottereau, S.Joblot, F.Semond, J.Massies, L.Di Cioccio, H.Moriceau
Superlattices & Microstructures **(40)** (2006) 359-362

177. Strong light-matter coupling in GaN microcavities grown on silicon (111) at room temperature
I.R.Sellers, F.Semond, M.Leroux, J.Massies, A-L.Henneghien, P.Disseix, J.Leymarie and A.Vasson
Phys. Stat. Sol. (b) **243(7)** (2006) 1639

178. Investigation of growth mechanisms of GaN quantum dots on (0001) AlN surface by ammonia MBE
V.G. Mansurov, Yu. G. Galitsyn, A. Yu. Nikitin, K.S. Zhuralev, P. Vennéguès
Phys. Stat. Sol. (c) **3, No.6** (2006) 1548

179. Characterization of structural defects in GaN films grown on sapphire substrates
P. Vennéguès, F. Mathal, and Z. Bougrioua
Phys. Stat. Sol. (c) **3/6** (2006) 1658-1661

180. Modelling of the Anomalous Field-Effect Mobility Peak of O-Ta_2Si/4H-SiC High-k MOSFETS Measured in Strong Inversion
A. Pérez-Tomas, M. Vellvehi, N. Mestres, J. Millan, P. Vennéguès and J. Stoemenos
Materials Science Forum **527-529** (2006) 1059

181. InAs/$In_{0.15}Ga_{0.85}As_{1-x}N_x$ quantum dots for 1.5 µm laser applications
M. Richter, B. Damilano, J. Massies, and J.-Y. Duboz
Mater. Res. Soc. Symp. Proc. **891** (2006) 0891-EE03-29.1

182. Influence of crystal quality on electron mobility in AlGaN/GaN HEMTs grown on Si(111), SiC and GaN templates
Y.Cordier, P.Lorenzini, M.Hugues, F.Semond, F.Natali, Z.Bougrioua, J.Massies, E.Frayssinet, B.Beaumont, P.Gibart, J-P.Faurie
Journal de Physique IV **132** (2006) 365-368

183. Comparison of high quality GaN-based light-emitting diodes grown on alumina-rich spinel and sapphire substrates

F. Tinjod, P. de Mierry, D. Lancefield, S; Chenot, E. Virey, J.L. Stone-Sundberg, M.R. Kokta, D. Pauwels
Phys. Stat. Sol. (c) **(6)** (2006) 2199-202

184. AlGaN/GaN HEMTs grown on silicon (001) substrates by molecular beam epitaxy
S. Joblot, Y. Cordier, F. Semond, S. Chenot, P. Vennéguès, O. Tottereau, P. Lorenzini and J. Massies
Superlattices & Microstructures **40** (2006) 295-299

185. Field-effect-modulated SAW devices on AlGaN/GaN heterostructures
J. Pedros,R. Cuerdo,F. Calle,J. Grajal,J.L. Martinez-Chacon,Z. Bougrioua
IEEE Ultrasonics Symposium (2006)

186. Structural characterisation of Sb-based heterostructures by X-ray scattering methods
C. Renard, O. Durand, X. Marcadet, J. Massies, O. Parillaud
Applied Surface Science **253** (2006) 112

187. Investigation of the optical properties of epitaxial-lateral-overgrown GaN on R- and M-sapphire
T. Gühne, Z. Bougrioua, M. Albrecht, P. Vennéguès, M. Leroux, M. Laügt, S. Ndiaye, M. Teisseire, L. Nguyen, and P. Gibart
Mater. Res. Soc. Symp. Proc. (2006)

188. Cylindric resonators with coaxial Bragg reflectors
R. Schmidt-Grund, T. Gühne, H. Hochmuth, B. Rheinländer, A. Rahm, V. Gottschalch, J. Lenzner, and M. Grundmann
Proc. SPIE (2006)

189. Investigation of the interface properties of MOVPE grown AlGaN/GaN high electron mobility transistor (HEMT) structures on sapphire
T. Aggerstam, S. Lourdudoss, H.H. Radamson, M. Sjödin, P. Lorenzini, D.C. Look
Thin Solid Films **515** (2006) 705–707

2007

190. AlGaN-based focal plane arrays for selective UV imaging at 310nm and 280nm and route toward deep UV imaging
J.L. Reverchon , J.A. Robot, J.P. Truffer, J.P. Caumes, I. Mourad, J. Brault and J.Y. Duboz
SPIE procedings **6744** (2007) 674417

191. AlGaN/GaN HEMTs on (001) oriented silicon substrate based on 100 nm SiN recessed gate technology for low cost device fabrication
S. Boulay, S. Touati, A. Sar, V. Hoel, C. Gaquiere, J.C. De Jacger, S. Joblot, Y. Cordier, F. Semond, J. Massies

European Microwave Integrated Circuits Conference **2007** (2007) 96-99

192. Time-resolved spectroscopy of excitonic transitions in ZnO/(Zn, Mg)O quantum wells
T. Guillet, T. Bretagnon, T. Taliercio, P. Lefebvre, B. Gil, C. Morhain, X.D. Tang XD
Superlattice et Microstructures **41** (2007) 352

193. Magnetic properties of single crystalline Zn1-xCoxO thin films
P. Sati, S. Schafer, C. Morhain, C. Deparis, A. Stepanov
Superlattices et Microstructures **42** (2007) 191

194. Magnetotransport characterization of AlGaN/GaN interfaces
R. Tauk, A. Tiberj, P. Lorenzini, Z. Bougrioua, M. Azize, M. Sakowicz, K. Karpierz, W. Knap
Phys. Stat. Sol. A **204** (2007) 586

195. Double-dielectric-mirror InGaN/GaN microcavities formed using selective removal of an AlInN layer
F. Rizzi, P.R. Edwards, K. Bejtka, F. Semond, et al.
Superlattices and microstructures **41** (2007) 414-418

196. From evidence of strong light-matter coupling to polariton emission in GaN microcavities
I.R. Sellers, F. Semond, M. Zamfirescu, et al.
Phys. Stat. Sol. B **244** (2007) 1882-1886

197. Micro-photoluminescence of isolated hexagonal GaN/AlN quantum dots: Role of the electron-hole dipole
R. Bardoux, T. Guillet, P. Lefebvre, F. Semond, et al.
Physics of semiconductors **B893** (2007) 941-942

198. $Al_xGa_{1-x}N$ focal plane arrays for imaging applications in the extreme ultraviolet (EUV)
J. John, P. Malinowski, P. Aparicio, J.-Y. Duboz, F. Semond, et al.
Optical sensing technology and applications **6585** (2007) 33-40

199. ***Growth of non-polar ZnO/(Zn,Mg)O quantum well structures on R-sapphire by plasma-assisted molecular beam epitaxy***
J. M. Chauveau, D. A. Buell, M. Laugt, P. Vennéguès, M. Teisseire-Doninelli, S. Berard-Bergery, C. Deparis, B. Lo, B. Vinter, and C. Morhain
J. Cryst. Growth **301-302** (2007) 366-9

200. Growth and characterization of A-plane ZnO and ZnCoO based heterostructures
J.-M. Chauveau, C. Morhain, B. Lo, B. Vinter, P. Vennéguès, M. Laügt, M. Tesseire-Doninelli, and G. Neu
Applied Physics A: Materials Science & Processing **88 (1)** (2007) 65-9

201. Deuterium Out-diffusion Kinetics in Magnesium-doped GaN
J. Chevallier, F. Jomard, N. H. Nickel, P. de Mierry, S. Chenot, Y.Cordier, M. A. di Forte-Poisson, and S. Delage
Mat. Res. Soc. Symp. Proc. **994** (2007) F03-22

202. Radiative lifetime in wurtzite GaN/AlN quantum dots
R. Bardoux, T. Bretagnon, T. Guillet, P. Lefebvre, T. Taliercio, P. Valvin, B. Gil, N. Grandjean, B. Damilano, A. Dussaigne, J. Massies
Phys. Stat. Sol. (c) **4, Issue 1** (2007) 183-186

203. Structural and morphological characterization of ZnO films grown on GaAs substrates by MOCVD
S. Agouram, J. Zúñiga-Pérez, and V. Muñoz-Sanjosé
Appl. Phys. A **88** (2007) 83

204. Nanoscale determination of surface orientation and electrostatic properties of ZnO thin films
J. Zúñiga-Pérez, E. Palacios-Lidón, V. Muñoz-Sanjosé, and J. Colchero
Appl. Phys. A **88** (2007) 77

205. X-ray and transmission electron microscopy characterization of twinned CdO thin films grown on a-plane sapphire by metalorganic vapour phase epitaxy
C. Martínez-Tomás, J. Zúñiga-Pérez, P. Vennéguès, O. Tottereau and V. Muñoz - Sanjosé
Appl. Phys. A **88** (2007) 61

206. Strain and wafer curvature of 3C-SiC films on silicon: influence of the growth conditions
M. Zielinski, S. Ndiaye, T. Chassagne, S. Juillaguet, R. Lewandowska, M. Portail, A. Leycuras; J. Camassel
Phys. Stat. Sol. (a) **204** (2007) 981

207. Low Specific Contact Resistance to 3C-SiC grown on (100) Si substrates
A. E. Bazin, T. Chassagne, J. F. Michaud, A. Leycuras, M. Portail, M. Zielinski, E. Collard; D. Alquier
Materials Science Forum **556-557** (2007) 721

208. Trends in nitrogen doping for 3C-SiC films on silicon
M. Zielinski, M. Portail, H. Peyre, T. Chassagne, S. Ndiaye, B. Boyer, A. Leycuras and J. Camassel
Materials Science Forum **556-557** (2007) 207

209. In situ measurements of wafer bending curvature during growth of group-III-nitride layers on silicon by molecular beam epitaxy
Y.Cordier, N.Baron, F.Semond, J.Massies, M.Binetti, B.Henninger, M.Besendahl, T.Zettler
J. Cryst. Growth **301-302** (2007) 71-74

210. Monolithic white light emitting diodes with a broad emission spectrum
A. Dussaigne, J. Brault, B. Damilano, J. Massies
Phys. Stat. Sol. (c) **4, Issue 1** (2007) 57-60

211. All-optical characterisation of carrier lifetimes and diffusion lengths in MOCVD-, ELO-, and HVPE grown GaN
T. Malinauskas, R. Aleksiejunas, K. Jarasiunas, B. Beaumont, P. Gibart, A. Kakanakova, E. Janzen, D. Gogova, B. Monemar, M. Heuken
J. Cryst. Growth **300** (2007) 223-227

212. Intersubband transitions in InGaAsN/AlGaAs quantum wells with a high confinement energy
J.-Y. Duboz
Phys. Stat. Sol. (c) **7** (2007) 2391

213. Developments for the production of high quality and high uniformity AlGaN/GaN heterostructures by Ammonia MBE
Y.Cordier, F.Semond, J.Massies, M.Leroux, P.Lorenzini, C.Chaix
J. Cryst. Growth **301-302** (2007) 434-436

214. Energetically deep defect centers in vapor-phase grown zinc oxide
T. Frank, G. Pensl, R. Tena-Zaera, J. Zúñiga-Pérez, C. Martínez-Tomás,V. Muñoz-Sanjosé, T. Ohshima, H. Itoh, D. Hofmann, D. Pfisterer, J. Sann and B. Meyer
Appl. Phys. A **88** (2007) 141

215. Realization of AlGaN/GaN HEMTs on Si-on-polySiC substrates
Y. Cordier, S. Chenot, M. Laügt, O. Tottereau, S. Joblot, F. Semond, J. Massies, L. Di Cioccio and H. Moriceau
Phys. Stat. Sol. (c) **4, n°7** (2007) 2670-2673

216. Electron Scattering Spectroscopy by High Magnetic Field in Mid-Infrared Quantum Cascade Lasers
A. Leuliet, A. Wade, A. Vasanelli, G. Fedorov, D. Smirnov, M. Giovannini, J. Faist, G. Bastard, B. Vinter, and C. Sirtori
ICPS, AIP Conference Proceedings **893** (2007) 497-498

217. Reduction of stacking faults in (11-20) and (11-22) GaN films by ELO techniques and benefit on GaN wells emission
Z. Bougrioua, M. Laügt, P. Vennéguès, I. Cestier, T. Gühne, E. Frayssinet, P. Gibart, and M. Leroux
Phys. Stat. Sol. (a) **204, n°1** (2007) 282-289

218. Structural and electrical characterization of n-type GaN/$Al_xGa_{1-x}N$ superlattices grown by metalorganic vapour phase epitaxy
H.P.D. Schenk, P. Demolon, S. Ndiaye, M. Laügt, T. Gühne, Z. Bougrioua, P. de Mierry, J.Y. Duboz, A.D. Dräger, C. Netzel, and A. Hangleiter
Proc. Int. Workshop Nitride Based Nanostruct. (2007) 127

219. Photoelectric properties of highly excited GaN-Fe epilayers grown by modulation- and continuous-doping techniques
Z. Bougrioua, M. Azize, B. Beaumont, P. Gibart, T. Malinauskas, K. Neimontas, A. Mekys, J. Storasta, K. Jarasiunas
J. Cryst. Growth **300** (2007) 228-232

220. Development and analysis of low resistance ohmic contact to n-AlGaN/GaN HEMT
A. Soltani, A. BenMoussa, S. Touati, V. Hoël, J.-C. De Jaeger, J. Laureyns, Y. Cordier, C. Marhic, M.A. Djouadi, C. Dua
Diamond and Related Materials **16** (2007) 262–266

221. X-ray photoemission studies of the electronic structure of single-crystalline CdO(100)
L.F.J. Piper, P.H. Jefferson, T.D. Veal, C.F.C. McConville, J. Zúñiga-Pérez, V. Muñoz-Sanjosé
Superlattices & Microstructures **42** (2007) 197

222. Polariton emission in GaN microcavities
M. Gurioli, M. Zamfirescu, F. Stokker-Cheregi, A. Vinattieri, I. R. Sellers, F.Semond, M. Leroux, and J.Massies
Superlattices & Microstructures **41** (2007) 284

223. Polariton thermalization in GaN microcavities in the strong light-matter coupling regime
F. Stokker-Cheregi, M. Zamfirescu, A. Vinattieri, M. Gurioli, I. Sellers, F. Semond, M. Leroux, and J. Massies
Superlattices & Microstructures **41** (2007) 376

224. Fabrication of monocrystalline 3C-SiC resonators for MHz frequency applications
M. Placidi, P. Godignon, N. Mestres, G. Abadal, G. Ferro, A. Leycuras, T. Chassagne
Sensors and Actuators B (2007)

225. ZnO micro-pillar resonators with coaxial Bragg reflectors
R. Schmidt-Grund, B. Rheinländer, T. Gühne, H. Hochmuth, V. Gottschalch, A. Rahm, J. Lenzner, and M. Grundmann
AIP Conference Proceedings (2007)

226. High indium content AlInGaN films: growth, structure and optoelectronic properties
M. Nemoz, E. Beraudo, P. De Mierry, P. Vennéguès, L. Hirsch
Phys. Stat. Sol. (c) **4, No. 1** (2007) 137-140

227. Electric-field screening effects in the micro-photoluminescence spectra of as-grown stacking faults in 4H-SiC
S. Juillaguet, T. Guillet, R. Bardoux, J. Camassel and T. Chassagne

Materials Science Forum 556-557, (2007), 351-354

2008

228. Mechanisms of ammonia-MBE growth of GaN on SiC for transport devices
H. Tang, S. Rolfe, F. Semond, J.A. Bardwell, J.M. Baribeau
J. Cryst. Growth **311** (2008) 2091-2095

229. Selectively grown AlGaN/GaN HEMTs on Si(111) substrates for integration with Silicon microelectronics
S. Haffouz, F. Semond, J.A. Bardwell, T. Lester, H. Tang
J. Cryst. Growth **311** (2008) 2087-2090

230. Performance of Unstuck Γ Gate AlGaN/GaN HEMTs on (001) Silicon Substrate at 10GHz
J.-C. Gerbedoen, A.Soltani, N. Defrance, M. Rousseau, C. Gaquiere, J-C. De Jaeger, S. Joblot, Y.Cordier
European Microwave Integrated Circuits Conference **2008** (2008) 330-333

231. Mosaicity and stress effects on luminescence properties of GaN
A. Toure, A. Bchetnia, T.A. Lafford, Z.Benzarti, I. Halidou, Z. Bougrioua, B. El Jani
Phys. Stat. Sol. A **208** (2008) 2042

232. Influence of $In_{0.15}Ga_{0.85}As$ capping layers on the electron and hole energy levels of InAs quantum dots
M. Richter, D. Reuter, J.-Y. Duboz, A. D. Wieck
PhysicaE **40** (2008) 1891

233. Growth and Characterization of Non-Polar (Zn,Mg)O/ZnO Quantum Wells and Multiple Quantum Wells
J.-M. Chauveau, B. Vinter, M. Laugt, M. Teisseire, P. Vennéguès, C. Deparis, J. Zúñiga-Pérez and C. Morhain
J. Kor. Phys. Soc. **53(5)** (2008) 2934

234. Growth of AlGaN/GaN HEMTs on Silicon Substrates by MBE
F. Semond, Y. Cordier, F. Natali, A. Le Louarn, S. Vézian, S. Joblot, S. Chenot, N. Baron, E. Frayssinet, J.-C. Moreno, J. Massies
MRS symposium proceedings **1068** (2008) 51-56

235. Strong light-matter coupling in GaN-based microcavities grown on silicon substrates
F. Semond, I.R. Sellers, N. Ollier, et al.
MRS proceedings **1068** (2008) 95-100

236. Molecular Beam Epitaxy of AlN Layers on Si (111)
J.-C. Moreno, E. Frayssinet, F. Semond, et al.
MRS symposium proceeding **1068** (2008) 141-145

237. Temperature dependence of the polariton relaxation bottleneck in a GaN microcavity
F. Stokker-Cheregi, A. Vinattieri, M. Colocci, F. Semond, et al.
Phys. Stat. Sol. C **5** (2008) 2257

238. Strong coupling in bulk GaN microcavities grown on silicon
F. Reveret, I.R. Sellers, P. Disseix, F. Semond, et al.
Phys. Stat. Sol. C **4** (2008) 108-111

239. Dry etching of N-face GaN using two high-density plasma etch techniques
F. Rizzi,; K. Bejtka,; F. Semond, et al.
Phys. Stat. Sol. C **4** (2008) 200-203

240. Growth of AlGaN/GaN HEMTs on 3C-SiC/Si(111) Substrates
Y. Cordier, M. Portail, S. Chenot, O. Tottereau, M. Zielinski and T. Chassagne
MRS Symposium Proceedings **1068** (2008) C04-05

241. AlGaN photodetectors for applications in the extreme UV range
P. Malinowski, J. John, A. Lorrenz, P.A. Alonso, M. Germain, J. Derluyn, K. Cheng, G. Borghs, R. Mertens, J.Y. Duboz, F. Semond, U. Kroth, M. Richter, J.F. Hochedez, A. Ben Moussa
Proc. SPIE (2008)

242. Structural and morphological characterization of 3C-SiC films grown on (111), (211) and (100) silicon substrates
M. Portail, M. Nemoz, M. Zielinski, T. Chassagne
Materials Science Forum **600-603** (2008) 231

243. Strain in 3C-SiC heteroepitaxial layers grown on (100) and (111) oriented silicon substrates
M. Zielinski, M. Portail, T. Chassagne, Y. Cordier
Materials Science Forum **600-603** (2008) 207-210

244. Comparison of GaInN laser structures grown on different substrates
A.D. Dräger, D. Fuhrmann, C. Netzel, U. Rossow, H.P.D. Schenk, and A. Hangleiter
Phys. Stat. Sol. (c) **5** (2008) 2277

245. High temperature behaviour of GaN HEMT devices on Si(111) and sapphire substrates
R. Cuerdo, F. Calle, A. F. Braña, Y. Cordier, M. Azize, N. Baron, S. Chenot, and E. Muñoz
Phys. Stat. Sol. (c) (2008)

246. Realization of AlGaN/GaN HEMTs on 3C-SiC/Si(111) substrates
Y. Cordier, M. Portail, S. Chenot, O. Tottereau, M. Zielinski, and T. Chassagne
Phys. Stat. Sol. (c) **5, No. 6** (2008) 1983–1985

247. Optical and structural properties of $Al_{1-x}In_xN$ epilayers grown in three different MOVPE reactors
R.W. Martin, E. Alves, N. Franco, C.J. Humphreys, M.J. Kappers, M. Korytov, M. Leroux, K. Lorenz, S. Magalhães, K.P. O'Donnell, R.A. Oliver, T.C. Sadler, H.P.D. Schenk, L.T. Tan, P. Vennéguès, K. Wang, and I.M. Watson
International Workshop on Nitride Semiconductors (2008)

248. Structural and optical properties of $Zn_{(1-x)}Cd_xO$ solid solutions grown on ZnO substrates by using MOCVD
A. Lusson, N. Hanèche, V. Sallet, P. Galtier, V. Muñoz-Sanjosé, J. Zúñiga-Pérez, S. Agouram, J. A. Bastos Segura, E. Leroy
J. Kor. Phys. Soc. **53** (2008) 158

249. Characterization of non-polar ZnO layers with positron annihilation spectroscopy
A. Zubiaga, F. Tuomisto, J. Zúñiga-Pérez and V. Muñoz-Sanjosé
Acta Physica Polonica A **114** (2008) 1457

250. Subsurface Fe doped semi-insulating GaN templates for inhibition of regrowth interface pollution in AlGaN/GaN HEMT structures
Y. Cordier, M. Azize, N. Baron, Z. Bougrioua, S. Chenot, O. Tottereau, J. Massies, and P. Gibart
J. Cryst. Growth **310** (2008) 948

251. P Implantation Effect on Specific Contact Resistance in 3C-SiC Grown on Si
A. E. Bazin, J. F. Michaud, M. Portail, T. Chassagne, M. Zielinski, J. F. Lecoq, E. Collard, D. Alquier
Mater. Res. Soc. Symp. Proc. **1068** (2008) 1068-C07-09

252. Observation of Asymetric Wafer Bending for 3C-SiC Thin Films Grown on Misoriented Silicon Substrates
M. Zielinski, M. Portail, T. Chassagne, S. Kret, M. Nemoz, Y. Cordier
Mater. Res. Soc. Symp. Proc. **1069** (2008) 1069-D07-09

2009

253. Croissance d'héterostructures à base de Nitrure de Gallium pour applications en électronique de puissance
Y.Cordier, N.Baron, M.Azize, S.Chenot
Revue de l Electricite et de l Electronique **10** (2009) 73-77

254. First demonstration and performance of AlGaN based focal plane array for deep-UV imaging
J.-L. Reverchon, S. Bansropun, J. A. Robo, J. P. Truffer, E. Costard, E. Frayssinet, J. Brault, F. Semond, J. Y. Duboz, M. Idir
SPIE procedings **7474** (2009) 74741G

255. Al and Ti/Al contacts on n-GaN
L. Dobos, B. Pecz, L. Toth, Z.J. Horvath, Z.E. Horvath, E. Horvath, A. Toth, B. Beaumont, Z. Bougrioua
Vacuum **84** (2009) 228

256. Perturbing GaN/AlN quantum dots with uniaxial stressors
O. Moshe, D. H. Rich, B. Damilano, J. Massies
Phys. Stat. Sol. C **6** (2009) 1432

257. Electroluminescence analysis of 1.3-1.5 µm InAs quantum dot LEDs with (Ga,In)(N,As) capping layers
M. Montes, A. Hierro, J. M. Ulloa, A. Guzmán, M. Al Khalfioui, M. Hugues, B. Damilano, J. Massies
Phys. Stat. Sol. C **6** (2009) 1424

258. Optical study of bulk ZnO for strong coupling observation in ZnO-based microcavities
F. Médard, J. Zúñiga-Pérez, E. Frayssinet, J. C. Moreno, F. Semond, S. Faure, P. Disseix, J. Leymarie, M. Mihailovic, A. Vasson, T. Guillet, and M. Leroux
Photonics and Nanostructures **7** (2009) 26

259. Optical characterization of zinc oxide microlasers and microwire core-shell heterostructures
C. Czekalla, C. Sturm, R. Schmidt-Grund, B. Cao, J. Zúñiga-Pérez, M. Lorenz, and M. Grundmann
J. Vac. Sci. Technol. B **27** (2009) 1780

260. Expected progress based on aluminium gallium nitride focal plane arrays for near and deep ultraviolet
J-L Reverchon, K. Robin, S. Bansropun, Y. Gourdel, J.-A. Robo, J.-P. Truffer, E. Costard, J. Brault, E. Frayssinet and J.-Y. Duboz
EDP **37** (2009) 207

261. Recent ROB developments on wide bandgap based UV sensors
B. Giordanengo, A. Ben Moussa, J.F. Hochedez, A. Soltani, P.de Moor, K. Minouglou, P. Malinowski, J.Y. Duboz, Y.M. Chong, Y.S. Zhou, W.J. Zhang, S.T. Lee, R. Dahal, J. Li, J.Y. Lin, and H.X. Jiang
EDP_EAS **37** (2009) 199

262. Strain engineering in GaN layers grown on silicon by molecular beam epitaxy: The critical role of growth temperature
Y.Cordier, N.Baron, S.Chenot, P.Vennéguès, O.Tottereau, M.Leroux, F.Semond, J.Massies
J. Cryst. Growth **311** (2009) 2002-2005

263. High temperature behaviour of AlGaN/AlN/GaN Hall-FET sensors
L. Bouguen, L. Konczewicz, S. Contreras, B. Jouault, J. Camassel, Y. Cordier
Mat. Sci. Eng. **B 165-1-2** (2009) 1-4

264. Growth and characterization of AlGaN/GaN HEMT structures on 3C-SiC/Si(111) templates
Yvon Cordier, Marc Portail, Sébastien Chenot, Olivier Tottereau, Marcin Zielinski and Thierry Chassagne
Materials Science Forum **600-603** (2009) 1277-1280

265. Optical investigations of bulk and multi-quantum well nitride-based microcavities
F. Reveret, F. Medard, P. Disseix, F. Semond, et al.
Optical Materials **31** (2009) 505

266. Advances in quality and uniformity of (Al,Ga)N/GaN quantum wells grown by molecular beam epitaxy with plasma source
F.Natali, Y.Cordier, C. Chaix, P.Bouchaib
J. Cryst. Growth **311** (2009) 2029-2032

267. Epitaxial aluminium nitride on patterned silicon
J.C. Moreno, E. Frayssinet, F. Semond, et al.
Materials Science in Semicond. Processing **12** (2009) 31

268. Evaluation of SiN films for AlGaN/GaN MIS-HEMTs on Si(111)
Y. Cordier, A. Lecotonnec, S. Chenot, N. Baron, F. Nacer, A. Goullet, H. Lhermite, M. El Kazzi, P. Regreny, G. Hollinger, M. P. Besland
Phys. Stat. Sol. C **6 - S2** (2009) 1016-1019

269. Anomalous Hall Effect in Gd-Implanted Wurtzite $Al_xGa_{1-x}N$/GaN High Electron Mobility Transistor Structures
F.Y Lo, A. Melnikov, D. Reuter, Y. Cordier, A.D. Wieck
Materials Research Society Symposium Proceedings **1111** (2009) 61-69

270. Preliminary results of bench implementation for the study of terahertz amplification in gallium nitride quantum wells
T. Laurent, P. Nouvel, J. Torres, L. Chusseau, C. Palermo, L. Varani, Y. Cordier, J.-P. Faurie, B. Beaumont, E. Starikov, P. Shiktorov, V. Gruzˇinskis,
Journal of Physics : Conference Series **193** (2009) 012094

271. Analysis of the C-V characteristic SiO_2/GaN MOS capacitors
I Cortes, E Al-Alam, MP Besland, P Regreny, F Morancho, A Cazarré, Y Cordier, A Goullet and K Isoird
Proceedings 7th Spanish Conference on Electron Devices **7** (2009) 254-257

272. Selective area growth of GaN-based structures by molecular beam epitaxy on micrometer and nanometer size patterns
Y. Cordier, F. Semond, J-C. Moreno, E. Frayssinet, B. Benbakhti, Z. Cao, S. Chenot, L. Nguyen, O. Tottereau, A. Soltani and K. Blary
Materials Science in Semiconductor Processing **12** (2009) 16-20

273. Luminescence and reflectivity characterization of AlGaN/GaN high electron mobility transistors
N. Baron, M. Leroux, N. Zeggaoui, P. Corfdir, F. Semond, Z. Bougrioua, M. Azize, Y. Cordier, J. Massies
Phys. Stat. Sol. C **6 - S2** (2009) 715-718

274. AlGaN/GaN high electron mobility transistor grown by molecular beam epitaxy on Si(110): comparisons with Si(111) and Si(001)
Y. Cordier, J.-C. Moreno, N. Baron, E. Frayssinet, S. Chenot, B. Damilano, F. Semond
Phys. Stat. Sol. C **6 - S2** (2009) 1020-1023

275. AlInN optical confinement layers for edge emitting group III-nitride laser structures
H.P.D. Schenk, M. Nemoz, M. Korytov, P. Vennéguès, P. Demolon, A.D. Dräger, A. Hangleiter, R. Charash, P.P. Maaskant, B. Corbett, and J.Y. Duboz
Phys. Stat. Sol. (c) **S2** (2009) 897

276. Towards green lasing: ingredients for a green laser diode based on GaInN
A.D. Dräger, H. Jönen, H. Bremers, U. Rossow, P. Demolon, H.P.D. Schenk, J.Y. Duboz, B. Corbett, and A. Hangleiter
Phys. Stat. Sol. (c) **C6 (S2)** (2009) 792

277. Advances in liquid phase conversion of (100) and (111) oriented Si wafers into self standing 3C-SiC
M. Zielinski, M. Portail, T. Chassagne, S. Juillaguet, H. Peyre, A. Leycuras, J. Camassel
Materials Science Forum **615-617** (2009) 49

278. Role of substrate misorientation in relaxation of 3C-SiC layers on silicon
M. Zielinski, M. Portail, S. Roy, S. Kret, T. Chassagne, M. Nemoz, Y. Cordier
Materials Science Forum **615-617** (2009) 169

279. Optical and excitonic properties of ZnO films
M. Mihailovic, A. L. Henneghien, S. Faure, P. Disseix, J. Leymarie, A. Vasson, D. A. Buell, F. Semond, C. Morhain, and J. Zúñiga-Pérez
Optical Matérials **31** (2009) 532

280. UV Imaging Based on AlGaN Arrays
Jean-Yves Duboz, Julien Brault, Jean-Patrick Truffer, Jean-Alexandre Robot, Kristelle Robin, Jean Luc Reverchon
Phys. Stat. Sol. (c) **S2** (2009) S611

281. 8H Stacking Faults in a 4H-SiC Matrix: Simple Unit Cell or Double 3C Quantum Well?
Robert T., Juillaguet S., Marinova M., Chassagne T., Tsiaoussis I., Frangis N., Polychroniadis E. K. and Camassel J.
Materials Science Forum 615-617, (2009), 339-342

2010

282. Electrical behaviour of lateral Al/n-GaN/Al structures
Z.J. Horvath, L. Dobos, B. Beaumont, Z. Bougrioua, B. Pecza
App. Surf. Science **256** (2010) 5614

283. In-clustering effects in InAlN and InGaN revealed by high pressure studies
I. Gorczyca, T. Suski, A. Kaminska, G Staszczak, H.P.D. Schenk, N.E. Christensen, A. Svane
Phys. Stat. Sol. A **207** (2010) 1369

284. Asymmetric barrier composition GaN/(Ga,In)N/(Al,Ga)N quantum wells for yellow emission
Benjamin Damilano, Thomas Huault, Julien Brault, Denis Lefebvre, and Jean Massies
Phys. Stat. Sol. C **1-3** (2010) 200983426

285. GaN quantum dots in (Al,Ga)N-based Microdisks
S. Sergent, J. C. Moreno, E. Frayssinet, Y. Laaroussi, S. Chenot, J. Renard, D. Sam-Giao, B. Gayral, D. Néel, S. David, P. Boucaud, M. Leroux, F. Semond
J. Phys.: Conf. Ser. **210** (2010) 012005

286. Toward polariton lasing in a zinc oxide microcavity: Design and preliminary results
F. Médard, D. Lagarde, J. Zúñiga-Pérez, P. Disseix, J. Leymarie, M. Mihailovic, D. D. Solnyshkov, G. Malpuech, E. Frayssinet, S. Sergent, F. Semond, M. Leroux, S. Bouchoule
J. Phys.: Conf. Ser. **210** (2010) 012026

287. SiC on SOI resonators: a route for electrically driven MEMS in harsh environment
M. Placidi, A. Pérez-Tomás, P. Godignon, N. Mestres, G. Abadal, T. Chassagne, M. Zielinski
Materials Science Forum **645-648** (2010) 845-848

288. Epitaxial Graphene Elaborated on 3C-SiC(111)/Si Epilayers
A. Ouerghi, M. Portail, A. Kahouli, L. Travers, T. Chassagne, M. Zielinski
Materials Science Forum **645-648** (2010) 585-588

289. Thermally induced surface reorganization of 3C-SiC(111) epilayers grown on silicon substrates
M. Portail, T. Chassagne, S. Roy, C. Moisson, M. Zielinski
Materials Science Forum **645-648** (2010) 155-158

CNRS-CRHEA
PARC DE SOPHIA ANTIPOLIS,
RUE BERNARD GREGORY
06560 VALBONNE
Tél : 33 (0)4 93 95 42 00
www.crhea.cnrs.fr